# Vertex: Designing High-Performance Legs for Specialized Quadrupedal Robots

**Master Thesis**

**Author(s):**
Lau, Hong Fai

**Publication date:**
2019

**Permanent link:**
https://doi.org/10.3929/ethz-b-000373460

Eidgenössische Technische Hochschule Zürich
Swiss Federal Institute of Technology Zurich

Robotic Systems Lab
Prof. Dr. Marco Hutter

Master Thesis

# Vertex: Designing High-Performance Legs for Specialized Quadrupedal Robots

**Spring Term 2019**

**Supervised by:**
Hendrik Kolvenbach
Fabio Dubois

**Author:**
Hong Fai Lau

# Declaration of Originality

I hereby declare that the written work I have submitted entitled

**Vertex: Designing High-Performance Legs for Specialized Quadrupedal Robots**

is original work which I alone have authored and which is written in my own words.[1]

**Author(s)**

| | |
|---|---|
| Hong Fai | Lau |

**Student supervisor(s)**

| | |
|---|---|
| Hendrik | Kolvenbach |
| Fabio | Dubois |

**Supervising lecturer**

| | |
|---|---|
| Marco | Hutter |

With the signature I declare that I have been informed regarding normal academic citation rules and that I have read and understood the information on 'Citation etiquette' (`https://www.ethz.ch/content/dam/ethz/main/education/rechtliches-abschluesse/leistungskontrollen/plagiarism-citationetiquette.pdf`). The citation conventions usual to the discipline in question here have been respected.

The above written work may be tested electronically for plagiarism.

Zürich, 28/10/2019

Place and date

Signature

[1] Co-authored work: The signatures of all authors are required. Each signature attests to the originality of the entire piece of written work in its final form.

## Intellectual Property Agreement

The student acted under the supervision of Prof. Hutter and contributed to research of his group. Research results of students outside the scope of an employment contract with ETH Zurich belong to the students themselves. The results of the student within the present thesis shall be exploited by ETH Zurich, possibly together with results of other contributors in the same field. To facilitate and to enable a common exploitation of all combined research results, the student hereby assigns his rights to the research results to ETH Zurich. In exchange, the student shall be treated like an employee of ETH Zurich with respect to any income generated due to the research results.
This agreement regulates the rights to the created research results.

### 1. Intellectual Property Rights

1. The student assigns his/her rights to the research results, including inventions and works protected by copyright, but not including his moral rights ("Urheberpersönlichkeitsrechte"), to ETH Zurich. Herewith, he cedes, in particular, all rights for commercial exploitations of research results to ETH Zurich. He is doing this voluntarily and with full awareness, in order to facilitate the commercial exploitation of the created Research Results. The student's moral rights ("Urheberpersönlichkeitsrechte") shall not be affected by this assignment.
2. In exchange, the student will be compensated by ETH Zurich in the case of income through the commercial exploitation of research results. Compensation will be made as if the student was an employee of ETH Zurich and according to the guidelines "Richtlinien für die wirtschaftliche Verwertung von Forschungsergebnissen der ETH Zürich".
3. The student agrees to keep all research results confidential. This obligation to confidentiality shall persist until he or she is informed by ETH Zurich that the intellectual property rights to the research results have been protected through patent applications or other adequate measures or that no protection is sought, but not longer than 12 months after the collaborator has signed this agreement.
4. If a patent application is filed for an invention based on the research results, the student will duly provide all necessary signatures. He/she also agrees to be available whenever his aid is necessary in the course of the patent application process, e.g. to respond to questions of patent examiners or the like.

### 2. Settlement of Disagreements

Should disagreements arise out between the parties, the parties will make an effort to settle them between them in good faith. In case of failure of these agreements, Swiss Law shall be applied and the Courts of Zurich shall have exclusive jurisdiction.

Zürich, 28/10/2019

Place and date

Signature

# Contents

# Preface

This master thesis was undoubtedly challenging. While it was strenuous at times, the experience that I have gained was well worth it. This work would not have been made possible without the help of several people. I would like to firstly thank my supervisors, Hendrik Kolvenbach and Fabio Dubois who have guided and supported me throughout this entire thesis. For that, I am grateful to you both. I would also like to thank my colleague, Michael Chadwick who I have collaborated closely with during this thesis. Your help was much appreciated. Last but certainly not least, I would like to thank Prof. Dr. Marco Hutter for making this thesis happen.

# Abstract

Legged robots have demonstrated how versatile all-terrain robot locomotion can be. Coupling this with other capabilities such as running at high speeds, carrying heavy payloads or any other general ones, make them appealing for outdoor applications. The typical design approach used to develop the legs of these robots has been actuator-centric. While this approach has worked well for general-purpose legged robots as seen from their promising performance in outdoor applications, it may not necessarily be the case for specialized robots. This is because such a straightforward design approach may not uncover the design intricacies required to facilitate their specific requirements in order to achieve high performance. Hence, this calls for an alternative design approach.

This master thesis studies the question of what it means to design a specialized robotic leg holistically. It begins with the exploration of leg designs meant for two different specialized robots: one for high-speed applications and the other to carry heavy payloads. The legs of various animals and that of previous robotic works were first examined to gain inspiration and insights. Design concepts based on these were then drawn up. Eventually, only a single leg concept intended for heavy payload applications was pursued. This design concept was subsequently developed using a thorough design framework. This holistic design approach eventually led to a leg design intended for a centaur-like heavy payload quadrupedal robot which is deployable in construction-related scenarios. The finalized leg design uses an average of 24.5% less total joint torque for a walking task as compared to a naively designed one. The high-performance leg design encapsulates the critical ideas explored as well as serves as a proof of concept of the proposed design approach.

# Symbols

## Indices

| | |
|---|---|
| $d$ | Design |
| $i$ | Time Index |
| $j$ | Joint Index |
| $KFE$ | Knee Flexion and Extension |
| $max$ | Maximum Value |
| $min$ | Minimum Value |

## Acronyms and Abbreviations

| | |
|---|---|
| AAA | Ankle Abduction and Adduction |
| AFE | Ankle Flexion and Extension |
| CAD | Computer-Aided Model |
| CFRP | Carbon Fibre Reinforced Polymer |
| CoM | Center of Mass |
| DoF | Degree of Freedom |
| ETH | Eidgenössische Technische Hochschule |
| FEM | Finite Element Method |
| HAA | Hip Abduction and Adduction |
| HFE | Hip Flexion and Extension |
| KFE | Knee Flexion and Extension |
| LF | Left Foreleg |
| LH | Left Hindleg |
| PDD | Pseudo-Direct Drive |
| PEA | Parallel Elastic Actuator |
| RF | Right Foreleg |
| RH | Right Hindleg |
| RoM | Range of Motion |
| ROS | Robot Operating System |
| SEA | Series Elastic Actuator |
| SDA | Series Damper Actuator |
| SLIP | Spring-Loaded Inverted Pendulum |
| TOWR | Trajectory Optimizer for Walking Robots |
| VSA | Variable Stiffness Actuator |

# Chapter 1

# Introduction

Legged robots have long been recognized for their versatility in all-terrain locomotion [1]. Their defining subsystem, the legs, enable them to possess unique locomotion capabilities which include: i) the ability to maneuver through arduous terrain, ii) requiring only a few defined foot placements instead of a continuous path, and iii) easily maintaining their stability using their intrinsic multiple Degrees of Freedom (DoFs) [2]. These benefits motivate the research field to push the application of mobile robots from mere factory floors to the outside world.

The research field has recently seen some significant progress. The unprecedented dynamism demonstrated by various legged robots such as Agility Robotics Cassie [3, 4], ANYbotics ANYmal [5], Boston Dynamics Spot[1] and the MIT Cheetahs [6, 7, 8, 9] are evidence of this. The design approach used to develop the legs of such robots has generally been actuator-centric. Here, actuator development takes the top priority, while the mechanical design of the leg merely serves as a means to an end. While this approach has been relatively effective for such legged robots, it may not be the case for more specialized ones, such as one that can run at high speeds or carry heavy payloads, and whose development may be the future direction of the research field. This is because such a straightforward design approach may not reveal the often complex and counter-intuitive design intricacies required to facilitate the specific demands of these robots. This may result in a final design that performs poorly. Hence, this calls for a proper investigation into the design of robotic legs.

This master thesis puts forth the notion that a robotic leg is more than just actuators coupled together using rigid links, and hence it needs to be designed holistically. In other words, when designing robotic legs, their actuators together with their functions and projected tasks, have to be considered simultaneously. This thesis starts with the search for two leg designs meant for two different robots, one that can run at high speeds and another that can carry heavy payloads. Animals and previous robotic works were first studied to seek for inspiration and insights. These were then used to generate potential design concepts for the legs. After some evaluation, one that can bear heavy payloads was eventually selected. This design concept was then built upon using a meticulous design framework. This holistic design approach led to a high-performance leg design meant for a centaur-like heavy payload legged robot which is suitable for construction-related applications. When compared to a naively designed leg, the leg as depicted in Fig. 1.1, uses 24.5% less total joint torque for a walking task. Hence, the design embodies the fundamental ideas explored and is a proof-of-concept of the holistic design approach introduced.

The thesis is organized as follows: Chapter 2 details the design problem and re-

[1]Product link: https://www.bostondynamics.com/spot

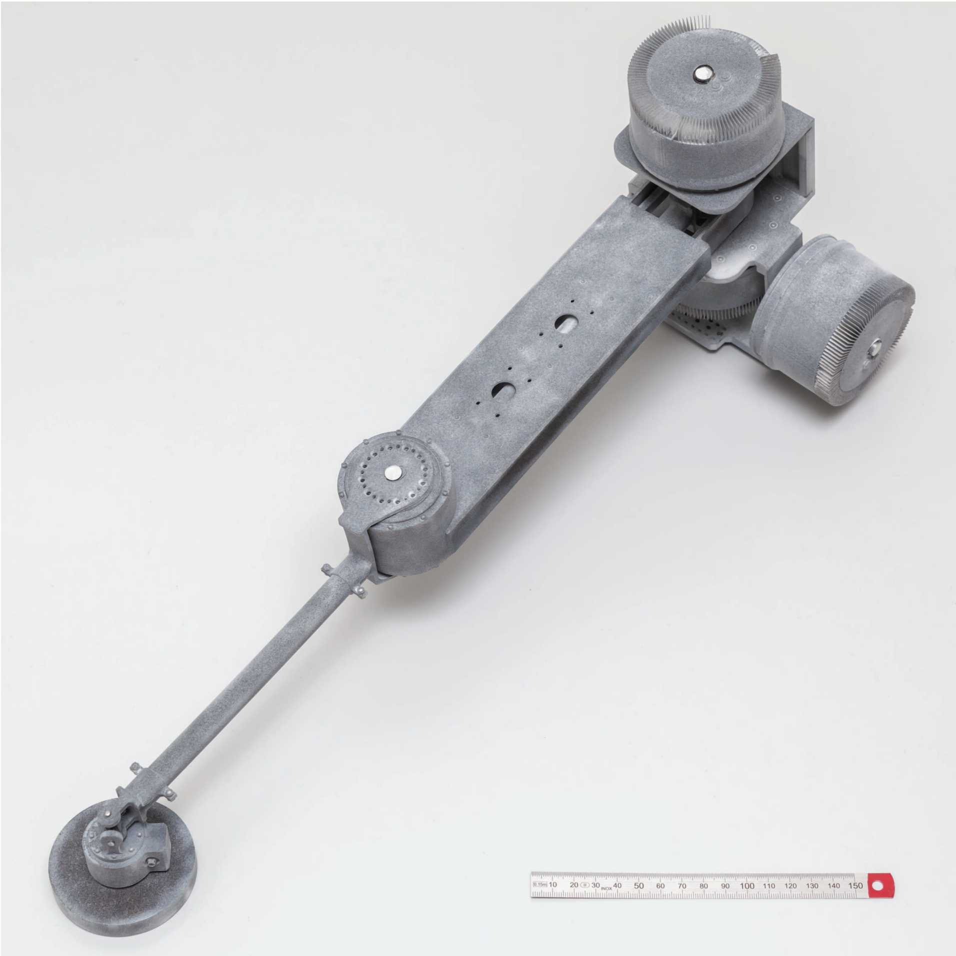

Figure 1.1: A 1:2 scale 3D-printed prototype of the finalized leg design developed using the proposed holistic design approach.

views existing literature. Chapter 3 covers the concept generation and evaluation phases. Chapter 4 explains how a selected leg concept was systematically analyzed, optimized, and engineered. Chapter 5 details the finalized leg design of the heavy payload leg. Last but not least, Chapter 6 concludes the thesis. The relevant project management and supporting documents can be found in the appendices.

# Chapter 2

# Design Process and Literature Review

This chapter begins with the introduction of the design objective of this master thesis. The associated design problem is then abstracted and analyzed. A holistic design approach suitable for tackling the design problem is subsequently proposed. Literature regarding animals and existing robotic works are finally reviewed at the end of the chapter.

## 2.1 Design Objective

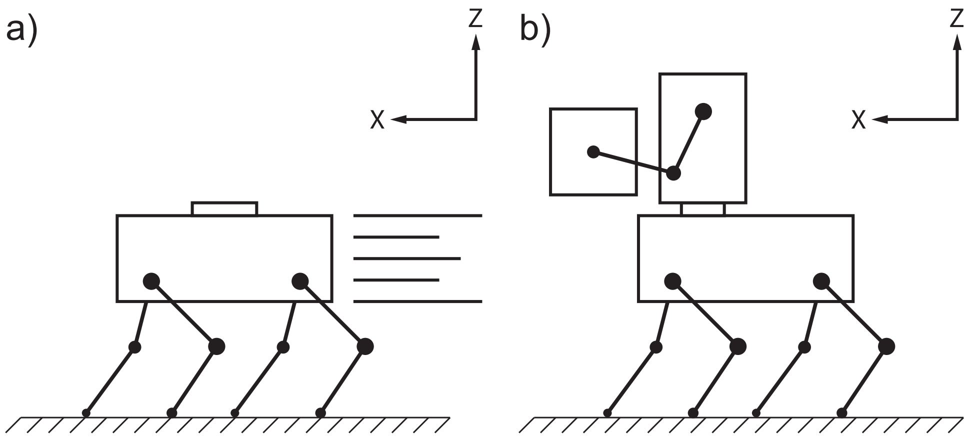


Figure 2.1: Envisioned specialized quadrupedal robots. a) High-speed. b) Heavy payload.

| **Requirement** | **High-speed robot** | **Heavy payload robot** |
|---|---|---|
| Maximum speed [$ms^{-1}$] | 10 | 1 |
| Maximum payload [$kg$] | 1 | 20 |
| Autonomy [$h$] | 1 | 4 |

Table 2.1: Requirements of the future robots.

The primary objective of this thesis was to explore leg designs intended for two future quadrupedal robots, namely one that can run at high speeds and the other that can carry heavy payloads. Figures 2.1a-b respectively illustrate these two specialized robots and their requirements are listed in Table 2.1. The high-speed robot was envisioned to be a regular quadrupedal robot that was suitable for search and rescue deployment. It should expend most of its energy transversing the terrain at high speeds while carrying a small payload (e.g. first aid kit). The heavy payload robot, on the other hand, was envisioned to be a quadrupedal robot that has an arm or a torso with arms attached to it. This configuration enables the robot to manipulate its environment, hence, making it suitable for the construction industry. This robot should also be able to operate for a sizeable period of time (e.g. drilling holes into the walls of a floor). By the end of this thesis, it was planned that only one leg design that facilitates the realization of either of these robots would be developed.
The following section analyzes the underlying design problem of these two robots in detail.

## 2.2 Design Problem

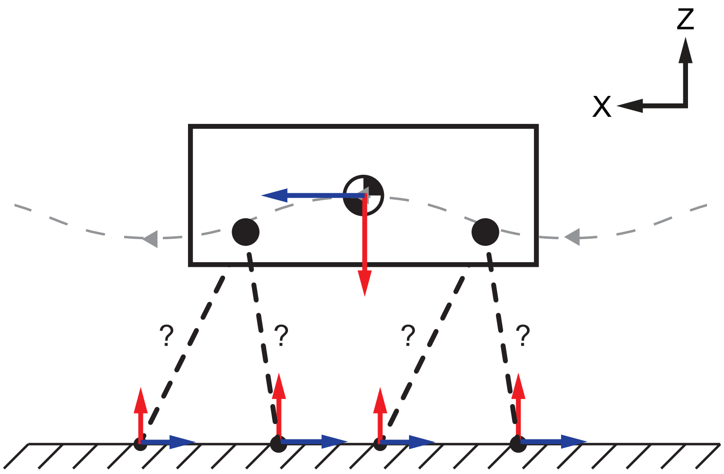


Figure 2.2: Fundamental design problem of legged robot locomotion; 2D case on the sagittal (XZ) plane.

The fundamental design problem of robot locomotion is the development of mechanisms that utilize ground interaction forces to propel an elevated mass along a given desired trajectory. In the domain of legged robots, these mechanisms take on the form of vertical extensions which periodically make contact with the ground as illustrated by Fig. 2.2. These vertical extensions, which are better known as legs, can be analyzed in three ways, namely the forces that they apply, their motion as well as their energetics. In the following paragraphs, each of these will be explained in greater detail.
The stance phase of legged robot locomotion begins when the leg comes into contact with the ground. For this simplified 2D analysis, during the stance phase, the leg only applies forces that act along the X and Z axes. Along the Z-axis, the leg supports a proportion of the weight of the robot while also applying any additional force required to accelerate the mass vertically. As this force is primarily vertical to the ground, it gives rise to a frictional force (traction) which acts along the X-axis. It is this horizontal force that enables the leg to move the mass forward as

it actuates backward. Once the leg has reached the backward limit of its reach, it shortens its length to create some clearance before swinging forward. This marks the start of the swing phase, where the actuators produce forces which act on the leg to counter the inertial forces. Upon reaching the forward limit of its reach by swinging and extending, the leg impacts the ground (its velocity instantaneously changes to $0ms^{-1}$) and enters back into the stance phase.
As the robot tracks its desired trajectory, the above phases are repeated one after another to form a periodic cycle. The timings to which individual leg is in the stance or swing phase characterize the motion of the robot. The overarching pattern of these timings is called a gait. The different types of gaits in animals and robots are generally well studied and can be explained analytically using the Spring-Loaded Inverted Pendulum (SLIP) model [10].
By considering the energetics of this design problem, an ideal leg is one that expends an amount of energy that is equivalent to the theoretical work required to move the mass along its desired trajectory. However, in reality, the theoretical work required only forms a lower bound on the energy expenditure due to the inevitability of energy losses. The sources of these energy losses include but are not limited to the following: i) ground impacts [11], ii) friction and other dissipative nonlinearities in the actuators and its transmission system [12], and iii) leg configuration; geometric work where the actuators are working against one another [13].
With the above analysis, the leg of a legged robot can be defined as follows: it is a subsystem that applies accurate and repeatable forces in a well-defined workspace surrounding it. These forces together with their ground interactions, propel the Center of Mass (CoM) of the robot along its desired trajectory. The mechanical design of the leg should seek to achieve the following: i) facilitate the locomotion of the robot (predominantly periodic), ii) minimize overall energy consumption (lower bounded by physical laws), and iii) mitigate any short yet high-intensity impacts that may occur at the end effector. If these are fulfilled, the leg is deemed to be a high performing one.
In the following section, the insights from this analysis were used to develop a holistic design approach for this thesis.

## 2.3 Holistic Design Approach

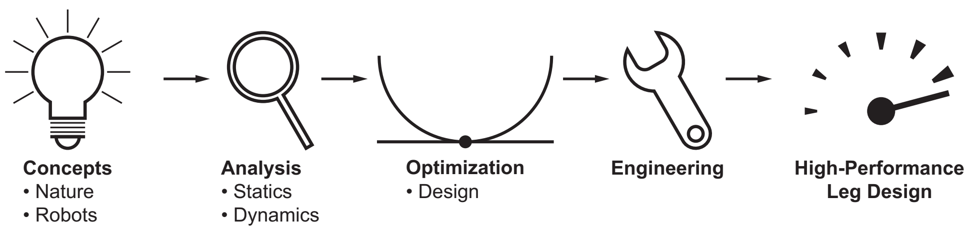


Figure 2.3: Proposed holistic design approach for designing high-performance robotic legs.

Referring back to Table 2.1, it was expected that a high-performance leg design for each of the two envisioned robots would be very different from one another. This was because each leg has to cater to the particular requirements of each robot. By intuition, the high-speed leg has to move quickly and efficiently, while also being able to mitigate very high-intensity impacts. The heavy payload leg, on the other hand, has to use very little power to maintain its configuration, even when it is loaded heavily. In other words, the design emphasis of the high-speed leg lies in the application of horizontal forces, while that of the heavy payload leg was in the application of vertical forces. This insight and the demanding requirements suggested that the straightforward actuator-focused design approach typically employed in robotic legs development today may not be adequate enough. This was because when designing high-performance legs for specialized legged robots, the often complex and counter-intuitive design intricacies required to facilitate the performance of these robots are only revealed when its actuators, various functions, and projected tasks are simultaneously considered in the design process. These would most likely be overlooked should attention be paid only to the actuators of the leg. Hence, this called for a more holistic design approach.

Figure 2.3 presents the holistic design approach that was used to design high-performance robotic legs for this thesis. The 5-phase process started with the generation of concepts using insights from both nature[1] and previous robotic works. These are then evaluated and narrowed down. The most promising concept was further developed before being analyzed, both statically and dynamically based on the projected tasks of the robot. The design parameters of the leg were later optimized to one of the tasks and then engineered to increase their feasibility. The high-performance robotic leg was then finally designed using these parameters.

The above summary serves as a guide for the remainder of this thesis. The following section presents the findings from the comprehensive literature review.

## 2.4 Literature Review

An extensive literature review that spanned across nature and previous related works is presented in this section. The findings are organized in pointers to highlight specific insights. These were useful when the design concepts of the high-speed and heavy payload legs were being constructed.

### 2.4.1 Nature

The following pointers relate to animals:

- Morphology:
  - Quadrupedal mammals have asymmetrical loadings on their limbs due to their forward CoM; dogs have higher loadings on their forelegs than their hindlegs [14]. Therefore, this highlights that symmetry is not a common natural phenomenon. Hence, one should expect that the forelegs and hindlegs of animals are morphologically different from one another.
  - The cross-sectional bone structures of a fast dog and a strong one are different; the former is elliptical while the latter is circular [14]. This highlights the interconnectedness of form and functions seen in nature.
- Locomotion:
  - Energetically efficient locomotion:
    - People who run with a midfoot or forefoot strike are more energy-efficient than those who run with a heel strike as it reduces the

[1]Based on the Theory of Evolution, there exist adaptations in animals in which inspiration can be sought from. While it is clear for the case of high-speed animals since they relate to survival (chasing prey, running away from predators), it may not be the case for carrying heavy payloads. This is because such an act may not be necessary for survival and is more of a human-related activity (transporting materials around). Hence, adaptations that enable larger animals to carry their massive weights were investigated instead.

ground contact time. This consequently minimizes the unnecessary movement of their CoM [15].

    * During walking, the human pelvis restrains the motion of the CoM such that it is only able to track its trajectory. Hence, achieving energetically efficient locomotion [16].
    * When horses gallop, they retract their legs during the swing phase to reduce the inertia of their limbs. Hence, reducing the amount of torque required for the swing phase.
    * Animals tend to locomote at their resonance frequencies. Therefore, they move with very little energy input [17].
  - Adaptations that increase ground traction:
    * Animals such as dogs have claws that dig into soft ground for traction.
  - Factors affecting animals moving at different speeds:
    * The acceleration and deceleration of animals are affected by different constraints at different speeds. At low speeds, geometric constraints such as the ratio of how forward the CoM is to their leg lengths limit their speed. This is done to avoid pitching while also increasing ground traction. At higher speeds, they are limited by physiological constraints [18].

- Impact mitigation:
  - It primarily takes place in the foot.
  - Adaptations that decreases the rate of change of momentum:
    * There are movable links present in the hoof of a horse that increases its compliance.
    * Cushioning in the feet of animals is a common feature. Examples include the footpads of humans, the paw pads in digitigrade animals (animals which walk on their digits), the digital cushion in unguligrade animals (animals which walk on hoofs)
  - Different control strategies affect the magnitude of impacts:
    * People who run barefoot typically land on their midfoot or forefoot instead of the usual heel. Doing so increases the compliance of their ankle joint and consequently, the effective mass which impacts the ground. Hence, this results in smaller impacts [19].
    * Elephants tend to land on their cushioned heels when walking [20]
- Maintaining configuration:
  - Locking mechanisms:
    * Some birds have a locking mechanism similar to a hook and pawl which allow them to stand upright for long periods of time [21]
    * Flamingos can support their entire body weight on a single foot by changing their configuration such that their CoM is close to being directly above their foot. Hence, very little ankle joint torque is needed to maintain its configuration [22].
    * Horses have a group of soft tissues called the stay apparatus which lock their joints with little muscular effort when maintaining a configuration.
  - Cushioning:
    * Elephants have large feet cushions for bearing their massive weights [23].

### 2.4.2 Robots

The following pointers relate to previous robotic works:

- Design approach:
  - Every robotic leg comprises of two subsystems, its passive dynamics and its active control system [24].
  - Passive dynamics relate to the passive components (e.g. springs, dampers) and the configuration of the leg.
    - These components may be used to increase the performance of the robot with little to no energetic cost.
    - They can be viewed as an instantaneous and energy-efficient feedback control since no sensors that cause delays are involved [10].
    - However, it may increase the design complexity of the leg, and they may also be seen as a dead mass when not in used.
  - The active control system relates to the active components (e.g. actuators).
    - They can overwrite the passive dynamics to output a desired behavior.
    - They are also able to fulfill a variety of tasks.
    - They tend to be energetically expensive.
  - Passive dynamics may be viewed as a filter which reduces the task that the active control system has to perform. It also damps the high-frequency impacts.
    - Typically in a leg, its high-frequency behavior is handled by the passive dynamics, while the active control system manages its low-frequency behavior. This highlights the close relationship shared between its mechanical design and control [25].
    - However, it may be difficult to categorize what tasks are high- frequency and what tasks are low-frequency.
  - The inclusion of passive dynamics into the leg may reduce the closed-loop force control bandwidth of the leg [7].
  - Decoupling the actuation required for locomotion and gravity compensation may simplify the design problem [26, 27].
- Morphology:
  - In a nominal stance configuration, a mammalian configuration generally requires lesser joint torque as compared to a reptilian or insectile configuration [28].
  - A pantograph leg mimics that of mammals [29].
  - A spider configuration promotes a better power balance between the actuators during gait than a conventional serial configuration [13]. However, this may be limited to a particular case ($3ms^{-1}$ running trajectory generated using a SLIP model).
  - A parallel kinematic leg has a smaller Range of Motion (RoM) as compared to a serial leg [8].
  - Legs that have a tarsus which faces the direction of motion is prone to lesser impacts [24].

- Design practices and heuristics:
  - Proprioceptive force control is enabled by coupling a high torque actuator with a low mass and inertia leg [7].
  - The impact mitigation capability of a leg is inversely proportional to its mass and inertia [7].
  - The inertia of a leg can be reduced by minimizing its gearing since reflected link inertia is increased by the square of the gearing ratio [30].
  - Backdrivability enables energy to be regenerated [31].
  - A compliant leg may protect its actuators from impacts [32, 33].
  - Operating at resonant frequencies enables compliant actuators to achieve desirable performance metrics such as: i) minimal mechanical peak power, ii) minimal mechanical energy per cycle, and iii) minimal electrical energy per cycle [34, 35, 36].

### 2.4.3 Database of Animals and Robots

A database containing information regarding animals and robots was compiled. This spreadsheet can be found in Appendix B.1. The following are the insights that were gained: i) the shank of fast animals are generally longer than their thigh, ii) the shank of heavy animals are generally shorter than their thigh, and lastly, iii) both classes of animals generally walk on their digits or are hoofed.

In the following chapter, these insights were used to developed promising design concepts for the high-speed and heavy payload legs.

# Chapter 3

# Design Concepts and Evaluation

This chapter describes how a heavy payload leg design concept was eventually selected. The technical requirements for the high-speed and heavy payload legs, as well as the function structure of a robotic leg, were first formalized using the insights gained from the literature review. A morphological box containing possible solutions for each of these functions were subsequently constructed. These were then put together to form concepts for the two legs. These were evaluated against the corresponding objective-based evaluation tree. The top-scoring ones were further developed until the mentioned heavy payload leg was selected. This chapter ends with an overview of this concept.

## 3.1 Technical Requirements and Function Structure

The technical requirements for the high-speed and heavy payload legs were compiled into a spreadsheet, as seen in Appendix B.2. These represented the goals to which the final designs of the two legs sought to achieve. The requirements were organized into categories that relate to their mechanical design, functions, performance metrics, and interfaces (mechanical, electrical, data). They can be briefly summarized into the following pointers: i) the high-speed leg was expected to be a lightweight, low inertia leg which can track fast trajectories, ii) the heavy payload leg, on the other hand, was expected to be more massive, and it should maintain its configuration for an extended period of time with a relatively low energy consumption, and iii) both were expected to have a high composition of active elements while also being ingress protected to make them suitable for outdoor applications.
The function structure of a robotic leg was also derived using the insights gained from the literature review. It is as shown in Fig. 3.1. More details regarding the individual functions can be found in Appendix B.3. The function structure illustrates the flow of forces and data between the various functions of the leg. Energetics wise, a leg can be essentially viewed as a medium in which mechanical energy flows through. Hence, in order to achieve high performance, a leg design has to facilitate this flow. This is especially the case for the primary functions as highlighted in red. These functions which relate to the specializations of the high-speed and heavy payload leg should be designed to be either highly energy-efficient or low-powered.
The following section describes how these additional insights were combined with

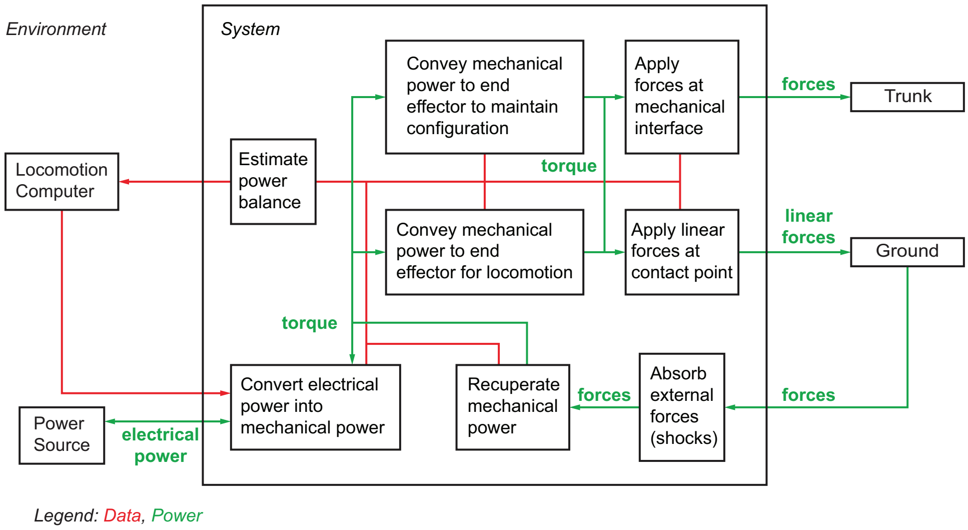


Figure 3.1: General function structure of a robotic leg. The primary functions of the leg are highlighted in red.

that from the literature review to generate possible design concepts for the high speed and heavy payload legs.

## 3.2 Concept Generation

A morphological box containing possible solutions for each function of the function structure was compiled. It is as shown in Fig. 3.2. The following highlights some of the solutions that were explored:

- Convert electrical power into mechanical power:
  - For this thesis, it was decided that either the DynaDrive or NEO Pseudo-Direct Drive (PDD) actuators were to be used in the eventual leg.
  - The DynaDrive actuator has a gear ratio of 1:8, while that of the NEO actuator is 1:6.6. These are relatively low gear ratios as compared to conventional high torque actuators which use harmonic gearboxes that have gear ratios typically ranging from 1:30 and upwards. Adopting such a low gear ratio allows leg inertia to be reduced, energy efficiency to be increased, and also transparent (feedforward) control to be enabled.
  - The peak torques of these in-house actuators are estimated to be $40Nm$ and $230Nm$ respectively.
  - These actuators may be used directly, coupled with additional gearing, or other components such as a spring or damper.
  - When coupled with a spring, the configuration results in a Series Elastic Actuator (SEA; when coupled a fixed stiffness spring in series) [32], a Variable Stiffness Actuator (VSA; when coupled a variable stiffness spring in series) [33], or a Parallel Elastic Actuator (PEA; when coupled a fixed stiffness spring in parallel) [37, 38].
  - When coupled with a damper, it results in a Series Damper Actuator (SDA) configuration [39].

| Functions | Comments | | Concepts | | | | | |
|---|---|---|---|---|---|---|---|---|
| | | | 1 | 2 | 3 | 4 | 5 | 6 |
| Convert electrical power into mechanical power | Combinations of actuators and transmission | Actuator | Direct Drive Rotary Actuator | Design constraint imposed by project (3 DoF motion, max 3 actuators) | | | | |
| | | Gearbox | None | Gearbox | | | | |
| | | Component | None | Serial Spring | Parallel Spring | Damper | | |
| Convey mechanical power to end effector to maintain configuration | Mechanism that enables the leg to maintain its configuration | | Power from Motors | Spring-based Mechanism | Singularity Configuration | Hard Stops | Clutches | Brakes |
| Convey mechanical power to end effector for locomotion | Morphology of the overall leg and its transmission | Kinematics | Serial | Parallel | Serial-Parallel | | | |
| | | Transmission | Motor at Joints | Rigid Link | Bowden Cable | Chain | Rope | Belt |
| | | Material | Metals | Composites | Plastics | Ceramics | | |
| Apply linear forces to the ground | Interface between leg and ground; acting on the ground | Nature | Passive | Active | | | | |
| | | Type | Single-point Contact | Multiple-points Contact | Geometric Foot | Plantar Foot | Digits | Hoof |
| Apply forces to the mechanical interface | Attachment to trunk | | Rigid Attachment | Spring-loaded Joint | Suspended Joint | | | |
| Absorb external forces | Interface between leg and ground; receiving from the ground | | Damper | Spring-based Mechanism | Additional Degrees of Freedom | | | |
| Recuperate mechanical power | Storage mechanisms | | Direct Feedback to Actuators | Spring-based Mechanism | Flywheel | Tendons | Elastomer | |
| Estimate power balance | Sensors | | Proprioceptive | Force Sensor | Position Sensor | | | |

Figure 3.2: Morphological box.

- Convey mechanical power to end effector to maintain configuration:
  - Variable stiffness mechanisms that can actively change their equilibrium positions can be used [40, 41].
  - Alternatively, locking mechanisms that are mechanical, frictional or singularity-based such as brakes can be used [42].
- Convey mechanical power to end effector for locomotion:
  - An unconventional serial-parallel kinematic structure can be used [43].
  - Using polymer ropes to transmit torques seemed promising [31].
- Apply linear forces to the ground:
  - Solutions such as a passive spring-loaded [12, 44] or adaptive [45] foot , an active foot [46], or even a bioinspired hoof [47] are possible options.
- Apply force to the mechanical interface:
  - These solutions can be used to restrict the movement of the CoM of the robot during locomotion, hence increasing the energy efficiency of the robot.
- Absorb external forces (shocks):
  - A foot inspired by the insights from Section 2.4.1 may be used here.
- Recuperate mechanical power:
  - Tendons made from kevlar can be used to store energy [48].

| Functions | Generated Concepts | | | | | | | | | | |
|---|---|---|---|---|---|---|---|---|---|---|---|
| | Datum | 1 | 2 | 3 | 4 | 5 | 6 | 7 | 8 | 9 | 10 |
| Convert electrical power into mechanical power | Direct Drive Rotary Actuator | Direct Drive Rotary Actuator | Direct Drive Rotary Actuator | Direct Drive Rotary Actuator | Direct Drive Rotary Actuator | Direct Drive Rotary Actuator | Direct Drive Rotary Actuator | Direct Drive Rotary Actuator | Direct Drive Rotary Actuator | Direct Drive Rotary Actuator | Direct Drive Rotary Actuator |
| | Gearbox | Gearbox | Gearbox | Gearbox | Gearbox | Gearbox | Gearbox | Gearbox | Gearbox | Gearbox | Gearbox |
| | Serial Spring | None | None | None | Serial Spring | Serial Spring | None | Parallel Spring | Parallel Spring | Serial Spring | Serial Spring |
| Convey mechanical power to end effector to maintain configuration | Power from Motors | Power from Motors | Power from Motors | Power from Motors | Spring-based Mechanism | Power from Motors | Power from Motors | Clutches | Spring-based Mechanism | Spring-based Mechanism | Power from Motors |
| Convey mechanical power to end effector for locomotion | Serial | Serial | Serial | Serial-Parallel | Parallel | Parallel | Serial | Serial | Serial | Parallel | Parallel |
| | Motor at Joints | Belt | Rigid Link | Rope | Rope | Motor at Joints | Rigid Link | Chain | Rope | Rope | Motor at Joints |
| | Metals | Composites | Metals | Composites | Plastics | Metals | Metals | Composites | Metals | Metals | Metals |
| Apply linear forces to the ground | Passive | Passive | Active | Passive | Passive | Passive | Passive | Passive | Passive | Passive | Passive |
| | Single-point Contact | Geometric Foot | Plantar Foot | Plantar Foot | Plantar Foot | Geometric Foot | Geometric Foot | Plantar Foot | Geometric Foot | Plantar Foot | Geometric Foot |
| Apply forces to the mechanical interface | Rigid Attachment | Rigid Attachment | Rigid Attachment | Rigid Attachment | Rigid Attachment | Spring-loaded Joint | Rigid Attachment | Spring-loaded Joint | Rigid Attachment | Rigid Attachment | Spring-loaded Joint |
| Absorb external forces | Damper | Damper | Damper | Additional Degrees of Freedom | Damper | Damper | Damper | Spring-based Mechanism | Damper | Damper | Damper |
| Recuperate mechanical power | Spring-based Mechanism | Direct Feedback to Actuators | Spring-based Mechanism | Spring-based Mechanism | Tendons | Spring-based Mechanism | Direct Feedback to Actuators | Spring-based Mechanism | Direct Feedback to Actuators | Tendons | Spring-based Mechanism |
| Estimate power balance | Force Sensor | Proprioceptive | Force Sensor | Force Sensor | Force Sensor | Force Sensor | Proprioceptive | Force Sensor | Force Sensor | Force Sensor | Force Sensor |
| Platform | Universal | High Speed | High Speed | High Speed | High Speed | High Speed | Heavy Payload | Heavy Payload | Heavy Payload | Heavy Payload | Heavy Payload |
| Description | ANYbotics ANYmal V2 | Conservative serial leg design | Serial leg design that has a foot that has an active clutch to release energy that is stored in a spring at toe off | Serial leg design that has a parallel mechanism at the end effector to mitigate impacts | Parallel leg design that is based on a pantograph | Parallel leg design that uses the weight savings from one less motor to better mitigate impacts | Conservative serial leg design | Serial leg design that has an active clutch to aid in maintaining the configuration | Serial leg design that has a variable stiffness mechanism in parallel to aid in mataining the configuration | Parallel leg design that is based on a pantograph | Parllel leg design that uses the weight savings from one less motor to better mitigate impacts |

Figure 3.3: Summary of the generated leg design concepts.

- Estimate power balance:
  - The proprioceptive method [7], a force sensor, or a position sensor that measures the displacement in springs can be used.

The solutions from the morphological box were combined to form five possible design concepts each for the high-speed and heavy payload legs. Figure 3.3 summarizes the generated concepts. The associated design sketches, as well as additional information, can be found in Appendix B.4.

## 3.3 Concept Evaluation

The technical requirements from Appendix B.2 were translated into an objective-based evaluation tree for each type of leg. They are as shown in Appendix B.5. The two high-level objectives governing the evaluation trees were high performance and a short development time. For both of them, a slight emphasis was placed on the former than the latter (0.6 vs. 0.4). While both evaluation trees share the same set of evaluation criteria, they have different weights for each criterion. The differing weights represent the specialization of each type of leg. Regarding the performance-related criteria, a large emphasis was placed on being lightweight, having a low inertia, and being structurally strong for the high-speed leg. This was primarily due to the leg operating at high speeds and experiencing enormous impacts while doing so. For the heavy payload leg, the emphasis laid on consuming low amounts of energy while maintaining a configuration and also being structurally strong. This was because the leg has to resist the effects of the heavy weights that it typically carries. On achieving a short development time, criteria such as having a low design complexity, a small number of custom parts, and having many standard and off the shelf parts have large weights for both evaluation trees.

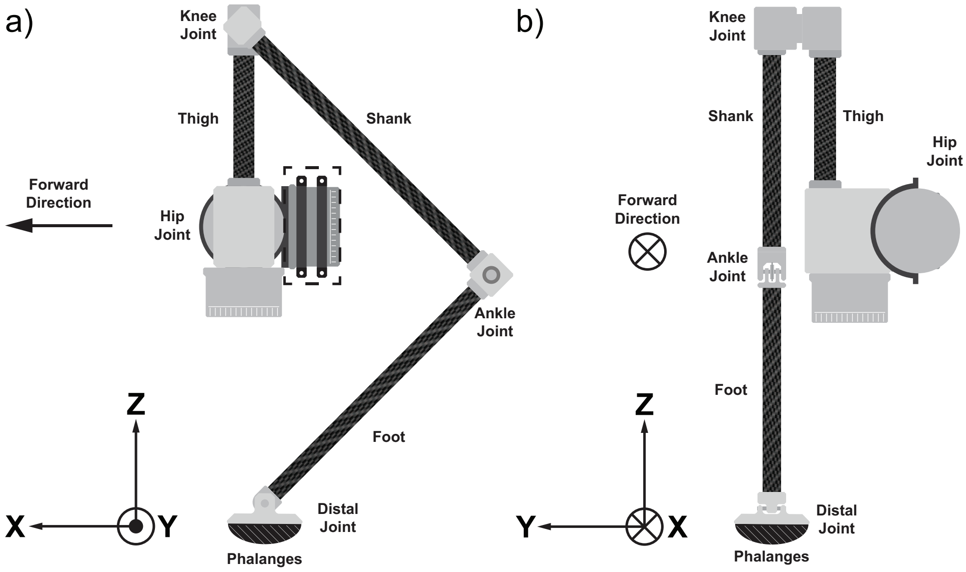


Figure 3.4: Selected heavy payload leg design concept. a) Front view. b) Side view. Note that the terminology for the link and joints of the spider leg are different from that of a conventional serial leg.

The evaluation trees were used to score the various concepts, as seen in Appendix B.6. The top two scoring concepts of each leg were subsequently developed. The four developed concepts are as depicted in Appendix B.7. Out of these four concepts, Concepts 3.1 and 7.1 were the most promising. The former is a high-speed leg that uses a simple serial leg configuration with a compliant foot. This foot enables the leg to operate energetically efficiently as it stores and releases energy as it runs at high speeds. The latter is a heavy payload leg that uses the spider configuration for a better power balance between its actuators. It is also equipped with a low-powered braking mechanism which enables it to hold its configuration efficiently. After much deliberation, Concept 7.1 was eventually selected. This was because it ranked the highest in its category and between the two types of legs, the realization of a heavy payload leg was the more certain one when the decision was made.
The design concept was further developed again after the selection. The following section presents an overview of the detailed version of this design concept.

## 3.4 Selected Heavy Payload Leg Design Concept

Figures 3.4a-b illustrate the selected heavy payload leg design concept. These design sketches were not drawn to scale and are meant only to highlight the key features of the concept. This concept sought to achieve the following objectives: i) it should be able to carry heavy payloads, ii) it should be energy efficient, and lastly, iii) it should be able to mitigate impacts effectively, given that it was expected to be heavy. The following pointers describe how these three objectives were being fulfilled:

- Ability to carry heavy payloads:
  - The leg uses the mentioned high-torque NEO actuators. The torque capability of these actuators should satisfy the demanding requirements set for the heavy payload leg.

  - The leg is made of custom aluminum alloy parts connected via standard Carbon Fibre Reinforced Polymer (CFRP) cylinders. This combination enables a lightweight, low inertia, and robust realization of the leg.
  - A force sensor located at its phalanges enables accurate and reliable force control.

- Energetically efficient operation:
  - The leg adopts a spider configuration that supports its actuators in providing powers of the same sign during gait; the actuator work with one another instead of braking against one another, hence possibly increasing the energy efficiency of the leg [13].
  - The leg incorporates a permanent magnet brake in its Ankle Flexion and Extension (AFE). This bioinspired feature enables the leg to lock its ankle joint and maintain a given configuration passively [21].

- Effective impact mitigation:
  - The leg has a distal joint that faces the direction in which it is moving; this geometrical feature enables the leg to experience lesser power dissipating impacts [24]
  - The leg uses ropes and pulleys to transmit the necessary torques to the various joints [31]. This allows the heavy actuators to be centralized near the supposed trunk of the heavy payload robot. Hence, a lightweight and low inertia leg (in the flexion and extension direction where it operates most of the time) can be realized. This consequently reduces the power dissipating impacts experienced by the leg.
  - Similar to animals as seen from Section 2.4.1, this leg integrates compliant material (e.g. silicone, foam) into its phalanges to mitigate impacts effectively. Additionally, the phalanges have a large surface area which not only increases the ground traction but also distributes the pressure more evenly so as not to destroy the environment.

Do note that the naming convention for the spider configuration is different from that of a regular serial leg since Hip Abduction and Adduction (HAA), and Hip Flexion and Extension (HFE) are no longer co-located. Hence, it will be useful to keep this naming convention in mind since it will appear regularly in the subsequent chapters.

The above features together formed a promising design concept for the heavy payload leg, which has the potential to emit a high performance. The concept also highlights the interconnectedness of the various features of the leg to its functions and tasks. It was the holistic design approach that revealed the necessary design considerations needed for the leg to achieve a high performance even in such an early phase of the design process. Therefore, the above suggests that the holistic design approach is indeed a feasible one when designing robotic legs. The above also demonstrated once again, the close relationship that form and function share. With the design concept in hand, one might proceed with the mechanical design phase, for example, by naively designing the leg with arbitrary link lengths. However, for this holistic design approach, the design concept was further analyzed, optimized, and engineered before doing so. The following chapter describes how these were carried out.

# Chapter 4

# Design Analysis, Optimization and Engineering

This chapter describes the design framework that was used to generate the final design parameters of the selected heavy payload leg. It begins with the sizing of a robot that uses the heavy payload leg. This robot was then analyzed statically and dynamically to deem its feasibility. The design parameters of its legs were subsequently optimized to a single task and were eventually engineered. The conducted procedure, as well as its findings, are presented in the following sections. Do note that this chapter heavily references the material seen in Appendix B.8, and it only serves as a guide behind the underlying thought process of the design framework.

## 4.1 Robot Sizing

The heavy payload robot was first sized to get a better understanding of the loadings and interfaces involved. It is as depicted in Fig. 4.1. The centaur-like robot is made from the trunk of ANYbotics ANYmal C[1] ($11kg$), the upper torso body of Halodi Robotics Eve[2] ($36kg$), and the updated iteration of the heavy payload legs which will be detailed in the following paragraph. This configuration enables the robot to not only transverse through the terrain, but also manipulate it. The torso was placed $0.2m$ in front of the center of the trunk to increase its reachability. This resulted in an asymmetry in the robot, which was further amplified by a $15kg$ payload (maximum payload of the arms). This was done so that the robot can be analyzed in a worst-case scenario manner.
Figure 4.2 shows the updated design concept for the selected heavy payload leg. As compared to the concept presented in Section 3.4, this design was further iterated with several design simplifications being adopted. These include the following: i) the vertical thigh has been integrated into the actuator mount for the Knee Flexion and Extension (KFE) NEO actuator, hence reducing the need of an extra transmission, ii) the rope transmission has been replaced by a belt transmission (assumed to have a mechanical advantage of 1.25) as the performance of the former cannot be guaranteed upon further research, and lastly iii) the gearing for AFE has been decoupled; the gearbox of the NEO actuator was placed at the joint itself after the belt transmission in order to reduce the torque transmission requirement of the belt,

[1]Product link: https://www.anybotics.com/anymal-legged-robot/
[2]Product link: https://www.halodi.com/ever3

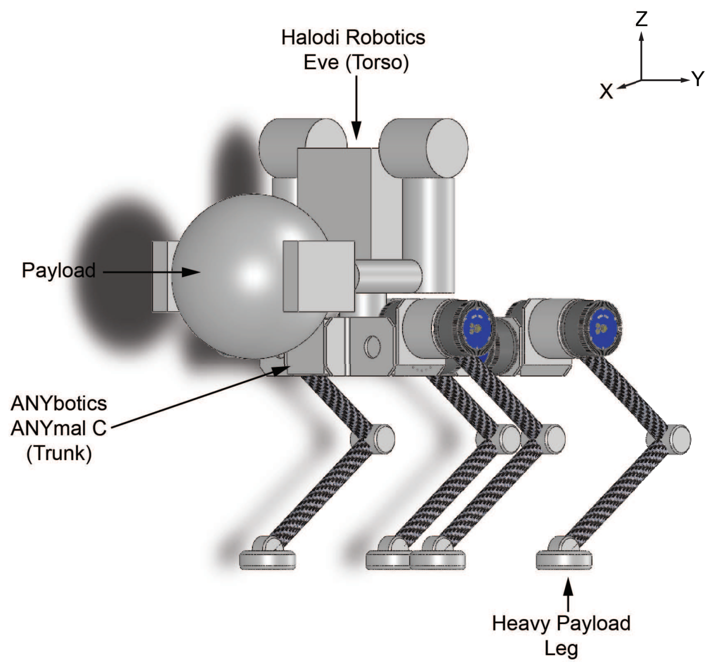


Figure 4.1: The envisioned heavy payload robot.

as well as to enable the amplification of the static torque provided by the permanent magnet brake. The leg was expected to have a total mass of approximately $18.8kg$, where $> 70\%$ of it was made up of active components. The nominal hip height of the leg was set at $0.6m$. This consequently led to the link lengths shown in Table 4.1 below:

| **Link** | **Length** $[m]$ |
|---|---|
| Thigh | 0.05 |
| Shank | 0.5 |
| Foot | 0.5 |
| Phalanges | 0.05 |

Table 4.1: Initial link lengths of the heavy payload leg.

With these, the heavy payload robot (with its maximum payload) was expected to have a total mass of $137.4kg$. This was concerning as it suggested that the loadings on the heavy payload leg would be very significant. Hence, it was clear that mass reduction was one of the priorities of this design framework.

The updated design concept of the heavy payload leg served as an initial design guess of what the heavy payload leg might eventually be. Nonetheless, it was expected that the leg design parameters would change as the framework uncovered more design intricacies that facilitate the performance of the leg. The following section details the analysis and optimization of this heavy payload leg.

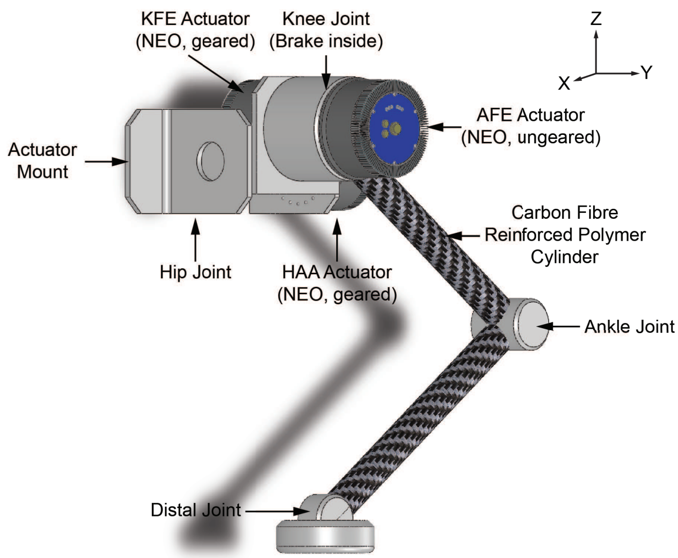


Figure 4.2: Updated heavy payload leg.

## 4.2 Analysis and Optimization

The heavy payload robot was analyzed first statically, and then dynamically. The insights from the analyses were used to guide the optimization of its leg design parameters. The following subsections detail how these were being carried out.

### 4.2.1 Static Analysis

The design parameters from the previous section were used to generate a mathematical model of the heavy payload robot. This model was then analyzed statically on the sagittal (XZ) plane. Here, the range of achievable hip heights, as well as the reachability of its arms, were studied. Additionally, the static joint torque required to hold different hip heights were also calculated. In this portion of the analysis, it was assumed that AFE solely provides the required torque. Hence, due to asymmetry, the joint torques required in the forelegs were more significant than that of the hindlegs. This hinted that it was possible to use smaller and lighter brakes in the hindlegs, which may result in a much needed mass reduction of $0.6kg$ per leg. Overall, this portion of the analysis showed that the initial design guess of the heavy payload while was feasible (joint torques required were below actuator limits), left much room for improvement.

### 4.2.2 Dynamic Analysis

Four potential tasks that the heavy payload robot might be subjected to were identified. Figures 4.3a-d illustrate these robot-level tasks, namely, pushing up from a crouched position, walking on flat ground, rotating on the spot, and climbing a flight of stairs. Out of these tasks, walking on flat ground was assessed to be the most likely worst-case scenario that the robot will face. Additionally, if the push up was done very slowly (quasi-statically), the joint torques required should be identical to those reflected in Section 4.2.1. Hence, half of these tasks has been technically accounted for.

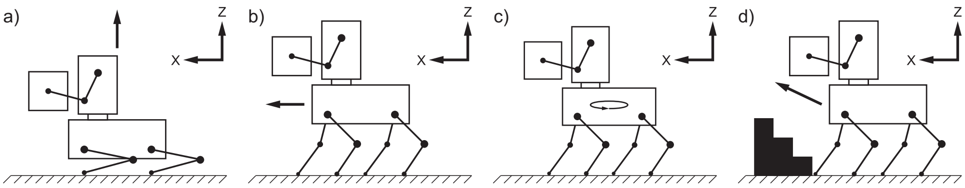


Figure 4.3: Four potential tasks of the heavy payload robot. a) Push up from a crouched position. b) Walking on flat ground. c) Rotating on the spot. d) Climbing a flight of stairs.

With this in mind, the design parameters of the heavy payload robot from Section 4.1 was used to generate a robot model in the Robot Operating System (ROS) environment. Using the Trajectory Optimizer for Walking Robots (TOWR) package[3] [49], this robot model was tasked to walk a distance of $1.5m$ in $12s$, which resulted in an average velocity of $\dot{x} = 0.153ms^{-1}$. The obtained robot trajectory is optimal in the sense that it did not violate any of the default constraints in TOWR. While this trajectory was far from the initial target of $\dot{x} = 1ms^{-1}$, it was a safe and feasible one; analysis showed that the initial target was both too ambitious (joint torques required were beyond the capability of the NEO actuators) and potentially dangerous (a $\approx 140kg$ robot walking at that speed is undoubtedly a safety hazard). This robot-level task was subsequently translated into leg-level tasks using Vitruvio[4]. The MATLAB toolbox has an extensive list of capabilities, one of which being the ability to generate the associated joint-level metrics, given the models of the robot and its leg, as well as its TOWR trajectory. Hence, the design parameters from Section 4.1 were being used to generate the respective robot and leg models[5] The analysis showed that while the leg-level tasks were feasible for the legs (the power, joint torques and joint velocity requirements were below the actuator limits), the resulting joint torques required were still very high (maximum joint torque, $\approx 250Nm$). Hence, it was decided that joint torques should be minimized.

### 4.2.3 Link Length Optimization

The other capability of Vitruvio is the ability to optimize the design parameters of the leg model. It uses the genetic algorithm of the MATLAB Optimization Toolbox[6] as its optimization method, and the MATLAB Parallel Computing Toolbox[7] to speed up its calculations. This stochastic optimization method searches for the optimal design parameters in a way that is similar to natural selection. The design parameters that were being optimized in this case were the thigh, shank, and foot lengths of the heavy payload legs. A composite penalty function guided the optimization. It is made up of a particular component that needs to be minimized and binary checks. The latter only penalize potential leg designs should they fail to meet specific requirements. These include: i) a low tracking error while tracking the end effector (foot) trajectory, ii) a maximum extension of $< 90\%$ of the total leg length, and finally, iii) a spider configuration with a forward-facing distal joint. The settings used in the optimization, unless otherwise stated, are as shown in the

[3] Github link: https://github.com/ethz-adrl/towr

[4] Bitbucket link: https://bitbucket.org/leggedrobotics/vitruvio/src/master/

[5] Vitruvio is only able to account for leg designs with point feet. Hence, assumptions were made for the selected heavy payload leg design concept. It was assumed that the geometric phalanges (foot) were always ground-facing, and the force that it applies was always through its center. Thus, rendering the geometric phalanges as a point foot.

[6] Toolbox link: https://www.mathworks.com/products/optimization.html

[7] Toolbox link: https://www.mathworks.com/products/parallel-computing.html

Table 4.2[8]. The link lengths obtained through this optimization were deemed to be optimal (in a local sense) and were synonymous with being high performing. Their performance was also compared and normalized to the initial design guess.

| **Setting** | **Value** |
|---|---|
| Generations | 5 |
| Population | 250 |
| Range of possible thigh lengths $[m]$ | [0.005,0.1] |
| Range of possible shank lengths $[m]$ | [0.4,0.6] |
| Range of possible foot lengths $[m]$ | [0.4,0.6] |

Table 4.2: Standardized optimization settings.

The following subsubsection describes how the optimal link lengths for torque minimization were being obtained.

### Total Joint Torque Minimization

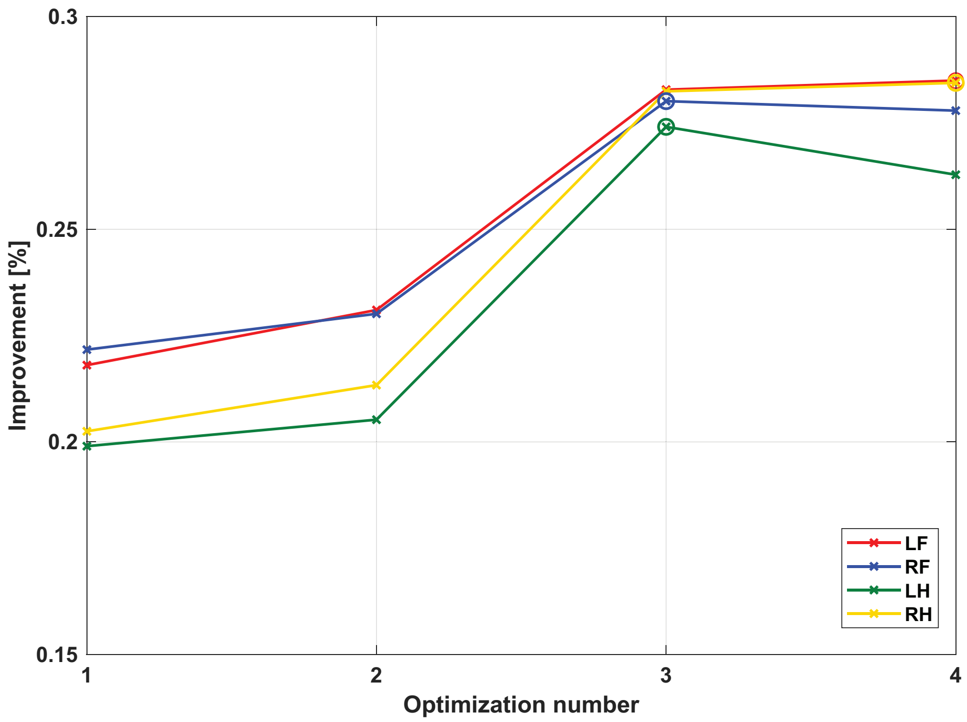


Figure 4.4: Improvement in total joint torque (reduction) by optimized link lengths after each round of optimization. The red, blue, green, and yellow lines represent the improvements recorded for LF, RF, LH, RH, respectively. A circled result indicates the particular set of optimized link lengths which gave rise to the largest improvement for that leg.

[8]It was realized that these generation and population settings were sufficient in obtaining a first insight about the optimization.

As mentioned in Section 4.2.2, it was desired that the joint torques of the walking task be minimized. Hence, the following component: $\sum_{j=1}^{j=3}\sum_{i=1}^{i=T}|\tau_{ji}|$, where $\tau$ is the joint torque, $i$ is the time index, $j$ is the joint index, and $T$ is the average period of a single gait cycle, was incorporated into the penalty function. Regarding the joint index, joint 1 refers to HAA, joint 2 refers to KFE, and joint 3 refers to AFE. This convention was abided for the various rounds of optimization, and the corresponding results are visualized in Fig. 4.4.

The first round of optimization was carried out at default settings, and it led to feasible link lengths which reduce the total joint torque by an average of $\approx 21.0\%$ across the legs. With this promising result, the optimization was reran, but this time the number of generations was increased to 25. This was done in a bid to find link lengths that can further reduce the total joint torque.

The second round of optimization did lead to better results with an average reduction in total joint torque of $\approx 22.0\%$. However, the optimal shank and foot lengths were hitting the lower bounds of possible link lengths. This suggested that in order to achieve better performance, the lower bound of the range of possible lengths for these links should be extended. Additionally, in a bid to further reduce design complexity, it could be worthwhile to check if a conventional serial leg will lead to similar results. Hence, the optimization was carried out once more at the default settings, with the thigh length set at $0.0005m$ (negligible) and the range of possible link lengths of the shank and foot set at $[0.3, 0.6]m$.

The third round of optimization resulted in even better improvements. On average, total joint torque was reduced by $\approx 28.0\%$. These results confirmed that the conventional serial leg configuration was feasible. Hence, like before, the optimization was reran with the number of generations increased to 25.

The fourth round of optimization led to better performance only for the Left Foreleg (LF) and the Right Hindleg (RH), and not for the Right Foreleg (RF) and Left Hindleg (LH). This result highlights the stochastic nature of the optimizer, where the amount of computing time is not necessarily proportional to the optimality of the results. Combining the results from the third and fourth rounds of optimization, the optimal link lengths which minimize total joint torque are summarized in Table 4.3 below. Do note that the naming convention of the leg used here is that of a conventional serial leg. One interesting observation regarding these parameters was that the ones for LF, RF were different from the ones for LH, RH. This is likely due to the asymmetry present in the heavy payload robot.

| **Leg** | **Thigh length** $[m]$ | **Shank length** $[m]$ | **Foot length** $[m]$ | **Improvement** $[\%]$ |
|---|---|---|---|---|
| Initial | 0.05 | 0.5000 | 0.5000 | - |
| LF | 0.0005 | 0.4772 | 0.3000 | $\approx 28.4$ |
| RF | 0.0005 | 0.4803 | 0.3000 | $\approx 28.0$ |
| LH | 0.0005 | 0.4560 | 0.3000 | $\approx 27.4$ |
| RH | 0.0005 | 0.4460 | 0.3016 | $\approx 28.4$ |

Table 4.3: Initial and optimal link lengths of the heavy payload leg for total joint torque minimization.

While the minimization of total joint torque was the main priority, other optimality criteria (components to be minimized) were also studied. The following subsubsection briefly summarizes the findings.

### Other Optimality Criteria

The following pointers describe the different optimality criteria being explored. The set of binary checks were still included, and the optimization settings used for these criteria are that of the default ones. This was because only first insights regarding the various optimality criteria were needed. Hence, the corresponding results which are visualized in Fig. 4.5 are only valid for this setup. The optimization procedure and the insights gained are also detailed in the text below.

| Penalty Function Component | LF, RF | Average Improvement [%] | LH, RH | Average Improvement [%] |
|---|---|---|---|---|
| Initial |  | - |  | - |
| Criterion 1 | 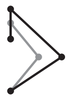 | ≈ 15.8 | 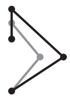 | ≈ 14.8 |
| Criterion 2 |  | ≈ 3.7 |  | ≈ 9.2 |
| Criterion 3 |  | ≈ 12.7 |  | ≈ 20.4 |
| Criterion 4 | 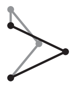 | ≈ 14.0 | 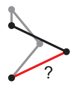 | ≈ 18.7 |
| Criteria 5 |  | ≈ 3.4 |  | ≈ 7.1 |
| Criteria 6 |  | ≈ 2.1 |  | ≈ 3.3 |
| Criteria 7 |  | ≈ 2.0 |  | ≈ 2.7 |

Figure 4.5: A graphical representation of the optimization results when different penalty function components were used. The referred criterion or criteria used are explained in greater detail in the text below. The results of LF, RF, and LH, RH are combined together as a left-right symmetry is generally observed in the results. A leg schematic in black represents the one referred in the first column, while a grey leg schematic represents the initial design guess as a basis for comparison. The red links indicate that the results were conflicting and hence, were inconclusive.

- Criterion 1 — Total Joint Velocity Minimization:
  - Component: $\sum_{j=1}^{j=3}\sum_{i=1}^{i=T}|\omega_{ij}|$, where $\omega$ is the joint velocity.
  - Results: i) Average improvement $\approx 15.3\%$, and ii) LF, RF, LH, RH: the thighs, shanks, and feet were maximized.
  - Insights: The optimal link lengths while were intuitive, were also infeasible as the resulting torques are over the actuator limits.
- Criterion 2 — Total Joint Mechanical Energy Minimization:
  - Component: If $\tau_{ij}\omega_{ji} < 0, \tau_{ji}\omega_{ji} := 0$ (no regeneration by actuators), else $\sum_{j=1}^{j=3}\sum_{i=1}^{i=T}\tau_{ji}\omega_{ji}$.
  - Results: i) Average improvement $\approx 6.4\%$, and ii) LF, RF: the thighs were minimized, the shanks were maximized, and the feet were shortened; LH, RH: the thighs and feet were minimized, while the shanks were maximized.
  - Insights: i) The optimal link lengths were feasible, and ii) total mechanical energy was reduced more in LH, RH than in LF, RF which is likely due to the asymmetry of the heavy payload robot.
- Criterion 3 — Power Quality Maximization:
  - Component: $\left(\left(\sum_{j=1}^{j=3}\sum_{i=1}^{i=T}\tau_{ji}\omega_{ji}\right)^2 - \left(\sum_{j=1}^{j=3}\sum_{i=1}^{i=T}(\tau_{ji}\omega_{ji})^2\right)\right)^{-1}$.
    - This component which is called power quality measures the extent to which the actuators were providing powers of the same sign while tracking the trajectories [13].
    - The component was inversed as it was to be maximized.
  - Results: i) Average improvement $\approx 16.5\%$, and ii) LF, RF, LH, RH: the thighs were maximized, the shanks were minimized, and the feet were shortened.
  - Insights: i) The optimal link lengths were feasible, and ii) power quality was improved more in LH, RH than in LF, RF which is likely due to the asymmetry of the heavy payload robot.
- Criterion 4 — Deviation of Condition Number from Unity Minimization:
  - Component: $\sum_{i=1}^{i=T}|\frac{\sigma_{i,min}}{\sigma i,max} - 1|$, where $\sigma$ is the singular value of matrix product of the jacobian at time index $i$, $J_iJ_i^T$.
    - $\frac{\sigma_{i,min}}{\sigma i,max}$ is called the condition number and relates to the shape of the manipulability ellipsoid of the leg.
    - It was desired that the leg should be able to move as easily as how it applies forces; condition number should be as close to 1 [50].
  - Results: i) Average improvement $\approx 16.4\%$, and ii) LF, RF: the thighs were minimized, the shanks and feet were maximized; LH, RH: the thighs were minimized, the shanks were maximized, and the feet were inconclusive.
  - Insights: i) The optimal link lengths were feasible, and ii) a greater improvement was observed in LH, RH than in LF, RF which is likely due to the asymmetry of the heavy payload robot.

- Criteria 5 — Total Joint Torque, Total Joint Velocity and Total Joint Mechanical Energy Minimization (Equal Component Weights):
  - Components: As above with equal weights.
  - Results: i) Average improvement $\approx 5.2\%$, and ii) LF, RF: the thighs were lengthened, the shanks maximized, and the feet were minimized; LH, RH: the thighs and shanks were maximized, and the feet were minimized.
  - Insights: i) The optimal link lengths were feasible, and ii) a greater improvement was observed in LH, RH than in LF, RF which is likely due to the asymmetry of the heavy payload robot.
- Criteria 6 — Total Joint Torque, Total Joint Velocity, Total Joint Mechanical Energy, Deviation of Condition Number from Unity Minimization and Power Quality Maximization (Equal Component Weights):
  - Components: As above with equal weights.
  - Results: i) Average improvement $\approx 2.7\%$, and ii) LF, RF, LH, RH: the thighs were minimized, the shanks were maximized, and the feet were shortened.
  - Insights: i) The optimal link lengths were feasible, and ii) a greater improvement was observed in LH, RH than in LF, RF which is likely due to the asymmetry of the heavy payload robot.
- Criteria 7 — Total Joint Torque, Total Joint Velocity, Total Joint Mechanical Energy, Deviation of Condition Number from Unity Minimization and Power Quality Maximization (Equal Category Weights):
  - Components: As above with the first three categorized as quantity-related ones, and the last two categorized as quality-related ones.
  - Results: i) Average improvement $\approx 2.4\%$, and ii) LF, RF: the thighs were inconclusive, the shanks maximized, and the feet were shortened; LH, RH: the thighs were minimized, the shanks were maximized, and the feet were shortened.
  - Insights: i) The optimal link lengths were feasible, and ii) a greater improvement was observed in LH, RH than in LF, RF which is likely due to the asymmetry of the heavy payload robot.

Thus far, it can be observed that the design framework can account for the projected tasks of the leg into its design. Not only can it verify if the current design is feasible for completing a task, but it can also optimize it according to a single or a set of complex objectives. While some optimization results may seem trivial and can be derived using intuition (e.g. total joint velocity minimization), the design framework has its advantages in more counter-intuitive cases (e.g. binary checks, total mechanical energy minimization, multi-components). Here, the computational approach finds the optimal design parameters with ease. However, the challenge then is to ensure that the task trajectory and penalty function are set up correctly. This is certainly not a simple task and comes with its own set of complexities (e.g. weighing the different components of a multi-objective optimization problem). The onus is then on the designer to ensure that the steps undertaken are reasonable and best represents the design problem. Nonetheless, accounting for the projected tasks in the leg design will undoubtedly lead to better performance as compared to a design that is naively designed (arbitrary link lengths which are typically equal). These also highlight once again the cornerstone of any design problem, that form is closely tied to function.

The following section details the process of how the optimal link lengths were engineered to make them fit for the final design of the heavy payload leg.

## 4.3 Engineering and Verification

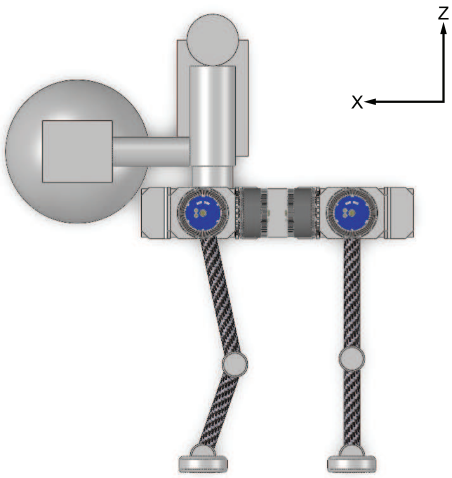


Figure 4.6: Heavy payload robot with optimal links at maximum hip height. The unequal total lengths of each leg result in unnecessary joint torques to be incurred at this hip height (bent knee joint).

The heavy payload leg design concept was updated using the optimal link lengths. The link lengths of the forelegs and hindlegs were averaged between their left and right ones since there was a left-right symmetry present. Additionally, smaller permanent magnet brakes were used for the hindlegs. This resulted in a total mass of 18.8$kg$ for a foreleg and 18.2$kg$ for a hindleg. The update legs were subsequently propagated into the robot-level. With the new legs, the heavy payload robot was expected to have a total mass of 136.2$kg$.
The updated design concepts were then analyzed statically. The following were the problems that arose early in the analysis: i) the range of possible hip heights have been substantially reduced due to the unequal thigh and shank lengths; $[0.42, 0.80]m$ instead of $[0.13, 1.00]m$ previously, ii) the unequal total length of the forelegs and hindlegs led to unnecessary joint torques at maximum hip height as shown in Fig. 4.6, and iii) the thighs were yet to be correctly sized for the belt transmission. It was clear from the above that the optimal link lengths left much room for improvement in terms of realizability. Hence, some engineering had to be done.
The optimal link lengths were engineered by first setting the total length of the thigh and shank to the larger one of the two legs (0.8$m$). This was done to ensure that the legs were still able to track their respective walking trajectories without any overextension. The thighs of each leg were then sized to the nearest available belt length of Misumi Super High Torque Timing Belts MTS8M line[9]. The shank lengths then followed suit. The following table summarizes the engineered link lengths of the various legs:
The design concepts were updated with these engineered link lengths, and the static analysis was performed again. The range of possible hip height was improved to $[0.42, 0.85]m$, and the static joint torques at these hip heights were feasible. Therefore, the engineered leg design was found to be statically feasible (maximum joint torque $\approx 160Nm < 283Nm$). With this, it was then analyzed dynamically in Vitruvio, which led to interesting results. While the engineered link lengths were not able to reduce total joint torque as well as the optimized ones (an average improvement of 24.5% as compared to 28.1%), they were found to consume less additional

[9]Product link: https://uk.misumi-ec.com/vona2/detail/110300414340/

| **Legs** | **Thigh lengths** $[m]$ | **Shank lengths** $[m]$ | **Improvement** [%] |
|---|---|---|---|
| LF, RF | 0.484 | 0.316 | $\approx 27.7$ |
| LH, RH | 0.452 | 0.348 | $\approx 21.4$ |

Table 4.4: Engineered link lengths of the heavy payload leg for total joint torque minimization.

mechanical energy per gait cycle than them (2.3% as compared to 3.9%). This was likely due to the engineered link lengths not being as short as the optimized ones. Hence, it did not lead to a substantial increase in joint velocity and, consequently, mechanical energy consumed.

Having verified that the engineered link lengths were both feasible and able to reduce the total joint torque during walking significantly, they were ready to be integrated into the heavy payload leg design concept properly. The following chapter details the final design of the high-performance heavy payload leg.

# Chapter 5

# Final Design

This chapter begins with an overview of the final design of the high-performance heavy payload leg. A Finite Element Method (FEM) analysis that was performed on several critical parts will be detailed. An evaluation of how well the final design matches up with the technical requirements set concludes the chapter.

## 5.1 Design Overview

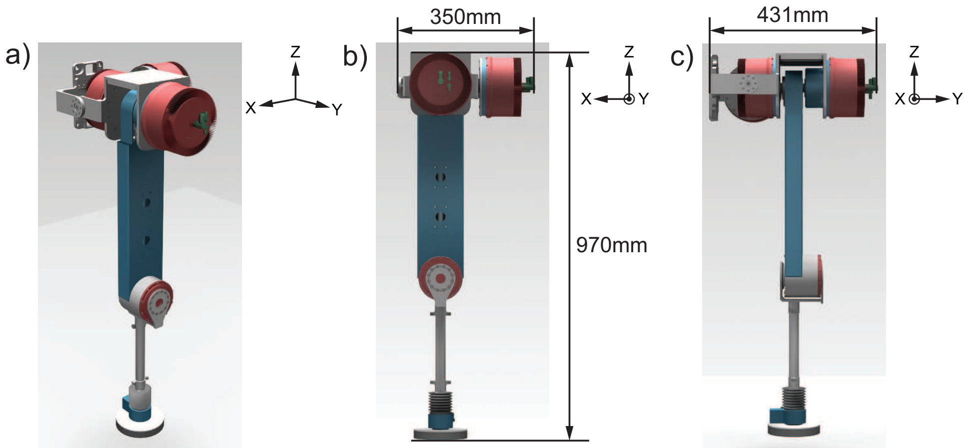


Figure 5.1: Various views of the high-performance heavy payload leg. a) Trimetric view. b) Front view. c) Side view.

Figure 5.1 presents the final design of the heavy payload leg. The leg is designed to be a serial LF leg which has 3 DoFs. The high torque NEO actuators actuate these DoFs. The leg has most of its mass concentrated at its top so that the portion that is frequently actuated (the parts which undergo flexion and extension) is lightweight and has low inertia. The technical specifications of the leg are listed in Table 5.1, and its mass distribution is illustrated in Fig. 5.2. Do note that the maximum payload was calculated by having the leg at the minimum hip height ($0.42m$) and both the HFE and KFE NEO actuators outputting maximum joint torque.
The following paragraphs detail the design. Table 5.2 shows the color code used in this Computer-Aided Design (CAD) model.
Figure 5.3 shows the HAA subassembly of the heavy payload leg. The leg is designed to be mounted onto a vertical leg rail for testing. It interfaces with the rail through

| **Specification** | **Value** |
|---|---|
| Mass $[kg]$ | 24.1 |
| Proportion of active elements [%] | 76 |
| Leg inertia $[kgm^2]$ | 1.86, 1.41, 0.950, 0.00235, 0.00233 (HAA, HFE, KFE, AAA, AFE) |
| Maximum joint torques $[Nm]$ | 230, 230, 283 (HAA, HFE, KFE) |
| Maximum joint velocities $[rads^{-1}]$ | 18.8, 18.8, 15.3 (HAA, HFE, KFE) |
| RoM [°] | [-95,95], [-95,95], [-95,95], [-90,90], [-90,90] (HAA, HFE, KFE, AAA, AFE) |
| Maximum payload $[kg]$ | 166 |

Table 5.1: Specifications of the high-performance heavy payload leg.

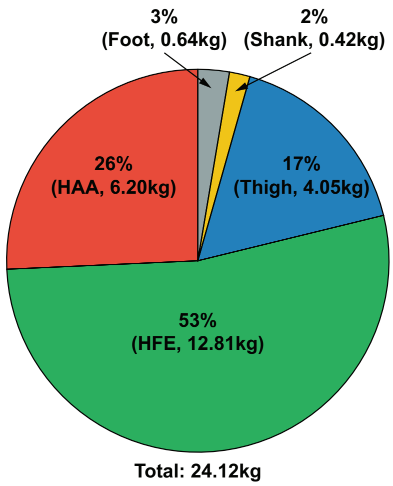


Figure 5.2: Mass distribution of the high-performance heavy payload leg.

an aluminum alloy part that simulates the trunk of the heavy payload robot. The NEO actuator responsible for HAA actuation is mounted onto one end of this trunk plate, while a radial ball bearing is mounted onto the other end. The sole purpose of this ball bearing is to share the loadings borne by the leg. The NEO actuator actuates the rest of the leg through a stainless steel flange that has a mounting plate at the other end.
Figure 5.4 shows the HFE subassembly of the heavy payload leg. It consists of two aluminum alloy mounting parts connected via a horizontal aluminum alloy plate. The NEO actuators responsible for the HFE and KFE actuation are mounted here. A Kendrion 86 61109K00 high torque permanent magnet brake [1] which provides the static torque in KFE to hold a configuration, is also mounted here. The minimum static torque that this brake can provide is $31Nm$, which is approximately the same as the ungeared KFE NEO actuator. Hence, it can statically output the same torques as the NEO actuator at the knee joint. A 3D-printed nylon cover surrounds the brake to provide some protection from the environment. This subassembly

[1] Product link: https://www.kendrion.com/industrial/ids/en/products/permanent-magnet-brakes/permanent-magnet-brake-high-torque.html

| Color | Category/material |
|---|---|
| Red | Actuation |
| Green | Electronics |
| Light blue | Foam |
| Blue | 3D-printed nylon |
| Yellow | Dampening foam |
| Light grey | Aluminum alloy |
| Grey | Titanium alloy |
| Dark grey | Stainless steel |
| Black | Rubber |

Table 5.2: Color code used in the CAD model.

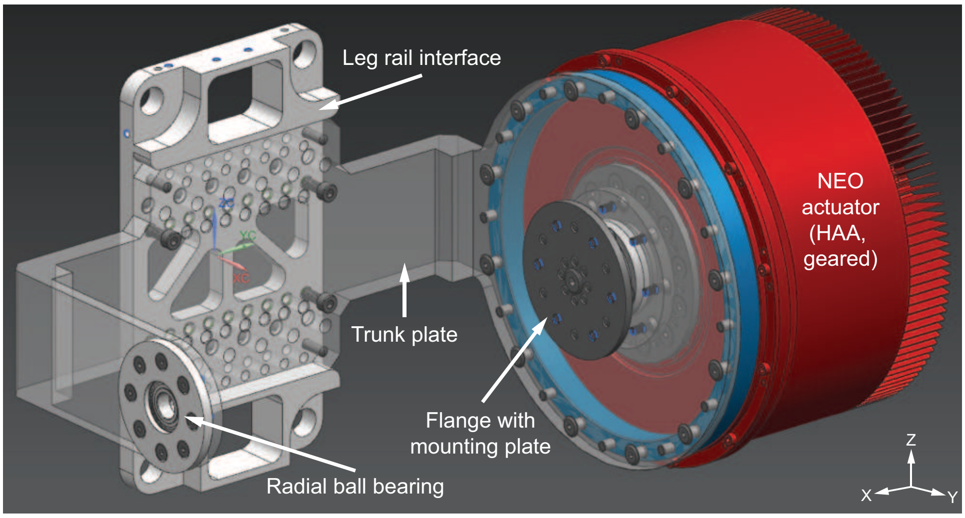


Figure 5.3: HAA subassembly of the high-performance heavy payload leg.

is actuated in the HAA direction by the mentioned mounting plate while being supported by another stainless steel flange. HFE and KFE actuation, on the other hand, are coaxial. The NEO actuator responsible for HFE actuates an aluminum alloy pitchfork piece that holds the thigh. The NEO actuator responsible for KFE actuates a stainless steel flange that runs through the permanent magnet brake, and eventually connects with the pulley of the belt transmission. The belt transmission which is of the mentioned Misumi Super High Torque Timing Belts MTS8M line was sized to a design power $P_d$ of $1.44kW$. This power was assumed to be the worst-case scenario for the belt transmission, and was formulated using the following equation:

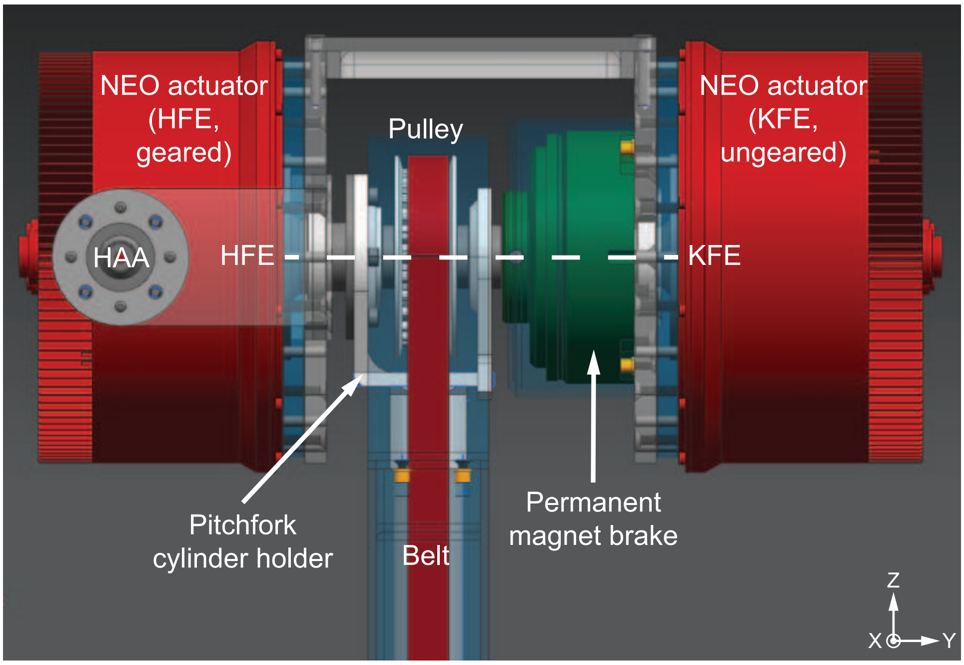


Figure 5.4: HFE subassembly of the high-performance heavy payload leg.

$$
\begin{aligned}
P_d = & \; 34.8 \text{ (Maximum torque of ungeared NEO motor)} \\
& * 5 \text{ (Maximum KFE joint velocity recorded)} \\
& * 6.6 \text{ (Gearing ratio of NEO planetary gearbox)} \\
& * 1.25 \text{ (Mechanical advantage of belt transmission)} \\
& * 1.25 \text{ (Safety factor)} \\
& \approx 1.44kW
\end{aligned}
$$

Figure 5.5a shows the thigh subassembly of the heavy payload leg. The thigh which is a titanium alloy cylinder, has a diameter of $25mm$ and a thickness of $1mm$. It was sized similar to a human femur as the leg is subjected to similar loads of a human leg of $\approx 30kg$ per leg. Similar to the permanent magnet brake, the belt transmission is protected from the environment by a 3D-printed nylon cover as it transmits torque from the hip joint to the knee joint.

Figure 5.5b shows the internals of the knee joint of the heavy payload leg. Here, the belt actuates a pulley which drives a flange. This flange is connected to the sun gear of the NEO planetary gearbox via dowel pins. Hence, the maximum KFE torque is given by the following equation:

$$
\begin{aligned}
\tau_{KFE,max} = & \; 34.8 \text{ (Maximum torque of ungeared NEO motor)} \\
& * 6.6 \text{ (Gearing ratio of NEO planetary gearbox)} \\
& * 1.23 \text{ (Mechanical advantage of belt transmission)} \\
& \approx 283Nm
\end{aligned}
$$

Figure 5.5c shows the aluminum alloy pitchfork cylinder holder that is connected to the shank of the heavy payload leg. The shank is identical to the thigh in terms of diameter and thickness. On one side of the shank, it is secured to the output

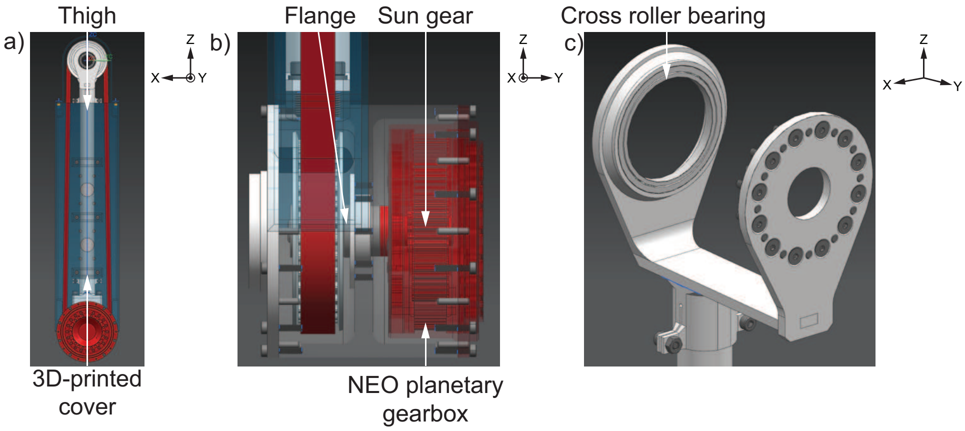


Figure 5.5: Thigh and knee joint subassembly of the high-performance heavy payload leg. a) Thigh. b) Internals of knee joint. c) Pitchfork cylinder holder which is connected to the knee joint.

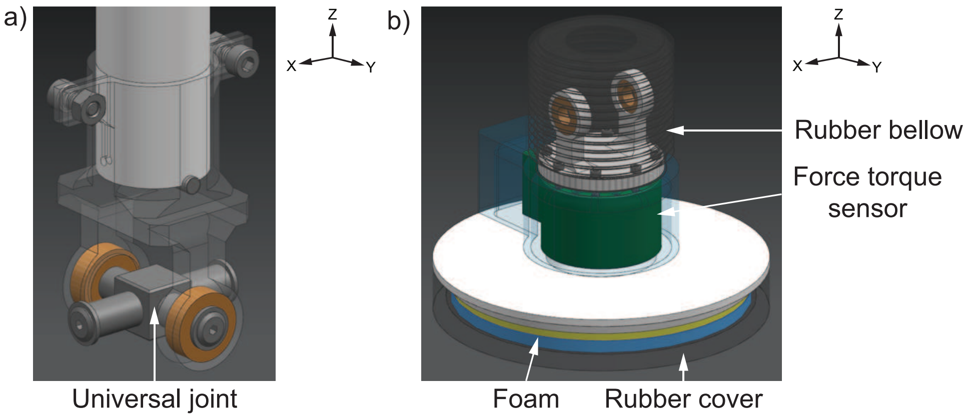


Figure 5.6: Ankle joint and foot subassembly of the high-performance heavy payload leg. a) Ankle joint. b) Foot.

of the NEO planetary gearbox via screws and dowel pins. On the other end, it is supported by a cross roller bearing that sits on the cover of the knee joint. The cross roller bearing was chosen as it was a slim and lightweight solution that could bear significant loads.

Figure 5.6a shows the other end of the shank, which is connected to a universal joint. This half of the universal joint is responsible for AFE.

Figure 5.6b shows the other half of the universal joint, which is responsible for AAA and is protected from the environment by a rubber bellow. It is connected to a BOTA Systems Rokubi EtherCAT force torque sensor[2] which measures the ground interaction forces needed for force control. This particular sensor was chosen as the maximum force that it can detect in the Z direction is well above the maximum force recorded in the analysis (1000N vs. 550N). A 3D-printed nylon cover is used to protect the sensor from the environment. The sensing end of the sensor is connected to an aluminum alloy plate which is sized similar to a human foot with an area of $\approx 100cm^2$ [51]. It is here where specialized dampening foam (Poron XRD[3]) and

[2]Product link: https://www.botasys.com/6-axis-force-torque-sensors
[3]Product link: http://www.xrd.tech/products/1/XRD-Technology.aspx

generic Shore 45C foam are attached to. These foam sheets protect the leg from impacts and are covered by rubber for traction.
In the following section, several critical parts were chosen and analyzed using FEM to deem the feasibility of their current design.

## 5.2 Finite Element Method Analysis

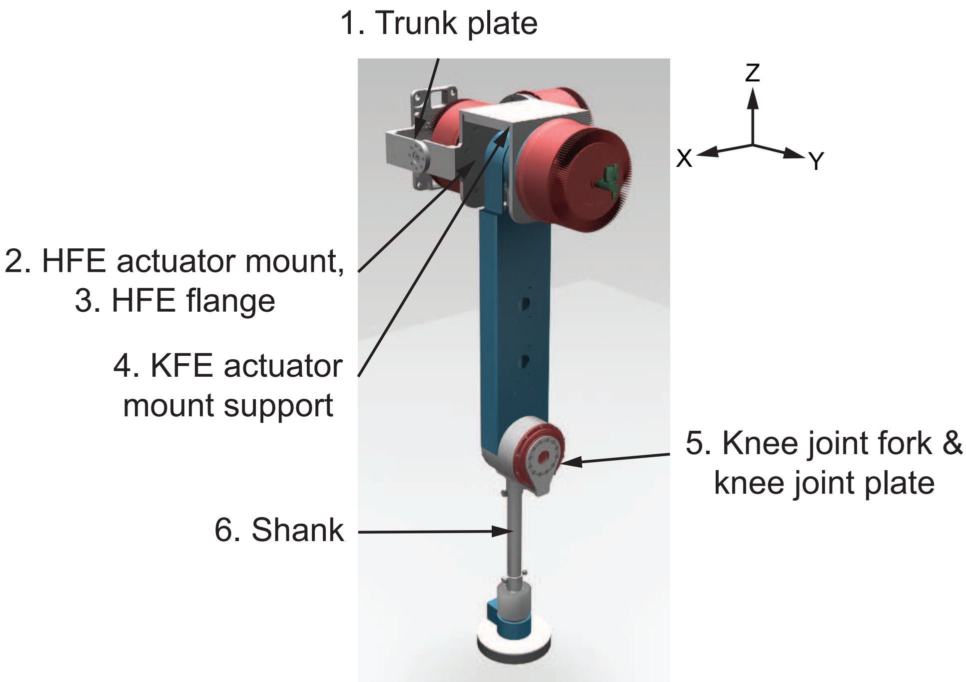


Figure 5.7: Location of parts analyzed using FEM.

Six parts of the heavy payload leg were identified for FEM analysis. Figure 5.7 shows the various locations of these parts. The parts were particularly chosen due to the high loadings (forces, torques) that they are projected to experience in a worst-case scenario manner. The conducted analysis is detailed in the following pointers while also being visualized in Fig. 5.8.

- Notes: i) All meshes were standardized to a size of $2.5mm$, ii) the maximum force applied by the leg in the simulation is recorded to be $550N$, iii) the peak torque of HAA, HFE and KFE are $[230, 230, 283]Nm$ respectively, and iv) all materials were assumed to be isotropic.
- Part 1 — Trunk plate:
  - This part was chosen as it was projected to experience high forces and torques.
  - Origin of forces or torques acting on parts:
    - Vertical forces applied by the leg: $550 * 1.25$ (safety factor) $\approx 700N$.
    - Peak torque of NEO actuator: $230Nm$.
  - Constraints:
    - Dowel pin and screw holes that interfaced with the vertical leg rail.

- Loads:
  - $700 \div 2 = 350N$ in the upward Z direction on the surfaces which interfaced with the bearings.
  - $230 \div (0.069 * 12) \approx 278N$ that were tangential in direction to the dowel pin holes. Forces act only on half of the surface area of each hole, and twelve dowel pins were used to anchor the NEO actuator in place.
- Findings:
  - There were stresses which were greater than the yield strength of aluminum alloy on the actuator side.
  - Generally low stresses everywhere else.
- Recommendations:
  - Reduce part thickness, while also making trusses on the bearing side to reduce weight.
  - Add additional supporting structures or material to the actuator side to reduce the stresses there.

- Part 2 — HFE actuator mount
  - This part was chosen as it was projected to experience high forces and torques.
  - Origin of forces or torques acting on parts:
    - Vertical forces applied by the leg: $700N$.
    - Peak torque of NEO actuator: $230Nm$.
  - Constraints:
    - Dowel pin and screw holes that interfaced with the flanges which interface with the trunk plate.
  - Loads:
    - $350N$ in the upward Z direction on the surfaces which interfaced with the bearing.
    - $350 \div 8 \approx 44N$ on each of the eight screw holes that were being pulled by the KFE actuator mount.
    - $278N$ that were tangential in direction to the dowel pin holes. Forces acted only on half of the surface area of each hole, and twelve dowel pins were used to anchor the NEO actuator in place.
  - Findings:
    - Generally low stresses everywhere.
  - Recommendations:
    - Reduce the thickness of the structure, while also making trusses to reduce weight.

- Part 3 — HFE flange
  - This part was chosen as it was projected to experience high torques.
  - Origin of forces or torques acting on parts:
    - Peak torque of NEO actuator: $230Nm$.
  - Constraints:
    - Fixed on the dowel pin holes at the end of the rotary shaft.

    - ∗ Cylinder constraint on the rotary shaft.
  - Loads:
    - ∗ $230 \div (0.03 * 10) \approx 767N$ that were tangential in direction to the dowel pin holes. Forces acted only on half of the surface area of each hole, and ten dowel pins were used to anchor the NEO actuator in place.
  - Findings:
    - ∗ Generally low stresses everywhere.
  - Recommendations:
    - ∗ Use aluminum alloy instead of stainless steel to reduce weight.
    - ∗ Reduce the number of holes in order to use fewer dowel pins and screws.

- Part 4 — KFE actuator mount support
  - This part was chosen as it was projected to experience high forces.
  - Origin of forces or torques acting on parts:
    - ∗ Vertical forces applied by the leg: $700N$.
  - Constraints:
    - ∗ Fixed on the surface that interfaced with the HFE actuator mount.
  - Loads:
    - ∗ $350N$ in the upward Z direction on the surfaces which interfaced with the KFE actuator mount.
  - Findings:
    - ∗ Generally low stresses everywhere.
  - Recommendations:
    - ∗ Reduce part thickness, remove supporting structure while also making trusses on the bearing side to reduce weight.

- Part 5 — Knee joint fork & knee joint plate
  - This part was chosen as it was projected to experience high torques.
  - Origin of forces or torques acting on parts:
    - ∗ Peak torque of NEO actuator with mechanical advantage from belt transmission: $230 * (32 \div 26)$ (mechanical advantage) $\approx 283Nm$.
  - Constraints:
    - ∗ Dowel pin and screw holes that interfaced with the NEO planetary gearbox.
    - ∗ Surface which interfaced with the cross roller bearing.
  - Loads:
    - ∗ $283 \div 0.035 \approx 8085N$ that acted tangentially on the inner surface of the titanium cylinder holder. Force acted only on half of the surface area.
  - Findings:
    - ∗ There were stresses which were greater than the yield strength of aluminum alloy on the cylinder side.
    - ∗ Generally low stresses everywhere else.

    - Recommendations:
        * Increase the moment arm where the torque acts on the titanium cylinder to reduce the forces and, subsequently, the stresses.
        * Add additional supporting material to the titanium cylinder holder to reduce stresses.

- Part 6 — Shank
    - This part was chosen as it was projected to experience high torques.
    - Origin of forces or torques acting on parts:
        * Peak torque of NEO actuator with mechanical advantage from belt transmission: $283Nm$.
    - Constraints:
        * End of the cylinder which interfaced with the other cylinder holder.
    - Loads:
        * $8085N$ that acted tangentially on the surface which interfaces with the titanium cylinder holder. Force acted only on half of the surface area.
    - Findings:
        * There were stresses which were greater than the yield strength of titanium grade 5 alloy on the constrained end of the cylinder.
    - Recommendations:
        * Increase the moment arm where the torque acts on the titanium cylinder to reduce the forces and, subsequently, the stresses.
        * Increase the thickness of the cylinder.

In summary, the structural components were oversized and could be trimmed down for mass reduction, while those that transmit forces or torques have to be reinforced as their current designs were inadequate. The following section evaluates the final design of the heavy payload based on the technical requirements that it was supposed to achieve.

## 5.3 Technical Requirements Evaluation

The final design of the heavy payload leg was evaluated against the technical requirements that it aimed to fulfill. The evaluation can be seen in Appendix B.9. The following pointers detail the key findings:

- Design requirements:
    - Most of these requirements were fulfilled. The ones that were not adequately satisfied relate to the mass and the link inertia of the heavy payload leg, and its level of ingress protection.
    - Regarding the former, updating the design with the recommendations from Section 5.2 should bring the mass of the leg down to the requirement. However, the link inertia requirement would still be challenging to achieve.
    - The latter can be realized when more information regarding the application of the heavy payload robot is obtained.

- Functional requirements:
  - These requirements were not fulfilled at all as it was realized that minimizing total joint torque for the walking task was the top priority. However, these may be easily achieved by rerunning the optimization portion with these represented in the penalty function and changing the link lengths of the heavy payload leg accordingly.
- Performance requirements:
  - These requirements, in general, can only be truly verified when the heavy payload leg is physically realized.
- Interface requirements:
  - These requirements were mostly satisfied as they were considered in the design of the heavy payload leg.

Nonetheless, the final design of the heavy payload leg is expected to be a high performing one. This is because the design intricacies that were revealed using the holistic design approach has been integrated into its design.
The thesis is concluded in the following chapter.

| Part | Loadings | Results |
|---|---|---|
| Trunk plate | 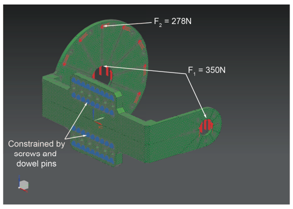 | 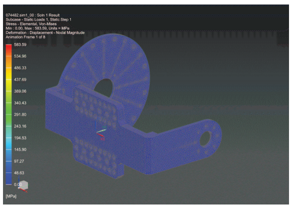 |
| HFE actuator mount | 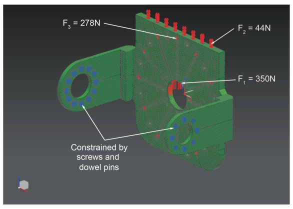 | 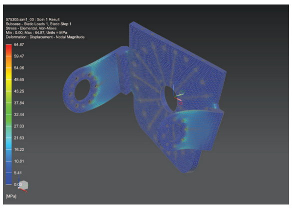 |
| HFE flange | 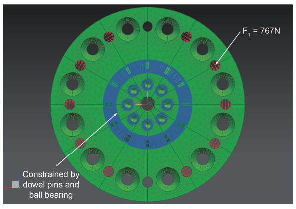 | 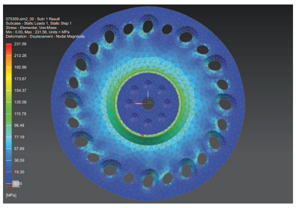 |
| KFE actuator mount | 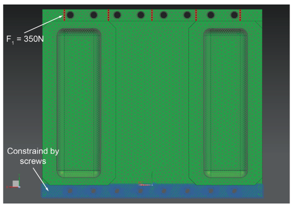 | 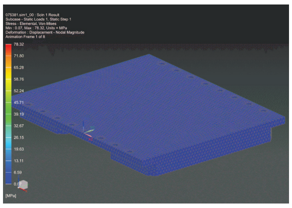 |
| Knee joint fork & knee joint plate | 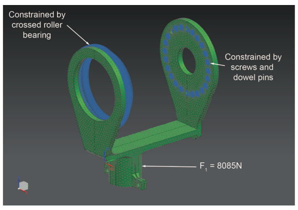 | 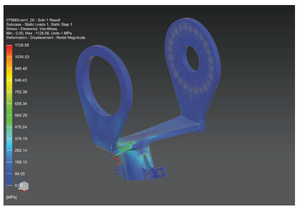 |
| Shank | 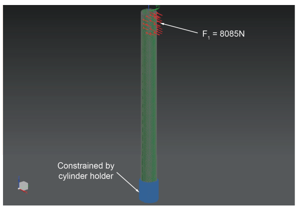 | 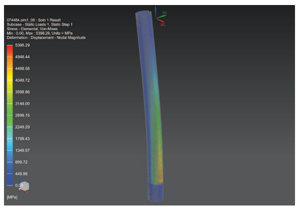 |

Figure 5.8: Summary of FEM Analysis.

# Chapter 6

# Conclusion

This master thesis sought to answer the question of what it meant to design a robotic leg holistically. Here, it aimed to develop a high-performance one for either a high-speed or a heavy payload robot. A literature review that spanned across nature and previous robotic works was first conducted. This was done to understand the different perspectives that nature and humans have on what a leg actually is. The insights gained from the study were then used to develop simple but practical design concepts. These concepts were then evaluated objectively based on their potential. Eventually, a heavy payload leg design concept was chosen to be further developed. By analyzing the projected tasks of the heavy payload robot and consequently the leg, the design parameters of the leg were optimized and engineered to increase their feasibility. Eventually, these cumulated into a final design of the heavy payload leg which has the potential to emit a high performance. In conclusion, the finalized design is indeed an embodiment of the key ideas explored, as well as a proof-of-concept of the proposed holistic design approach.
Future work involves the following:

- Optimizing the design further:
  - Trimming down the mass of the various structural parts, while strengthening those that are involved in transmitting the forces and torques.
  - Obtaining better performing design parameters by using more detailed and accurate models in simulation.
- Physically realizing the heavy payload leg and testing it

.
With the above, it is hoped that the heavy payload robot can be one day be realized.

# Bibliography


[1] D. J. Todd, *Walking Machines: An Introduction to Legged Robots.* Springer, 1985.

[2] C. D. Remy, M. Hutter, M. Hoepflinger, M. Bloesch, C. Gehring, and R. Siegwart, "Quadrupedal Robots with Stiff and Compliant Actuation," *Automatisierungstechnik*, vol. 60, no. 11, pp. 682–691, 2012.

[3] A. Abate and J. W. Hurst, "Oregon State's CASSIE Biped: Mechanical Design for Dynamic Locomotion," 2017.

[4] A. M. Abate, "Mechanical Design for Robot Locomotion," Ph.D. Thesis, Oregon State University, 2018.

[5] M. Hutter, C. Gehring, D. Jud, A. Lauber, D. Bellicoso, V. Tsounis, J. Hwangbo, K. Bodie, P. Fankhauser, M. Bloesch, R. Diethelm, S. Bachmann, A. Melzer, and M. Hoepflinger, "ANYmal - A Highly Mobile and Dynamic Quadrupedal Robot," in *IEEE/RSJ International Conference on Intelligent Robots and Systems*, 2016, pp. 38–44.

[6] S. Seok, A. Wang, M. Y. M. Chuah, D. J. Hyun, J. Lee, D. Otten, J. Lang, and S. Kim, "Design Principles for Energy Efficient Legged Locomotion and Implementation on the MIT Cheetah Robot," *IEEE/ASME Transactions on Mechatronics*, vol. 20, no. 3, pp. 1117–1129, 2015.

[7] P. M. Wensing, A. Wang, S. Seok, D. Otten, J. Lang, and S. Kim, "Proprioceptive Actuator Design in the MIT Cheetah: Impact Mitigation and High-Bandwidth Physical Interaction for Dynamic Legged Robots," *IEEE Transactions on Robotics*, vol. 33, no. 3, pp. 509–522, 2017.

[8] G. Bledt, M. J. Powell, B. Katz, J. Di Carlo, P. M. Wensing, and S. Kim, "MIT Cheetah 3: Design and Control of a Robust, Dynamic Quadruped Robot," in *IEEE/RSJ International Conference on Intelligent Robots and Systems*, 2018, pp. 2245–2252.

[9] B. G. Katz, "A low cost modular actuator for dynamic robots," Master Thesis, Massachusetts Institute of Technology, 2018.

[10] R. J. Full and D. E. Koditschek, "Templates and Anchors: Neuromechanical Hypotheses of Legged Locomotion on Land," *Journal of Experimental Biology*, vol. 202, pp. 3325–3332, 1999.

[11] N. Kashiri, A. Abate, S. J. Abram, A. Albu-Schaffer, P. J. Clary, M. Daley, S. Faraji, R. Furnemont, M. Garabini, H. Geyer, A. M. Grabowski, J. Hurst, J. Malzahn, G. Mathijssen, D. Remy, W. Roozing, M. Shahbazi, S. N. Simha, J.-B. Song, N. Smit-Anseeuw, S. Stramigioli, B. Vanderborght, Y. Yesilevskiy, and N. Tsagarakis, "An Overview on Principles for Energy Efficient Robot Locomotion," *Frontiers in Robotics and AI*, vol. 5, no. 129, pp. 1–13, 2018.

[12] J. Cho and K. Kong, “Realizing Natural Springy Motion of a Robotic Leg by Cancelling the Undesired Damping Factors,” in *IEEE International Conference on Robotics and Automation*, 2017, pp. 3062–3067.

[13] A. Abate, J. W. Hurst, and R. L. Hatton, “Mechanical Antagonism in Legged Robots,” in *Robotics: Science and Systems*, 2016.

[14] M. S. Fischer and K. Lilje, *Dogs in Motion.* VDH Service GmbH, 2011.

[15] H. Hasegawa, T. Yamauchi, and W. J. Kraemer, “Foot Strike Patterns of Runners at the 15-km Point during an Elite-level Half Marathon,” *Journal of Strength and Conditioning Research*, vol. 21, no. 3, pp. 888–893, 2007.

[16] C. L. Lewis, N. M. Laudicina, A. Khuu, and K. L. Loverro, “The Human Pelvis: Variation in Structure and Function During Gait,” *The Anatomical Record*, vol. 300, pp. 633–642, 2017.

[17] B. K. Ahlborn and R. W. Blake, “Walking and Running at Resonance,” *Zoology*, vol. 105, pp. 165–174, 2002.

[18] S. B. Williams, H. Tan, J. R. Usherwood, and A. M. Wilson, “Pitch then Power: Limitations to Acceleration in Quadrupeds,” *Biological Letters*, vol. 5, pp. 610–613, 2009.

[19] D. E. Lieberman, M. Venkadesan, W. A. Werbel, A. I. Daoud, S. D’Andrea, I. S. Davis, R. O. Mang’Eni, and Y. Pitsiladis, “Foot Strike Patterns and Collison Forces in Habitually Barefoot versus Shod Runners,” *Nature*, vol. 463, pp. 531–536, 2010.

[20] E. Muybrudge, “Animal Locomotion,” 1887.

[21] M. Stolpe, “Physiologisch-anatomische Untersuchungen über die hintere Extremität der Vögel,” *Journal für Ornithologie*, vol. 80, pp. 161–247, 1932.

[22] Y.-H. Chang and L. H. Ting, “Mechanical Evidence that Flamingos can Support their Body on One Leg with Little Active Musclar Force,” *Biology Letters*, vol. 13, pp. 1–5, 2017.

[23] G. E. Weissengruber, G. F. Egger, J. R. Hutchinson, H. B. Groenewald, L. Elsässer, D. Famini, and G. Forstenpointner, “The Structure of the Cushions in the Feet of African Elephants (Loxodonta Africana),” *Journal of Anatomy*, vol. 209, pp. 781–792, 2006.

[24] A. Abate, R. L. Hatton, and J. Hurst, “Passive-Dynamic Leg Design for Agile Robots,” in *IEEE International Conference on Robotics and Automation*, 2015, pp. 4519–4524.

[25] S. Rezazadeh, A. Abate, R. L. Hatton, and J. W. Hurst, “Robot Leg Design: A Constructive Framework,” *IEEE Access*, vol. 6, pp. 54 369–54 387, 2018.

[26] M. H. Raibert, H. B. J. Brown, and M. Chepponis, “Experiments in Balance with a 3D One-Legged Hopping Machine,” *The International Journal of Robotics Research*, vol. 3, no. 2, pp. 75–92, 1984.

[27] S. Hirose, Y. Fukuda, K. Yoneda, A. Nagakubo, H. Tsukagoshi, K. Arikawa, G. Endo, T. Doi, and R. Hodoshima, “Quadruped Walking Robots at Tokyo Institute of Technology,” *IEEE Robotics & Automation Magazine*, vol. 6, pp. 104–114, 2009.

[28] J.-W. Chung, I.-W. Park, and J.-H. Oh, "On the Design and Development of a Quadruped Robot Platform," *Advanced Robotics*, vol. 24, pp. 277–298, 2010.

[29] A. Spröwitz, A. Tuleu, M. Vespignani, M. Ajallooeian, E. Badri, and A. J. Ijspeert, "Towards Dynamic Trot Gait Locomotion: Design, Control, and Experiments with Cheetah-cub, a Compliant Quadruped Robot," *The International Journal of Robotics Research*, vol. 32, no. 8, pp. 932–950, 07 2013.

[30] J. W. Hurst, J. E. Chestnutt, and A. A. Rizzi, "An Actuator with Physically Variable Stiffness for Highly Dynamic Legged Locomotion," in *IEEE International Conference on Robotics and Automation*, 2004.

[31] J. Hwangbo, V. Tsounis, H. Kolvenbach, and M. Hutter, "Cable-Driven Actuation for Highly Dynamic Robotic Systems," in *IEEE/RSJ International Conference on Intelligent Robots and Systems*, 2018, pp. 8543–8550.

[32] G. A. Pratt and M. M. Williamson, "Series Elastic Actuators," in *IEEE/RSJ International Conference on Intelligent Robots and Systems*, 1995, pp. 399–406.

[33] R. Van Ham, T. G. Sugar, B. Vanderborght, K. W. Hollander, and D. Lefeber, "Compliant Actuator Designs," *IEEE Robotics & Automation Magazine*, vol. 16, no. 3, pp. 81–94, 2009.

[34] M. Grimmer, M. Eslamy, S. Gliech, and A. Seyfarth, "A Comparison of Parallel- and Series Elastic Elements in an Actuator for Mimicking Human Ankle Joint in Walking and Running," in *IEEE International Conference on Robotics and Automation*, 2012, pp. 2463–2470.

[35] T. Verstraten, P. Beckerle, R. Furnémont, G. Mathijssen, B. Vanderborght, and D. Lefeber, "Series and Parallel Elastic Actuation: Impact of Natural Dynamics on Power and Energy Consumption," *Mechanism and Machine Theory*, vol. 102, pp. 232–246, 2016.

[36] P. Beckerle, T. Verstraten, G. Mathijssen, R. Furnémont, B. Vanderborght, and D. Lefeber, "Series and Parallel Elastic Actuation: Influence of Operating Positions on Design and Control," *IEEE/ASME Transactions on Mechatronics*, vol. 22, no. 1, pp. 521–529, 2017.

[37] U. Mettin, P. X. La Hera, L. B. Freidovich, and A. S. Shiriaev, "Parallel Elastic Actuators as a Control Tool for Preplanned Trajectories of Underactuated Mechanical Systems," *The International Journal of Robotics Research*, vol. 29, no. 9, pp. 1186–1198, 2010.

[38] D. F. B. Haeufle, M. D. Taylor, S. Schmitt, and H. Geyer, "A Clutched Parallel Elastic Actuator Concept: Towards Energy Efficient Powered Legs in Prosthetics and Robotics," in *IEEE RAS/EMBS Interanational Conference on Biomedical Robotics and Biomechatronics*, 2012, pp. 1614–1619.

[39] C.-M. Chew, G.-S. Hong, and W. Zhou, "Series Damper Actuator: A Novel Force/Torque Control Actuator," in *IEEE/RAS International Conference on Humanoid Robots*, 2004, pp. 533–546.

[40] V. Chalvet and D. J. Braun, "Criterion for the Design of Low Power Variable Stiffness Mechanisms," *IEEE Transactions on Robotics*, vol. 33, no. 4, pp. 1002–1010, 2017.

[41] T.-H. Chong, V. Chalvet, and D. J. Braun, "Analytical Conditions for the Design of Variable Stiffness Mechanisms," in *IEEE International Conference on Robotics and Automation*, 2017, pp. 1241–1247.

[42] M. Plooij, G. Mathijssen, P. Cherelle, D. Lefeber, and B. Vanderborght, "Lock Your Robot: A Review of Locking Devices in Robotics," *IEEE Robotics & Automation Magazine*, vol. 22, no. 1, pp. 106–117, 2015.

[43] K. G. Gim, J. Kim, and K. Yamane, "Design of a Serial-Parallel Hybrid Leg for a Humanoid Robot," in *IEEE International Conference on Robotics and Automation*, 2018, pp. 6076–6081.

[44] M. Hutter, C. Holenstein, D. Fenner, C. D. Remy, M. A. Hoepflinger, and R. Siegwart, "Improved Efficiency in Legged Running Using Lightweight Passive Compliant Feet," in *International Conference on Climbing and Walking*, 2012, pp. 1–8.

[45] R. Käslin, H. Kolvenbach, L. Paez, L. Klajd, and M. Hutter, "Towards a Passive Adaptive Planar Foot with Ground Orientation and Contact Foot Sensing for Legged Robots," in *IEEE/RSJ International Conference on Intelligent Robots and Systems*, 2018, pp. 2707–2714.

[46] J. A. Blaya and H. Herr, "Adaptive Control of a Variable-Impedance Ankle-Foot Orthosis to Assist Drop-Foot Gait," *IEEE Transactions on Neural Systems and Rehabilitation Engineering*, vol. 12, no. 1, pp. 24–31, 2004.

[47] S.-A. Abad, N. Sornkarn, and T. Nanayakkara, "The Role of Morphological Computation of the Goat Hoof in Slip Reduction," in *IEEE/RSJ International Conference on Intelligent Robots and Systems*, 2016, pp. 5599–5605.

[48] A. Ananthanarayanan, M. Azadi, and S. Kim, "Towards a Bio-Inspired Leg Design for High-Speed Running," *Bioinspiration & Biomimetics*, vol. 7, pp. 1–12, 2012.

[49] A. W. Winkler, D. C. Bellicoso, M. Hutter, and J. Buchli, "Gait and Trajectory Optimization for Legged Systems through Phase-Based End-Effector Parameterization," *IEEE Robotics and Automation Letters*, vol. 3, pp. 1560–1567, 2018.

[50] M. Engardt, A. Heimbürger, and P. Sydhoff, "Manipulability Index Optimization for a Planar Robotic Arm," Bachelor Thesis, KTH Royal Institute of Technology, 2012.

[51] M. Birtane and H. Tuna, "The Evaluation of Plantar Pressure Distribution in Obese and Non-Obese Adults," *Clinical Biomechanics*, vol. 19, pp. 1055–1059, 2004.

# Appendix A

# Project Management Documents

## A.1 Gantt Chart

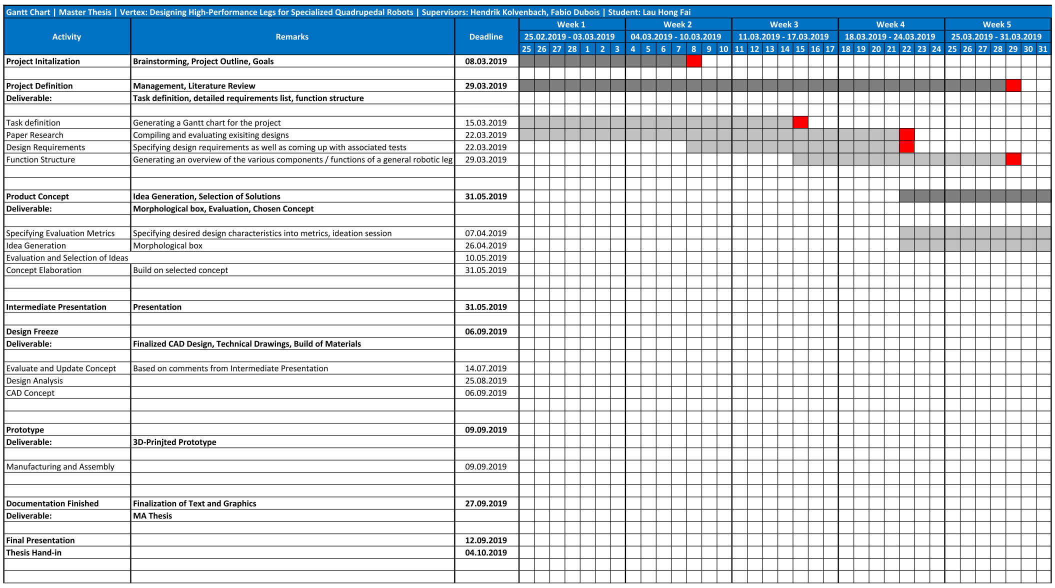


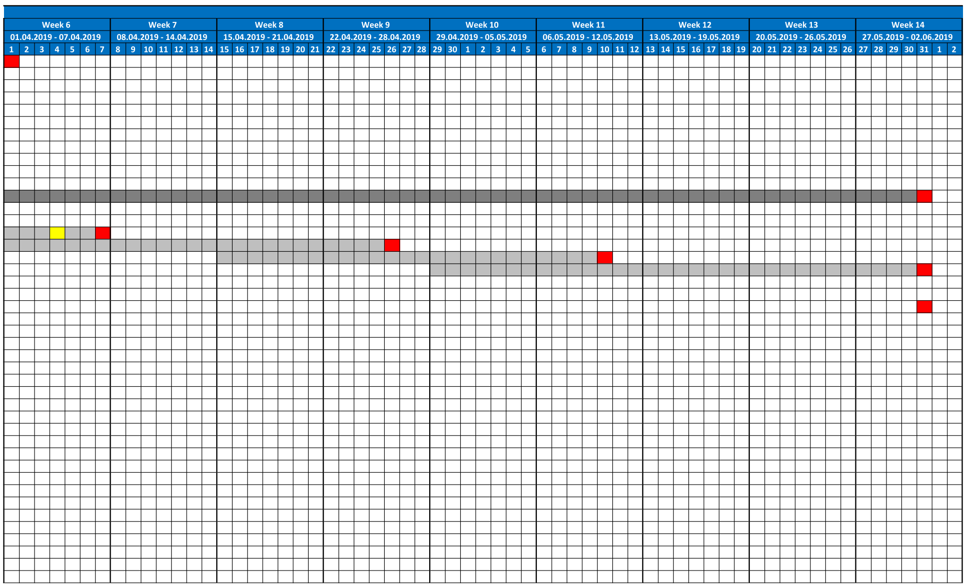

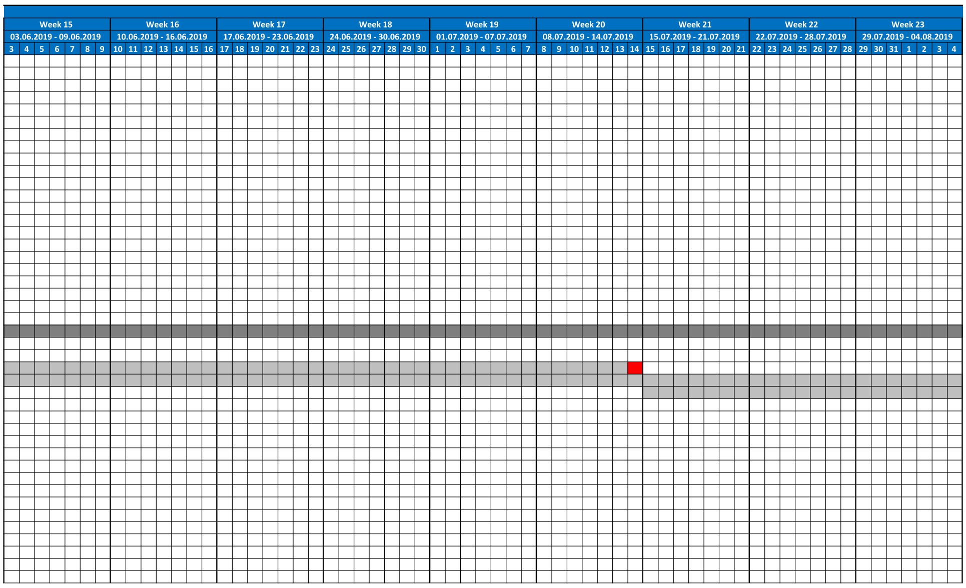
Week 15
03.06.2019 - 09.06.2019
Week 16
10.06.2019 - 16.06.2019
Week 17
17.06.2019 - 23.06.2019
Week 18
24.06.2019 - 30.06.2019
Week 19
01.07.2019 - 07.07.2019
Week 20
08.07.2019 - 14.07.2019
Week 21
15.07.2019 - 21.07.2019
Week 22
22.07.2019 - 28.07.2019
Week 23
29.07.2019 - 04.08.2019
3 4 5 6 7 8 9 10 11 12 13 14 15 16 17 18 19 20 21 22 23 24 25 26 27 28 29 30 1 2 3 4 5 6 7 8 9 10 11 12 13 14 15 16 17 18 19 20 21 22 23 24 25 26 27 28 29 30 31 1 2 3 4

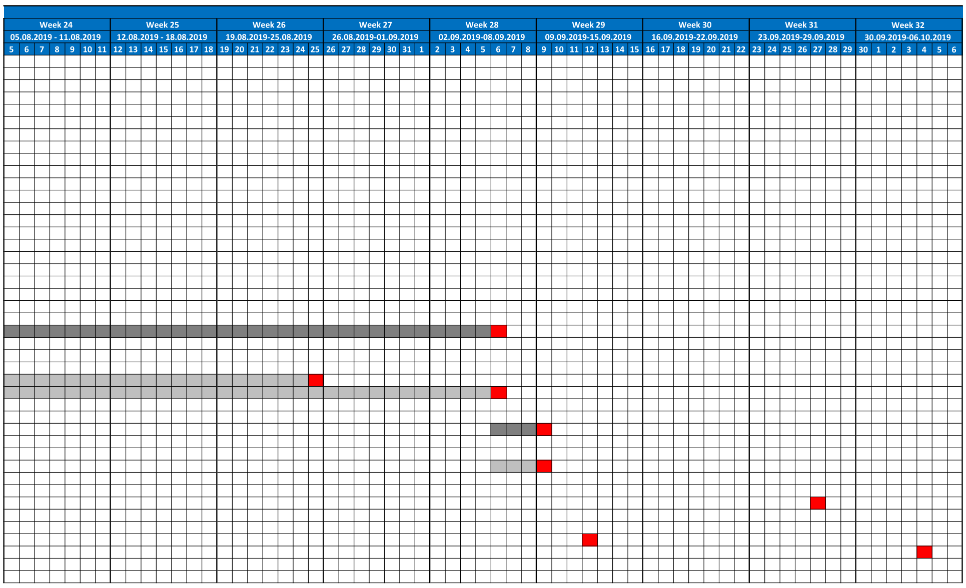
Week 24
05.08.2019 - 11.08.2019
Week 25
12.08.2019 - 18.08.2019
Week 26
19.08.2019-25.08.2019
Week 27
26.08.2019-01.09.2019
Week 28
02.09.2019-08.09.2019
Week 29
09.09.2019-15.09.2019
Week 30
16.09.2019-22.09.2019
Week 31
23.09.2019-29.09.2019
Week 32
30.09.2019-06.10.2019
5 6 7 8 9 10 11 12 13 14 15 16 17 18 19 20 21 22 23 24 25 26 27 28 29 30 31 1 2 3 4 5 6 7 8 9 10 11 12 13 14 15 16 17 18 19 20 21 22 23 24 25 26 27 28 29 30 1 2 3 4 5 6

# Appendix B

# Supporting Documents

## B.1 Database of Animals and Robots

| ID | Name (Animals: Beige / Robots: Grey) | Classification | Configuration | Kinematics | Number of Links | Leg Schematic | Leg Proportions (Joint to Joint, Normalized to Femur, Femur-(Fibula, Tibia)-(Tarsus-Metatarsus-Phalanges)) | Aspect Ratio (Hip to Withers: Contact Point to Hip; neutral position, | Feet Type | Material | Total Mass (kg) | Actuation (Rotary unless stated) | Performance Indexes | Gait | Forward Velocity (ms^-1) | Froude Number (V/sqrt (g*h)) | Focus | Inspiration | Leg Features | Comments | References |
|---|---|---|---|---|---|---|---|---|---|---|---|---|---|---|---|---|---|---|---|---|---|
| 1 | Agility Robotics Cassie | Biped | \|\| | Serial (with parallel constraints) | 6 | 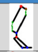 | 1,0.78,3.18,0.5,2.79,1.12 | - | Beam | Aluminium, CFRP | 31 | Electric | | Walking | 1.39 | 0.41 | Passive dynamics | Ostrich | Passive dynamics revolves around walking efficiently, fibre glass leaf springs at every joint, lands flatly on feet, hinge joints | Can be packed into a very compact form factor | "Oregon State's CASSIE biped: Mechanical design for dynamic locomotion", "Mechanical Design for Robot Locomotion", IEEE Robots database |
| 2 | ANYbotics ANYMAL | Quadruped | X | Serial | 2 |  | 1, 1.02 | 1.44:1 | Beam | Aluminium (Thigh), CFRP (Shank) | 30 | SEA (ANYdrives) | | Multiple | 1.25 | 0.48 | Active control | | Motors are located at each joint, off-axis link, V1 had a custom made shank that has a downward facing foot but it is weak to compressive loads | Benchmark for comparison | Internal data |
| 3 | Boston Dynamics LittleDog | Quadruped | X | Serial | 2 | 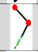 | 1,1.37 | 1.13:1 | Point | Plastic | 9 | Electric | | Multiple | | | Active control | Dog | | | Manual |
| 4 | Boston Dynamics SpotMini | Quadruped | M | Serial | 2 | 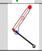 | 1, 1.08 | 1.18:1 | Point | | 25 | Electric (Slider-crank) | | Multiple | | | Active control | Dog | Motors are located high up in the leg, links are aligned, point foot is at an angle | | Boston Dynamics website |
| 5 | Cheetah | Quadruped | X | Serial | 4 | | 1, 1.13, 0.56,0.23 | 1.03:1 | Digits | Bones | 21-72 | Muscles | Accleration of 13ms^-2 (with claws) | Gallop | 27-33 | 10.71 | Speed | Nature; Evolution | | i) Fastest quadrupedal animal, ii) it uses its tail to aid in changing direction, iii) spine curves / compresses during motion | "Locomotion dynamics of hunting in wild cheetahs", Google, skeletal drawing |
| 27 | DLR Bert | Quadruped | \|\| | Serial | 2 |  | 1, 1.05 | 1.36:1 | Point | Plastic | 2.7 | SEA (Servo motors) | | Multiple | 1 | 0.53 | Active control | Cat | | | DLR Bert website |
| 6 | Elephant | Quadruped | X | Serial | 3 | | 1, 0.70, 0.26 | 1.09:1 | Digits | Bones | 2700-6000 | Muscles | | Amble | 7 | 1.29 | Strength | Nature; Evolution | | | Google, skeletal drawing |
| 7 | EPFL Cheetah-Cub Leg (Siegfried 2015) | Quadruped | M | Serial | 3 | 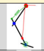 | 1,1.31,0.46 | 1.13:1 | Plantar | Steel, POM, CFRP | 1 | Servo motors with cable actuation | | Multiple | | | Passive dynamics | Cheetah | Each joint has an individual spring | | "Effect of Leg Design on Locomotion Stability for Quadruped Robot", Google |
| 8 | ETH ALoF | Quadruped | X | Serial | 2 |  | 1,1 | 1.3:1 | Point | Aluminium | 15 | Brushed motors | 3Nm,2Nm,4Nm / 0.84rads^-1, 1.13rads^-1, 1.69rads^-1 / 20W | Multiple | | | Active control | Dog | Rigid actuation results in lesser positional errors as well as the need for lesser sensing | No locomotion data | "Quadrupedal Robots with Stiff and Compliant Actuation" |
| 9 | ETH Capler-Leg | Leg | \| | Serial | 2 |  | 1, 1.04 | - | Point | Aluminium (Thigh), CFRP (Shank) | 4 | Cable (RoboDrive 115x25) | 70Nm / 4200W / 40rads^-1 / 300deg, 180deg | Multiple | | | Active control | | Motors are located high up in the leg, off-axis link, high performance cable actuation | Stretch goal to beat | "Cable-Driven Actuation for Highly Dynamic Robotic Systems", internal data |
| 10 | ETH FerrETH | Leg | \| | Serial | 2 | 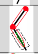 | 1,1.11 | - | Point | Aluminium | 15 | Brushed motors | Nonlinear >100Nm/rad, 12Nm/rad | Multiple | | | Passive dynamics | | Differential drive introduces coupling effects and is heavy, introduces collisions as damping | | "Efficient and Versatile Locomotion With Highly Compliant Legs", "Design of an articulated robotic leg with nonlinear series elastic actuation" |
| 11 | ETH MonoPogo | Hopper | \| | Serial | 2 |  | 1,1 | - | Point | Steel, Aluminium, CFRP | | SEA (ANYdrives) | | Hopping | | | Active control | Robotic hoppers | Uses springs to augment the knee torque, has an actively rotating bar to increase inertia | | "MonoPogo - Design of a Monopod Robot for 3D Locomotion" |
| 12 | ETH Multi Modal Linear Actuator | Leg | \| | Serial | 2 |  | 1,1 | - | Point | CFRP | 10 | Electric | 1000N | Multiple | | | Active control | | An actuator with multiple modes | | "Preloaded Hopping with a Linear Multi Modal Actuator" |
| 13 | ETH StarlETH | Quadruped | X | Serial | 2 | 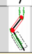 | 1,1 | 1.26:1 | Point | Aluminium | 23 | Brushless motors | 70Nm/rad, 80Nm/rad, 36Nm/rad / 20Nm, 12Nm,12Nm / 0.97rads^-1, 1.67rads^-1, 1.67rads^-1 / 200W | Multiple | 0.6 | 0.25 | Passive dynamics | Dog | Precompressed springs enable leg to be backlash free, springs enable energy storage during stance, mass is distributed around the leg resulting in high inertia, bumper and foam foot as dampers | Careful spring calculation based on eigenfrequencies | "Quadrupedal Robots with Stiff and Compliant Actuation", "Efficient and Versatile Locomotion With Highly Compliant Legs" |
| 14 | Gazelle | Quadruped | X | Serial | 4 | | 1,1.37, 1.20, 0.33 | 0.84:1 | Hoof | Bones | 14-25 | Muscles | | Multiple | 27 | 9.32 | Speed | Nature; Evolution | | | Google, skeletal drawing |
| 15 | Ghost Robotics Minitaur | Quadruped | \|\| | Parallel | 4 | 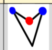 | 1,1.80, (1,1.80) | 2.22:1 | Point | Aluminium | | Brushless motors | | Multiple | 2 | | Active control | | Parallel leg setup | | "Taking Ground Robots to the Next Level" |
| 16 | Greyhound | Quadruped | X | Serial | 4 | | 1, 1.24, 0.76, 0.28 | 1.06:1 | Digits | Bones | 26-40 | Muscles | | Gallop | 20 | 7.53 | Speed | Nature; Evolution | Maximum linear acceleration at low speed is due to geometric constraint and muscle power for high speeds | Fastest breed of dogs | Google, skeletal drawing |
| 17 | Horse | Quadruped | X | Serial | 4 | | 1, 1.05, 0.97, 0.39 | 1.24:1 | Hoof | Bones | 380-1000 | Muscles | | Gallop | 11-13 | 3.28 | Speed | Nature; Evolution | | | Google, skeletal drawing |
| 18 | IHMC FastRunner | Biped | \|\| | Parallel | 7 | 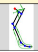 | 1, 2.25, 2.31, 1.88, (0.50, 0.37, 0.25) | - | Beam | Aluminium, 3D Printed parts | 30 | Electric | | Running | 10 | 2.7 | Passive dynamics | Ostrich | Complex parallel structure with springs at every joint | i) Results are from simulation, ii) relies on passive actuation, iii) design is based on real ostrich data | "FastRunner: A Fast, Efficient and Robust Bipedal Robot. Concept and Planar Simulation" |

| ID | Name (Animals: Beige / Robots: Grey) | Classification | Configuration | Kinematics | Number of Links | Leg Schematic | Leg Proportions (Joint to Joint, Normalized to Femur, Femur-(Fibula, Tibia)-(Tarsus-Metatarsus-Phalanges) | Aspect Ratio (Hip to Withers: Contact Point to Hip; neutral position, | Feet Type | Material | Total Mass (kg) | Actuation (Rotary unless stated) | Performance Indexes | Gait | Forward Velocity (ms^-1) | Froude Number (V/sqrt (g*h)) | Focus | Inspiration | Leg Features | Comments | References |
|---|---|---|---|---|---|---|---|---|---|---|---|---|---|---|---|---|---|---|---|---|---|
| 19 | IHMC HexRunner 1 | Wheel | O | Circular | 3 | 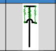 | 1,1,1 | - | Point | CFRP, 3D Printed parts | | Turbines / Brushless motors | | Rolling | 14 | | Passive dynamics | Geometric running | Simple spring-loaded point foot (rubber bands stores and releases energy, linearly moving contact point), forces act on point above COG, hitting the ground gives an upward pitch which is passively stabilizing | | IHMC YouTube video |
| 20 | IHMC HexRunner 2 | Biped | < | Parallel | 5 | 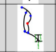 | 1 / (0.38,0.65), 0.96, 0.76 | - | Point | CFRP, 3D Printed parts | | Brushless motors | | Running | 14 | | Passive dynamics | Geometric running | Simple spring-loaded point foot (rubber bands stores and releases energy, linearly moving contact point), motion is encoded into parallel structure, forces act on point above COG, hitting the ground gives an upward pitch which is passively | Needs to run to be stable (CG in a relatively fixed position) | IHMC YouTube video |
| 21 | KAIST Raptor | Biped | >> | Parallel | 5 | 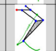 | (1,0.64), (1.10,1.17), 0.83 | - | Beam | Aluminium, CFRP | 3 | Electric | | Running | 13 | 6.05 | Passive dynamics | Raptor | Has an actively rotating bar to increase inertia, uses a spring as a link | | "Raptor: Fast Bipedal Running and Active Tail Stabilization" |
| 22 | KAIST Raptor 2 | Biped | >> | Parallel | 5 | 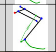 | (1,0.65), (1.08, 1.17), 0.78 | - | Beam | Aluminium, CFRP | 7 | Electric | | Running | | | Passive dynamics | Raptor | Has an actively rotating bar to increase inertia, uses a spring as a link | | "Raptor 2: Design of fast biped robot for 3D environments using active tail stabilization" |
| 23 | Kangaroo | Biped | \|\| | Serial | 3 | | 1, 2.03,1.03 | - | Plantar | Bones | 28-41 | Muscles | | Hopping | 19 | 4.95 | Speed | Nature; Evolution | Uses toe off to hop | It is able to leap up to 9m in a single jump | Google, skeletal drawing |
| 24 | Kwang Woon University HuboDog | Quadruped | X | Serial | 2 | 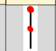 | 1,1 | 1.22:1 | Point | Aluminium | 42 | Brushless motors | 38.4Nm | Multiple | 1.24 | 0.36 | Active control | Dog | | Can carry a human | " On the Design and Development of a Quadruped Robot Platform" |
| 25 | MIT 3D One-legged Hopper | Hopper | \| | Serial | 0 | 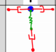 | - | - | Point | Steel, Aluminium | 17 | Pneumatic and hydraulic linear actuators | 1rad, 0.71rad, 83Nm | Hopping | 1.8 | | Active control | | Uses hydraulic actuators for positioning while uses pneumatic actuator as a combined spring and linear actuator | | "Experiments in Balance with a 3D One-Legged Hopping Machine" |
| 26 | MIT Cheetah 1 | Quadruped | X | Serial | 2 | 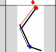 | 1, 0.88, 0.63 / 1, 1.32, 1.38 | 1.29:1 | Point | Foam core, resin shell | 33 | Direct drive motor (MIT Custom) | 0.5 (TCOT) | Multiple | 6 | | Active control | Cheetah | Composite and asymmetrical legs, actuated spine, tendon-bone co-location, motors are located high up in the leg, links are aligned | Joule heating was the primary source of energy losses | "Towards a bio-inspired leg desgin for high-speed running", "Design Principles for Energy Efficient Legged Locomotion and Implementation on the MIT Cheetah Robot" |
| 27 | MIT Cheetah 2 | Quadruped | X | Serial | 3 | 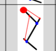 | 1,0.90, 0.74 | 1.42:1 | Point | ABS | 32 | Direct drive motor with rigid transmission (MIT Custom) | | Multiple | 6.4 | 2.89 | Active control | Cheetah | Pantograph legs made from ABS plastic, minimal compliance | It is able to jump over obstacles that are 0.4m in height | "Proprioceptive Actuator Design in the MIT Cheetah: Impact Mitigation and High-Bandwidth Physical Interaction for Dynamic Legged Robots" |
| 28 | MIT Cheetah 3 | Quadruped | M | Serial | 2 |  | 1,1 | 1.21:1 | Point | Aluminium | 45 | Direct drive motor with chain transmission (MIT Custom) | 230Nm / 21rads^-1 | Multiple | 3 | 1.07 | Active control | Cheetah | Strong and thin motors are located high up in the leg, links are aligned, inverted knee | It is able to jump onto a table that is 0.76 m tall | "MIT Cheetah 3: Design and Control of a Robust, Dynamic Quadruped Robot", MIT YouTube video |
| 29 | MIT Little Hermes | Biped | \|\| | Serial | 2 | 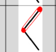 | 1,1 | - | Point | Aluminium | ≈10 | Direct drive motor with belt transmission (MIT Custom) | 17Nm | | | | Active control | Codesign of controller and mechanical design | Strong and thin motors are located high up in the leg, links are aligned, inverted knee, COM moves very little at extreme configurations | There are piezoresistive soft sensors at the foot to detect contact forces | "Facilitating Model-Based Control through Software-Hardware Co-Design" |
| 30 | MIT Mini Cheetah | Quadruped | M | Serial | 2 | 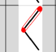 | 1, 1.28 | 1.32:1 | Point | Aluminium | 9 | Direct drive motor with belt transmission (MIT Custom) | | Multiple | 2.45 | 1.43 | Active control | Cheetah | Strong and thin motors are located high up in the leg, links are aligned, inverted knee | | MIT YouTube video |
| 31 | MIT Planar Robot | Biped | M | Serial | 2 | 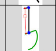 | 1, 0.45 | - | Beam | CFRP | 15 | SEA | 40Nm, 40Nm / 280W, 280W / 2.5Hz, 2.5 Hz | Pronking | | | Passive dynamics | Mathematical models | Uses a spring as a link | | "Design and Control of a Planar Robot to Study Quadrupedal Locomotion" |
| 32 | National Technical University Athens Heaxpod | Hexapedal | \|\| | Serial | 2 | 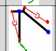 | 1,1.25 | - | Point | Steel | 1200 | Hydraulic actuators | 2700N | Multiple | 0.05 | 0.02 | Active control | | | | "Design, development, and control of a tough electrohydraulic hexapod robot for subsea operations" |
| 33 | Ostrich | Biped | \|\| | Serial | 4 | | 1, 2.48, 2.25, 1.19 | - | Digits | Bones | 100-120 | Muscles | | Running | 19 | 4.04 | Speed | Nature; Evolution | | Fastest bipedal animal | Google, skeletal drawing |
| 34 | Rhinoceras | Quadruped | X | Serial | 3 | | 1, 0.86, 0.73 | 1.62:1 | Hoof | Bones | 800-2300 | Muscles | | Gallop | 14 | 3.53 | Strength | Nature; Evolution | | | Google, skeletal drawing |
| 35 | Shanghai Jiao Tong University Little Elephant | Quadruped | \|\| | Parallel | 6 | 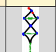 | (1,1), (1.90,1.90), 2.15 | 1.41:1 | Point | Aluminium | 130 | Hydraulic actuators | 100kg (Maximium payload) | Multiple | 0.5 | | Active control | Elephant | Uses a parallel mechanism to reduce mass and inertia, uses pressure sensor on hydraulic actuators to estimate ground reaction forces | | "A quadruped robot with parallel mechanism legs", YouTube video |
| 36 | Sogang University Cheetaroid 2 | Quadruped | M | Serial | 2 | 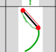 | 1:1.42 | 1.44:1 | Point | Aluminium, CFRP | 3 | Electric | | Multiple | 1.75 | | Active control | Cheetah | Uses a spring as a link, incorporates a pneumatic spring | | "Realizing Natural Springy Motion of a Robotic Leg by Cancelling the Undesired Damping Factors" |
| 37 | Sogang University Cheetaroid-I | Quadruped | M | Parallel | 4 | 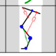 | 1, 0.88, 0.52, 0.18 | 1.28:1 | Plantar | Aluminium | 20 | Electrical linear actuators | 360N, 340N / 1.12ms^-1, 1.64ms^-1 / 3Hz, 3.5Hz | Multiple | | | Active control | Cheetah | Uses linear actuators over rotary actuators | | "Design of a Direct-Driven Linear Actuator for a High-Speed Quadruped Robot, Cheetaroid-I" |

## B.2 Technical Requirements

| Vertex: Designing High-Performance Legs for Specialized Quadrupedal Robots | | | | | | | | | | Additional comments |
|---|---|---|---|---|---|---|---|---|---|---|
| Technical Requirements List | | | | | | | | | | |
| ID | Requirement | Sign | HS Target | HS Type | HS Impt. | HP Target | HP Type | HP Impt. | Comments | |
| Design | | | | | | | | | | |
| D1 | The mass of the leg shall be | < | 3.1kg | D | 5 | 20kg | D | 3 | Including actuators | |
| D2 | The mass of active elements in the leg shall be | > | 1.9kg | D | 5 | 12kg | D | 3 | Relates to transmission related components, 60% of mass | |
| D3 | The link inertia of the leg shall be | < | 0.06kgm^2 | D | 5 | 0.1kgm^2 | D | 3 | Measured at hip joint when the leg is fully extended | On the sagittal plane |
| D4 | The dimensions of the leg when it is in its nominal stance shall be | < | 0.3m x 0.3m x 0.5m | W | 4 | 0.5m x 0.5m x 1.0 m | W | 3 | Length x Width x Height of envelope at nominal stance | |
| D5 | The volume of the leg when it is fully compacted should be minimized | - | - | W | 4 | - | W | 3 | Length x Width x Height of envelope, ease of transporting around | |
| D6 | The number of components of the leg shall be minimized | - | - | D | 5 | - | D | 5 | Strive for minimal design complexity, easy assembly and maintenance | |
| D7 | Frictional losses in the power transmission of the leg shall be minimized | - | - | D | 5 | - | D | 4 | Energy efficiency, transparency | |
| D8 | The possiblity of a static discharge of the leg shall be minimized | - | - | D | 4 | - | D | 4 | Safety; the robot is charging static electricity and rubber feet do not get rid of it | |
| D9 | The components of the leg shall be ingress protected | - | IP65 | D | 4 | IP65 | D | 5 | Possibility of wet missions, robustness | |
| D10 | The components of the leg should be waterproof | - | IP68 | W | 3 | IP68 | W | 3 | Possibility of wet missions, robustness | |
| D11 | The leg should be kinematically redundant | - | - | W | 1 | - | W | 1 | To avoid singularities | |
| Functional | | | | | | | | | | High-level matters |
| F1 | The kinematic velocity ellipsoid of the end effector shall be maximized | - | - | D | 5 | - | D | 3 | | |
| F2 | The kinematic force ellipsoid of the end effector shall be maximized | - | - | D | 4 | - | D | 4 | | |
| F3 | The dynamic force ellipsoid of the end effector shall be maximized | - | - | D | 4 | - | D | 4 | | |
| F4 | The workspace volume of the end effector shall be maximized | - | - | D | 3 | - | D | 4 | With ANYmal V3 trunk; relates to range of motion | |
| F5 | The normalized reachability of the end effector shall be maximized | - | - | D | 3 | - | D | 4 | Volume of reachable workspace / Volume of extended leg | |
| Performance | | | | | | | | | | Characterization of the leg |
| P1 | The maximum load that the leg can bear while standing up from a fully crouched configuration shall be | > | 7.8kg | D | 5 | 35kg | D | 5 | Mass(Platform + Payload) / 4 | |
| P2 | The maximum shear force that can be applied at the end effector when the leg is in its nominal stance shall be maximized | - | 10N | D | 5 | - | D | 5 | Important for efficient power transmission the ground; see test on the right | |
| P3 | The bandwidth for force control of the leg shall be | > | 70Hz | D | 3 | 70Hz | D | 3 | The higher it is, the better it is to control; numbers from Hutter 2016 | |
| P4 | The maximum force that can be applied by the end effector shall be maximized | - | - | D | 5 | - | D | 4 | Thrust; stance phase | |
| P5 | The maximum velocity of the end effector shall be maximized | - | - | D | 5 | - | D | 3 | Preparing for next step; swing phase | |
| P6 | The positioning accuracy of the end effector shall be | < | 5mm | D | 4 | 10mm | D | 3 | Accuracy; within a few mm but through the transmission it adds up (especially long links and transmissions) | |
| P7 | The positioning repeatability of the end effector shall be | < | 5mm | D | 4 | 10mm | D | 3 | Precision; within a few mm | |
| P8 | The end effector shall be able to track specific trajectories | - | 25% stance, 75% swing (Gallop) | D | 5 | 60% stance, 40% swing (Walk) | D | 5 | Related to gaits | |
| P9 | The minimum obstacle height that the leg can overcome shall be | > | 250mm | D | 3 | 375mm | D | 4 | Average height of a road curb and 20L bucket respectively | |

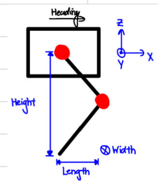


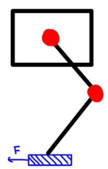


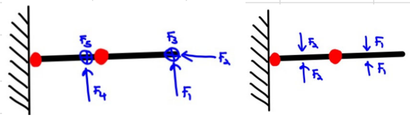

| | | | | | | | | | | |
|---|---|---|---|---|---|---|---|---|---|---|
| P10 | The structure of the leg shall withstand impact loads | - | Load cases | D | 5 | Load cases | D | 5 | Load cases to be determined (not only for walking but also falling); shank broke multiple times as load case was not accounted for | Load cases to simulate walking and falling |
| **Interface** | | | | | | | | | | |
| I1 | There should be a common electrical interface between the leg and the ANYmal V3 trunk | - | - | W | 2 | - | W | 2 | LEMO connectors | |
| I2 | There should be a common mechanical interface between the leg and the ANYmal V3 trunk | - | - | W | 2 | - | W | 2 | Compatible with HAA actuator | |
| I3 | The time required to replace the leg should be | < | 10 mins | W | 3 | 15 mins | W | 3 | To facilitate troubleshooting | |
| I4 | The leg shall be able to be mounted onto the Capler-leg rail | - | - | D | 5 | - | D | 5 | To facilitate testing; using the Capler-leg rail interface | |
| I5 | The leg shall have a mechanism that allows additional weight to be easily added | - | - | D | 5 | - | D | 5 | To facilitate testing; using the Capler-leg rail interface | |
| I6 | The length of the power and data cables in the leg shall be minimized | - | - | D | 2 | - | D | 2 | To ensure the robustness of operation | |
| I7 | The twisting of the power and data cables in the leg shall be minimized | - | - | D | 4 | - | D | 4 | To ensure the robustness of operation | |
| I8 | The movement of the power and data cables in the leg shall be minimized | - | - | D | 4 | - | D | 4 | To ensure the robustness of operation | |
| I9 | The power and data cables of the leg should be integrated into its structure | - | - | W | 2 | - | W | 2 | To ensure the robustness of operation | |
| I10 | The power and data cables of the leg shall be detachable | - | - | D | 3 | - | D | 3 | To ensure the robustness of operation; especially for the actuators | |
| I11 | Safe data communication should be ensured | > | 100 Mbps | W | 3 | 100 Mbps | W | 3 | To ensure the robustness of operation | |

## B.3 Function Structure

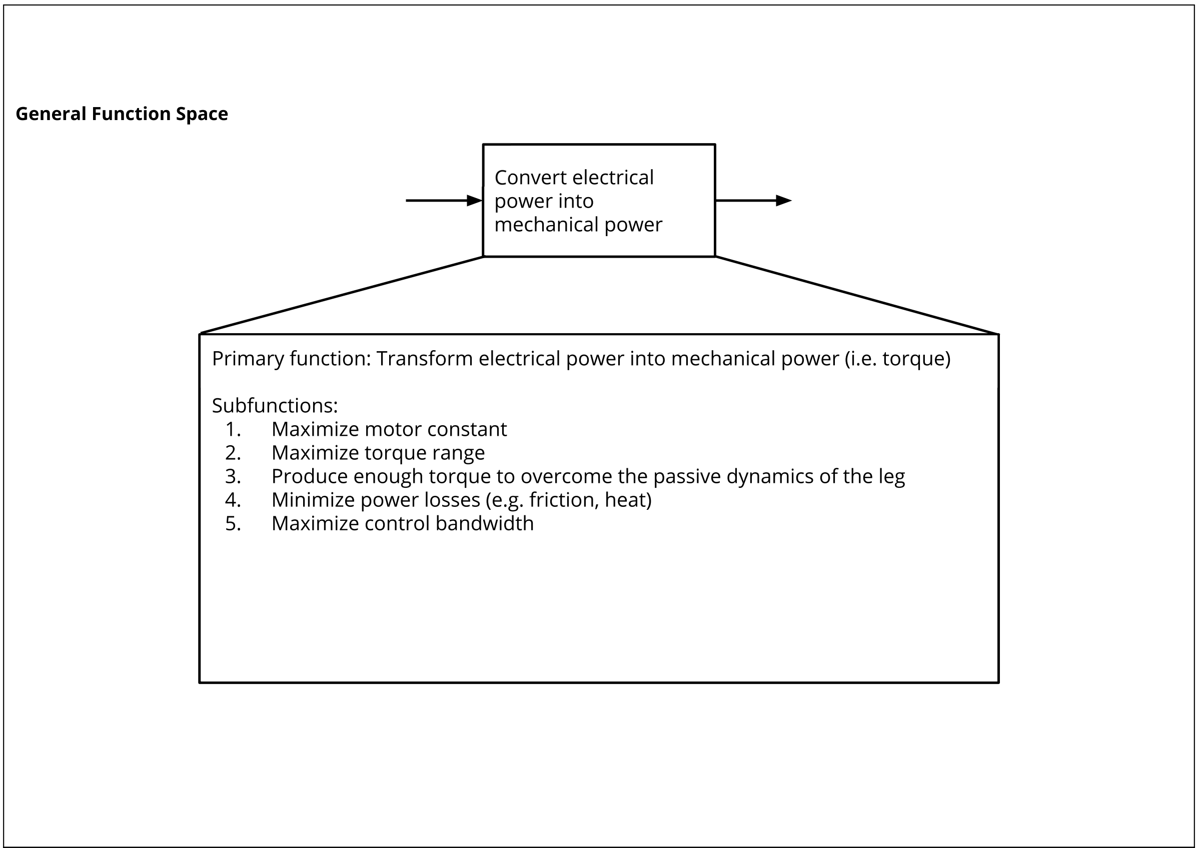


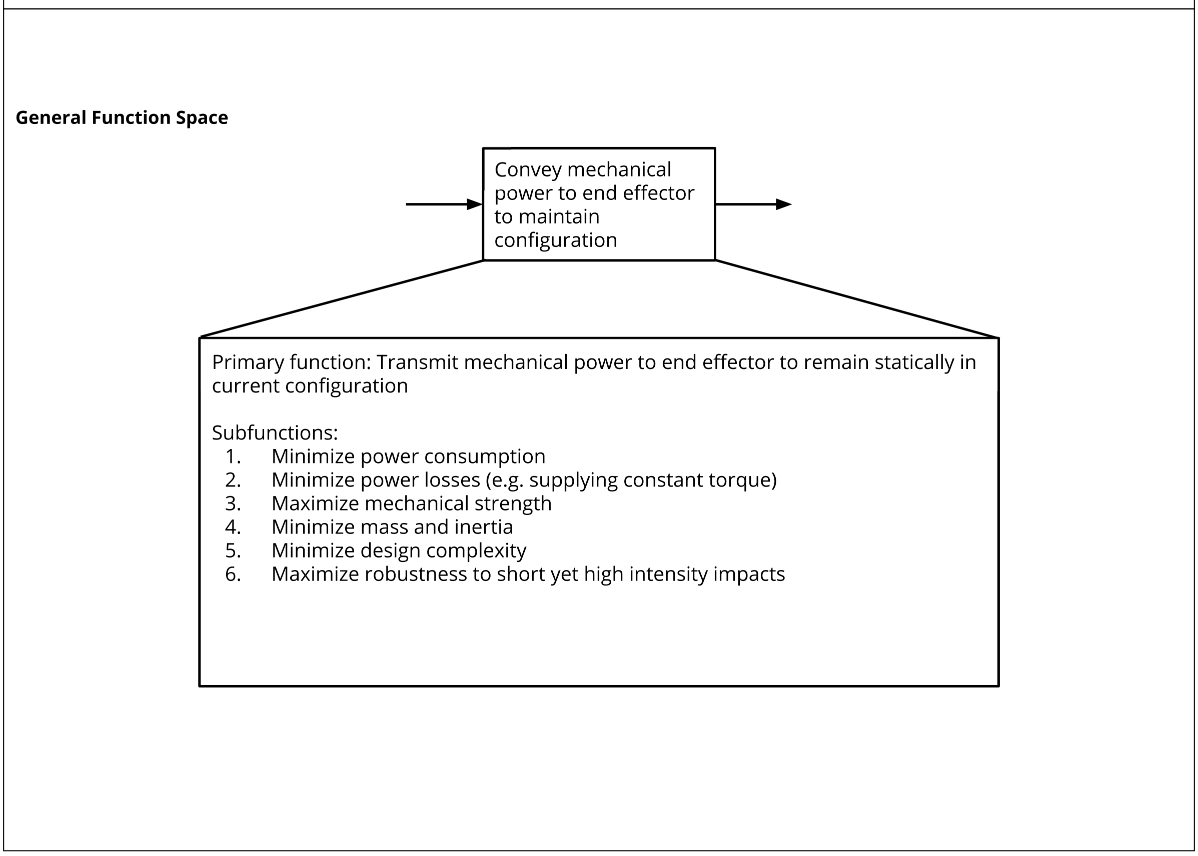

**General Function Space**

Convey mechanical power to end effector for locomotion

Primary function: Transmit mechanical power to end effector for locomotion (primarily horizontal motion)

Subfunctions:
1. Minimize power losses (e.g. sliding and rolling friction)
2. Minimize mass and inertia
3. Maximize reachability
4. Maximize mechanical strength
5. Maximize accuracy and precision of end effector position control
6. Minimize design complexity
7. Maximize robustness to short yet high intensity impacts

**General Function Space**

Apply linear forces to the ground

Primary function: Subject the contact point / area with the desired linear forces

Subfunctions:
1. Maximize the friction cone radius
2. Minimize power losses (e.g. sliding and rolling friction)

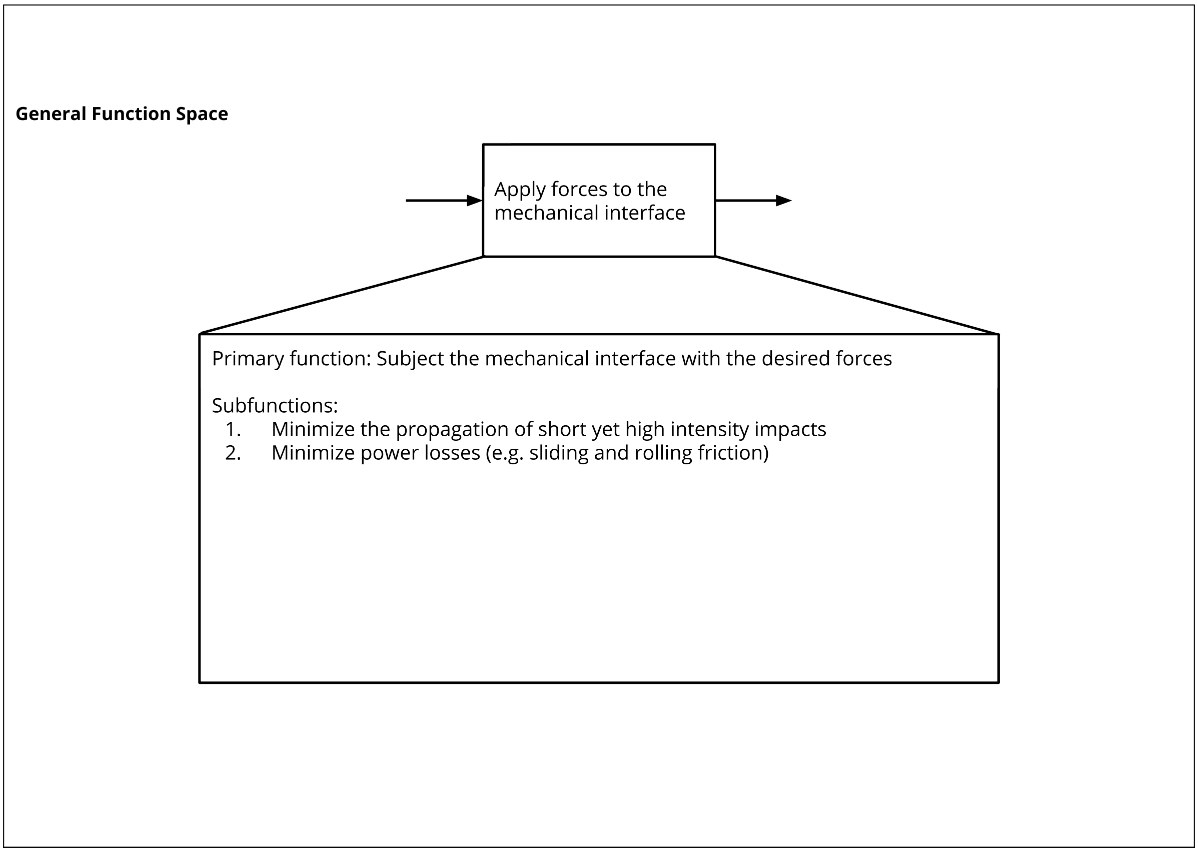
General Function Space
Apply forces to the mechanical interface
Primary function: Subject the mechanical interface with the desired forces
Subfunctions:
1. Minimize the propagation of short yet high intensity impacts
2. Minimize power losses (e.g. sliding and rolling friction)

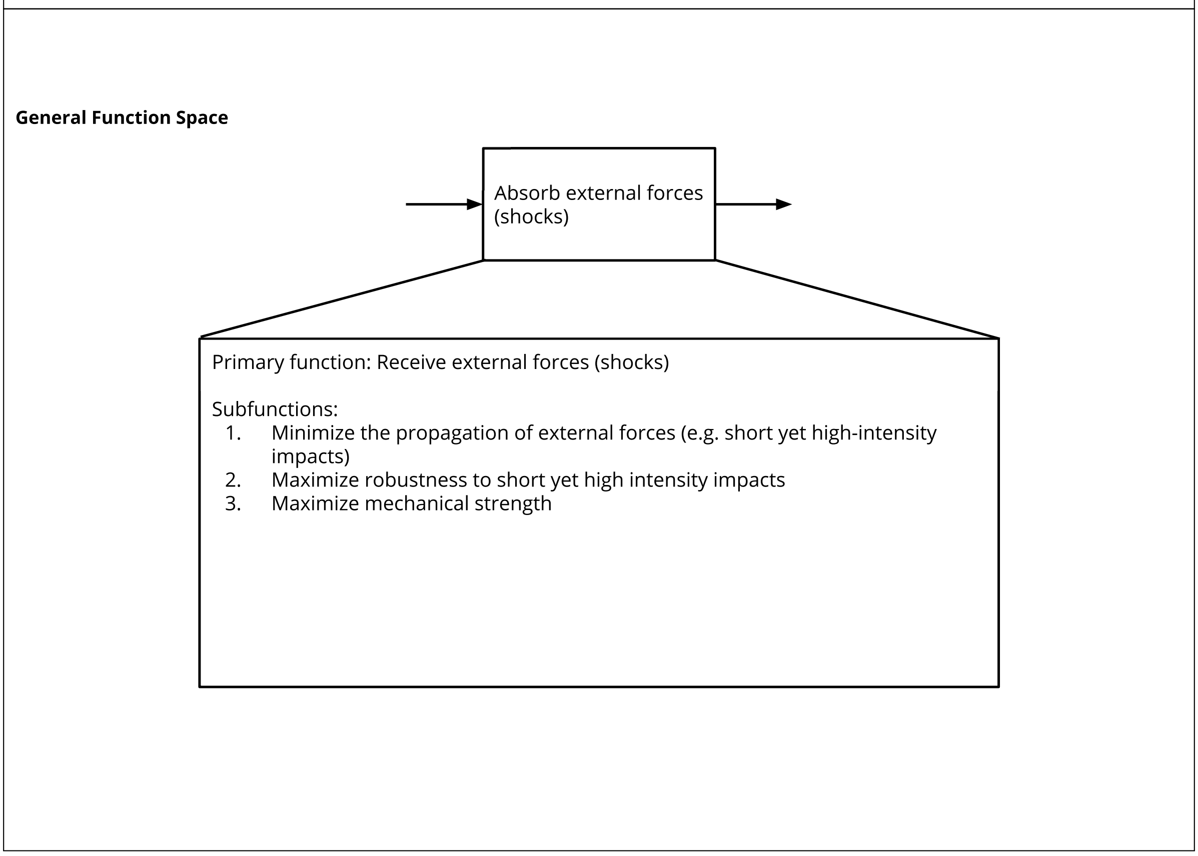
General Function Space
Absorb external forces (shocks)
Primary function: Receive external forces (shocks)
Subfunctions:
1. Minimize the propagation of external forces (e.g. short yet high-intensity impacts)
2. Maximize robustness to short yet high intensity impacts
3. Maximize mechanical strength

**General Function Space**

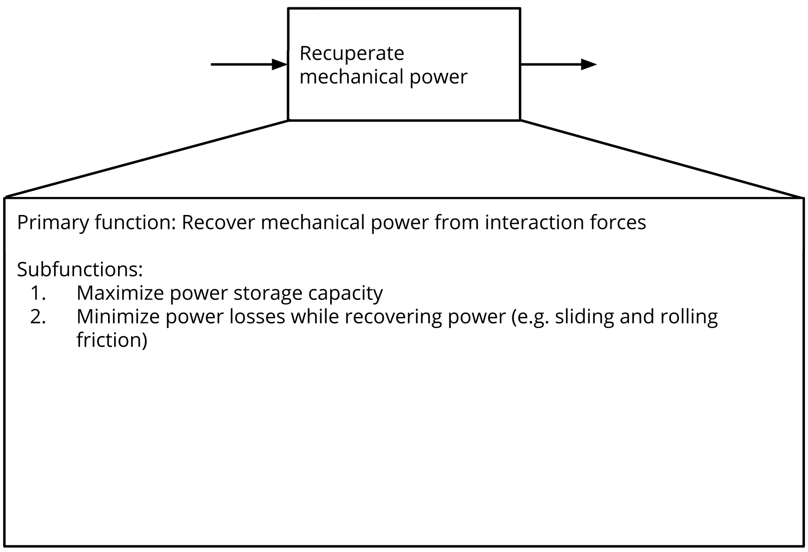


**General Function Space**

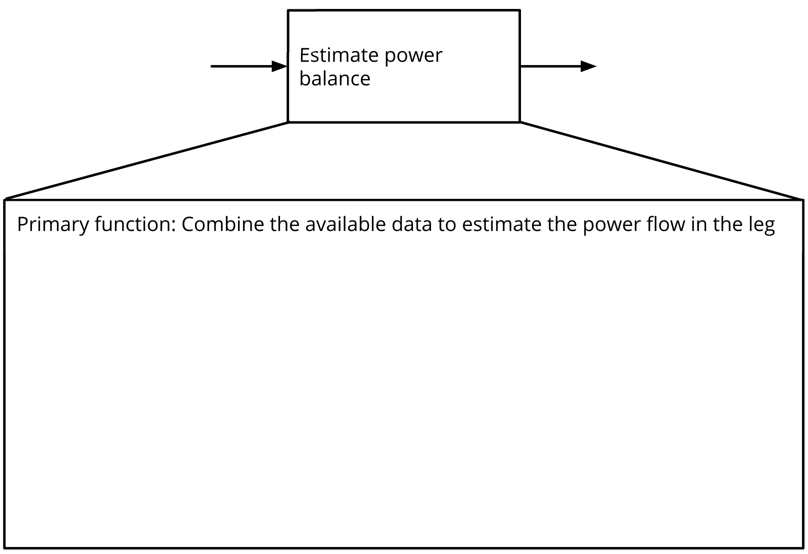

## B.4 Initial Leg Design Concepts

### Concept 1 (High Speed)

| Front View | Side View |
|---|---|
| 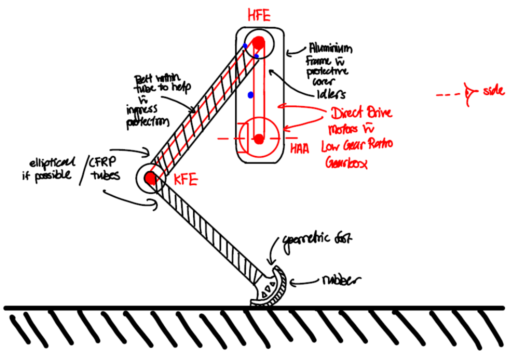 | 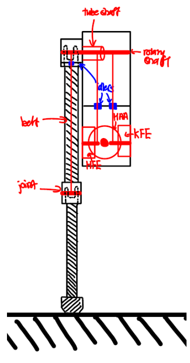 |





| Functions | Chosen Idea | Comments |
|---|---|---|
| **Convert electrical power into mechanical power** | Direct Drive Motor / Gearbox / No Spring | Choose a gear ratio such that:<br>• Motor provides sufficient torque<br>• Motor runs at high speeds (efficiency)<br>• Reflected inertia is not amplified too much |
| **Convey mechanical power to end effector to maintain configuration** | Power from Motors | Function is not particularly important for high speed<br><br>Neglecting the need of a specialized mechanism for this function leads to a reduction of overall leg mass and inertia |
| **Convey mechanical power to end effector for locomotion** | Serial / Belt / Composites | Spider configuration as it balances the actuator powers better (Abate 2016); knee facing forward so as to align the foot with the light force axis (Abate 2015)<br><br>Belt is used so as to relocate the knee motor higher up the limb and can use standard parts<br><br>Carbon fibre is used due to rigidity and availability; belt and other cables other cables (e.g. cables for knee joint angle data) can placed within the tube for ingress protection<br><br>Leg lengths should be as short as possible such that it can still overcome obstacles (Application of linear forces reduces with leg length) |
| **Apply linear forces to the ground** | Passive / Geometric Foot | Geometric feet is chosen so as to increase surface area of contact<br><br>Minimal compliance in the leg aids in maximizing the closed-loop force control bandwidth (Wensing 2017) |
| **Apply forces to the mechanical interface** | Rigid Attachment | Low platform mass reduces the need for any specialized features |
| **Absorb external forces** | Damper | Simplest solution which leads to a reduction of overall leg mass and inertia (as compared to other solutions) |
| **Recuperate mechanical power** | Direct Feedback to Actuators | Relying on backdrivability |
| **Estimate power balance** | Proprioceptive | Low gear ratio and low inertia leg permits this method of force estimation; inverse dynamics (Wensing 2017) |

**Concept 2 (High Speed)**

| Front View | Side View |
|---|---|

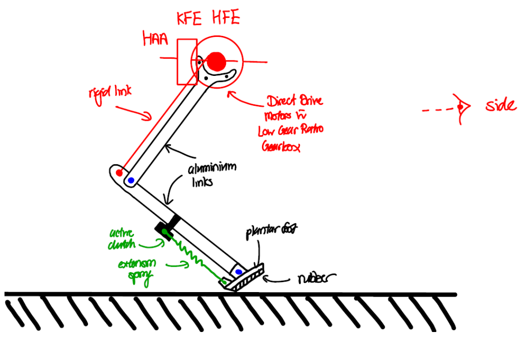


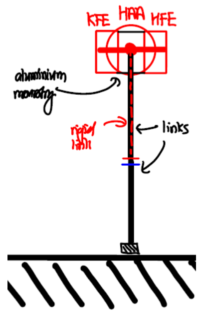


| Functions | Chosen Idea | Comments |
|---|---|---|
| **Convert electrical power into mechanical power** | Direct Drive Motor / Gearbox / No Spring | Choose a gear ratio such that:<br>● Motor provides sufficient torque<br>● Motor runs at high speeds (efficiency)<br>● Reflected inertia is not amplified too much |
| **Convey mechanical power to end effector to maintain configuration** | Power from Motors | Function is not particularly important for high speed<br><br>Neglecting the need of a specialized mechanism for this function leads to a reduction of overall leg mass and inertia |
| **Convey mechanical power to end effector for locomotion** | Serial / Rigid Link / Metals | Serial 2 link configuration is chosen due to its simplicity; knee facing forward so as to align the foot with the light force axis (Abate 2015)<br><br>Rigid link which connects the hip to the knee aids in the simplicity of the design<br><br>Aluminium chosen due to its low weight and strength<br><br>Leg lengths should be as short as possible such that it can still overcome obstacles (Application of linear forces reduces with leg length |
| **Apply linear forces to the ground** | Active / Plantar Foot | Spring with an active clutch captures energy upon touch down and releases at lift off<br><br>Plantar feet is chosen to increase surface area of contact |
| **Apply forces to the mechanical interface** | Rigid Attachment | Low platform mass reduces the need for any specialized features |
| **Absorb external forces** | Damper | Simplest solution which leads to a reduction of overall leg mass and inertia (as compared to other solutions) |
| **Recuperate mechanical power** | Spring-based Mechanism | As explained in the “Apply linear forces to the ground” section |
| **Estimate power balance** | Force Sensor | Compliance in the leg reduces the closed-loop force control feedback; there is a need for a force sensor to estimate the forces involved |

**Concept 3 (High Speed)**

| Front View | Side View |
|---|---|
| 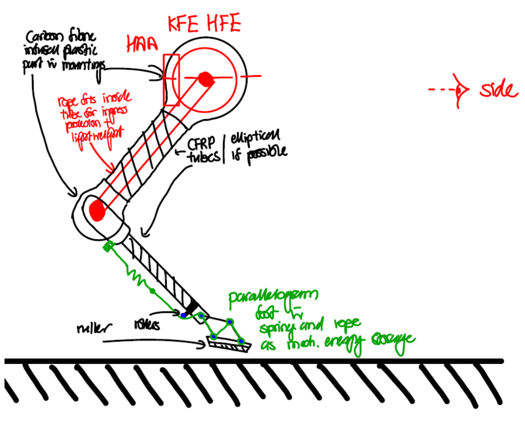 | 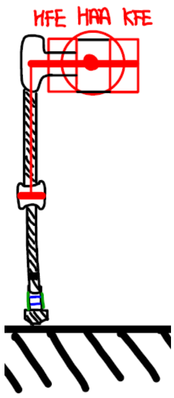 |





| Functions | Chosen Idea | Comments |
|---|---|---|
| **Convert electrical power into mechanical power** | Direct Drive Motor / Gearbox / No Spring | Choose a gear ratio such that:<br>• Motor provides sufficient torque<br>• Motor runs at high speeds (efficiency)<br>• Reflected inertia is not amplified too much |
| **Convey mechanical power to end effector to maintain configuration** | Power from Motors | Function is not particularly important for high speed<br><br>Reduction of overall leg mass and inertia |
| **Convey mechanical power to end effector for locomotion** | Serial-Parallel / Rope / Composites | Serial 2 link configuration is chosen due to its simplicity; knee facing forward so as to align the foot with the light force axis (Abate 2015)<br><br>Rope (Dyneema M20) is used so as to relocate the knee motor higher up the limb<br><br>Carbon fibre is used due to rigidity and availability; rope and other cables are placed within the limb for ingress protection<br><br>Leg lengths should be as short as possible such that it can still overcome obstacles (Application of linear forces reduces with leg length |
| **Apply linear forces to the ground** | Passive / Plantar Foot | Spring-loaded plantar feet made from 4 bar linkage mechanism adds compliance so as to mitigate impacts while storing mechanical energy<br><br>Plantar feet is chosen to increase surface area of contact |
| **Apply forces to the mechanical interface** | Rigid Attachment | Low platform mass reduces the need for any specialized features |
| **Absorb external forces** | Additional Degrees of Freedom | Inspired by the foot of horses |
| **Recuperate mechanical power** | Spring-based Mechanism | As explained in the "Apply linear forces to the ground" section |
| **Estimate power balance** | Force Sensor | Compliance in the leg reduces the closed-loop force control feedback; there is a need for a force sensor to estimate the forces involved |

## Concept 4 (High Speed)

| Front View | Side View |
|---|---|
| 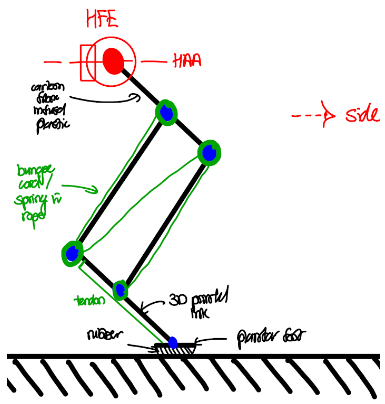 | 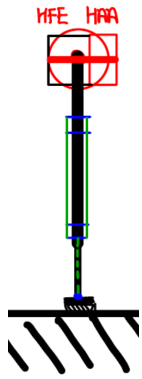 |




| Functions | Chosen Idea | Comments |
|---|---|---|
| **Convert electrical power into mechanical power** | Direct Drive Motor / Gearbox / Serial Spring | Choose a gear ratio such that:<br>• Motor provides sufficient torque<br>• Motor runs at high speeds (efficiency)<br>• Reflected inertia is not amplified too much<br><br>Serial spring allows for force estimation while also protecting the motor |
| **Convey mechanical power to end effector to maintain configuration** | Spring-based Mechanism | Due to the parallel kinematics of the leg as well as the spring configuration |
| **Convey mechanical power to end effector for locomotion** | Parallel / Rope / Plastics | Pantograph leg configuration is bioinspired (dogs)<br><br>Rope (Dyneema M20) along with a sufficiently stiff spring is used to hold the leg upright<br><br>3D printed carbon fibre infused plastic is used due to lightweight and strength; MIT Cheetah 2 uses ABS plastic as its links (Wensing 2017)<br><br>One less motor as well as lesser moving parts reduces the mass, inertia and chances of failure<br><br>Leg lengths should be as short as possible such that it can still overcome obstacles (Application of linear forces reduces with leg length |
| **Apply linear forces to the ground** | Passive / Plantar Foot | Plantar feet is chosen to increase surface area of contact |
| **Apply forces to the mechanical interface** | Rigid Attachment | Low platform mass reduces the need for any specialized features |
| **Absorb external forces** | Damper | Simplest solution which leads to a reduction of overall leg mass and inertia (as compared to other solutions) |
| **Recuperate mechanical power** | Tendons | Converts moments on 3D printed part into linear forces (Ananthanarayanan 2012) |
| **Estimate power balance** | Force Sensor | Compliance in the leg reduces the closed-loop force control feedback; there is a need for a force sensor to estimate the forces involved |

**Concept 5 (High Speed)**

| Front View | Side View |
|---|---|
| 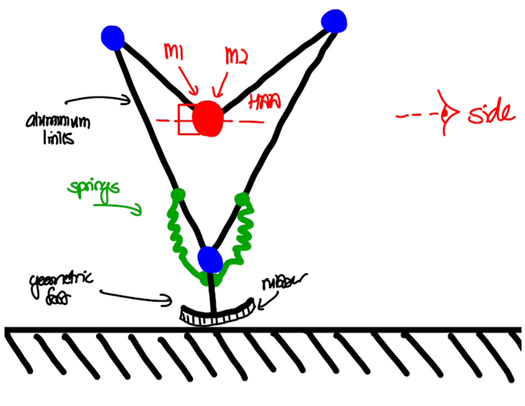  | 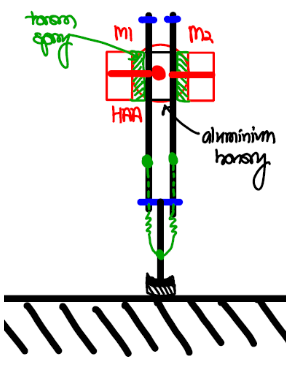  |

| Functions | Chosen Idea | Comments |
|---|---|---|
| **Convert electrical power into mechanical power** | Direct Drive Motor / Gearbox / Serial Spring | Choose a gear ratio such that:<br>• Motor provides sufficient torque<br>• Motor runs at high speeds (efficiency)<br>• Reflected inertia is not amplified too much<br><br>Serial spring allows for force estimation while also protecting the motor |
| **Convey mechanical power to end effector to maintain configuration** | Power from the Motors | Function is not particularly important for high speed<br><br>Neglecting the need of a specialized mechanism for this function leads to a reduction of overall leg mass and inertia |
| **Convey mechanical power to end effector for locomotion** | Parallel / Motors at Joints / Metals | Parallel leg configuration chosen due to simplicity<br><br>Aluminium chosen due to its low weight and strength<br><br>Leg lengths should be as short as possible such that it can still overcome obstacles (Application of linear forces reduces with leg length |
| **Apply linear forces to the ground** | Passive / Geometric Foot | Geometric feet is chosen to increase surface area of contact as a rolling point of contact |
| **Apply forces to the mechanical interface** | Spring-loaded Joint | Weight savings from this structured can be transferred into implementing better impact mitigation strategies |
| **Absorb external forces** | Damper | Simplest solution which leads to a reduction of overall leg mass and inertia (as compared to other solutions) |
| **Recuperate mechanical power** | Spring-based Mechanism | Foot is spring-loaded to store and release energy during locomotion |
| **Estimate power balance** | Force Sensor | Compliance in the leg reduces the closed-loop force control feedback; there is a need for a force sensor to estimate the forces involved |

**Concept 6 (Heavy Payload)**

| Front View | Side View |
|---|---|
| 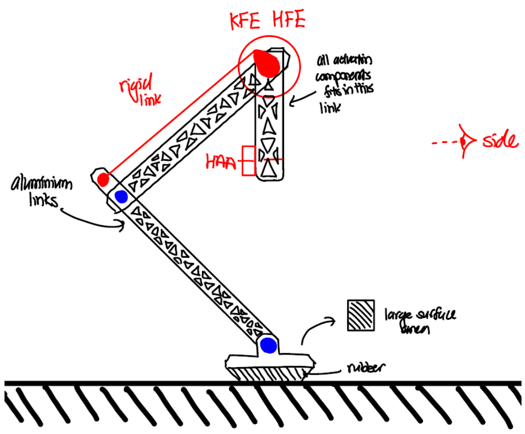  | 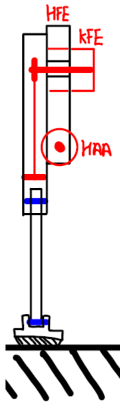  |

| Functions | Chosen Idea | Comments |
|---|---|---|
| **Convert electrical power into mechanical power** | Direct Drive Motor / Gearbox / No Spring | Choose a gear ratio such that:<br>• Motor provides sufficient torque<br>• Motor runs at high speeds (efficiency)<br>• Reflected inertia is not amplified too much |
| **Convey mechanical power to end effector to maintain configuration** | Power from Motors | This keeps the design complexity of the leg low at the cost of being energetically expensive |
| **Convey mechanical power to end effector for locomotion** | Serial / Rigid Link / Metals | Spider configuration as it balances the power better (Abate 2016); knee facing forward so as to align the foot with the light force axis (Abate 2015)<br><br>Rigid link that connects the hip to the knee aids in the simplicity of the design<br><br>Aluminium chosen due to its low weight and strength<br><br>Leg lengths should be as short as possible such that it can still overcome obstacles (Application of linear forces reduces with leg length |
| **Apply linear forces to the ground** | Passive / Geometric Foot | Geometric feet is chosen to increase surface area of contact<br><br>Minimal compliance in the leg aids in maximizing the closed-loop force control bandwidth (Wensing 2017) |
| **Apply forces to the mechanical interface** | Rigid Attachment | This keeps the design complexity of the leg low |
| **Absorb external forces** | Damper | Simplest solution which leads to a reduction of overall leg mass and inertia (as compared to other solutions) |
| **Recuperate mechanical power** | Direct Feedback to Actuators | Relying on backdrivability |
| **Estimate power balance** | Proprioceptive | Low gear ratio and low inertia leg permits this method of force estimation; inverse dynamics (Wensing 2017) |

**Concept 7 (Heavy Payload)**

| Front View | Side View |
|---|---|
| 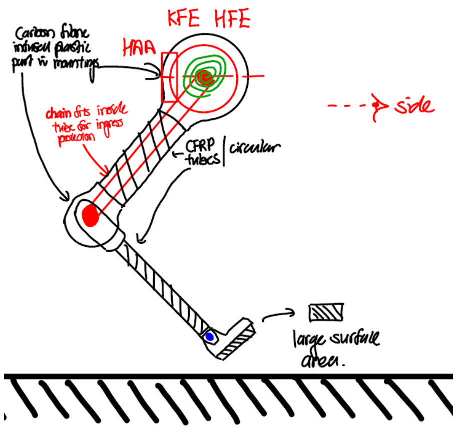 | 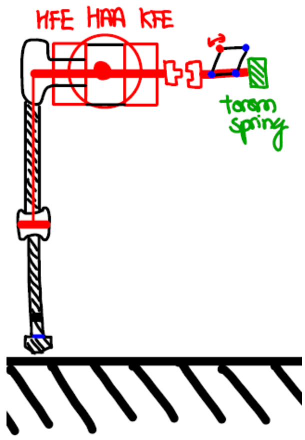 |





| Functions | Chosen Idea | Comments |
|---|---|---|
| **Convert electrical power into mechanical power** | Direct Drive Motor / Gearbox / Parallel Spring | Choose a gear ratio such that:<br>• Motor provides sufficient torque<br>• Motor runs at high speeds (efficiency)<br>• Reflected inertia is not amplified too much<br><br>Parallel spring is the spring-based mechanism explained below |
| **Convey mechanical power to end effector to maintain configuration** | Clutches | This leg relies on a torsion spring to provide the necessary torque to maintain the configuration (knee torque); the spring is engaged using a clutch mechanism |
| **Convey mechanical power to end effector for locomotion** | Serial / Chain / Composites | Serial 2 link configuration is chosen due to its simplicity; knee facing forward so as to align the foot with the light force axis (Abate 2015)<br><br>Chain is used so as to relocate the knee motor higher up the limb as well as to hold up the large mass of the platform<br><br>Carbon fibre is used due to rigidity and availability; chain and other cables are placed within the limb for ingress protection<br><br>Leg lengths should be as short as possible such that it can still overcome obstacles (Application of linear forces reduces with leg length |
| **Apply linear forces to the ground** | Passive / Plantar Foot | Plantar feet is chosen to increase surface area of contact |
| **Apply forces to the mechanical interface** | Spring-loaded Joint | Hip joint is spring-loaded to mitigate any impacts not filtered by the leg |
| **Absorb external forces** | Spring-based Mechanism | Using the clutchable parallel spring |
| **Recuperate mechanical power** | Spring-based Mechanism | Using the clutchable parallel spring |
| **Estimate power balance** | Force Sensor | Compliance in the leg reduces the closed-loop force control feedback; there is a need for a force sensor to estimate the forces involved |

**Concept 8 (Heavy Payload)**

<table>
<tr><th>Front View</th><th>Side View</th></tr>
<tr><td>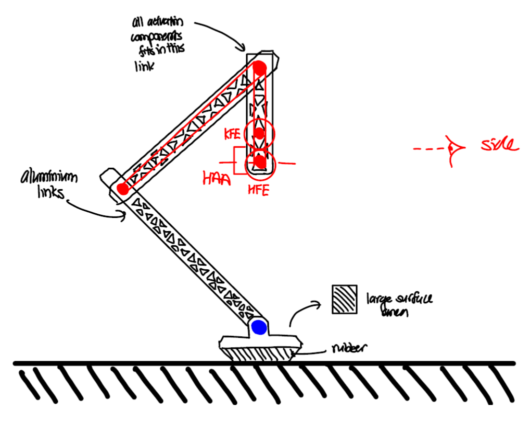
</td><td>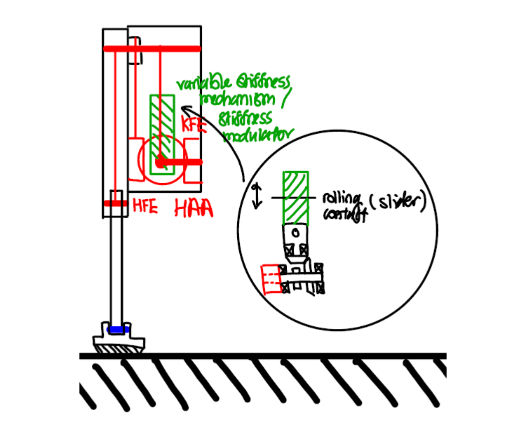
</td></tr>
</table>

| Functions | Chosen Idea | Comments |
|---|---|---|
| **Convert electrical power into mechanical power** | Direct Drive Motor / Gearbox / Parallel Spring | Choose a gear ratio such that:<br>● Motor provides sufficient torque<br>● Motor runs at high speeds (efficiency)<br>● Reflected inertia is not amplified too much<br><br>Parallel spring is the spring-based mechanism explained below |
| **Convey mechanical power to end effector to maintain configuration** | Spring-based Mechanism | The leg relies on a variable stiffness mechanism to provide the necessary torque to maintain the configuration (knee torque); by changing the stiffness of the mechanism, the equilibrium of the mechanism or configuration of the leg changes to the desired value (Chong 2017) |
| **Convey mechanical power to end effector for locomotion** | Serial / Rope / Metals | Spider configuration as it balances the power better (Abate 2016); knee facing forward so as to align the foot with the light force axis (Abate 2015)<br><br>Rope (Dyneema M20) is used so as to relocate the knee motor higher up the limb<br><br>Aluminium chosen due to its low weight and strength<br><br>Leg lengths should be as short as possible such that it can still overcome obstacles (Application of linear forces reduces with leg length |
| **Apply linear forces to the ground** | Passive / Geometric Foot | Geometric feet is chosen to increase surface area of contact |
| **Apply forces to the mechanical interface** | Rigid Attachment | This keeps the design complexity of the leg low |
| **Absorb external forces** | Damper | Simplest solution which leads to a reduction of overall leg mass and inertia (as compared to other solutions) |
| **Recuperate mechanical power** | Direct Feedback to Actuators | Relying on backdrivability |
| **Estimate power balance** | Force Sensor | Compliance in the leg reduces the closed-loop force control feedback; there is a need for a force sensor to estimate the forces involved |

**Concept 9 (Heavy Payload)**

| Front View | Side View |
|---|---|
| 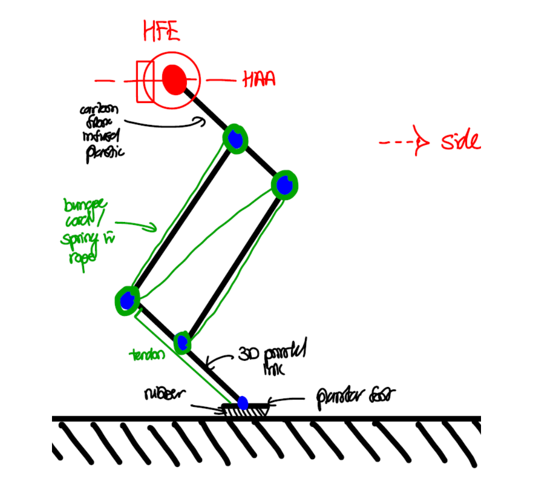  | 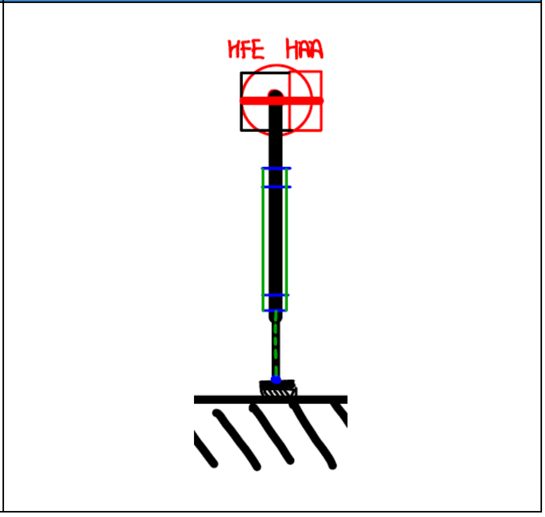  |

| Functions | Chosen Idea | Comments |
|---|---|---|
| **Convert electrical power into mechanical power** | Direct Drive Motor / Gearbox / Serial Spring | Choose a gear ratio such that:<br>• Motor provides sufficient torque<br>• Motor runs at high speeds (efficiency)<br>• Reflected inertia is not amplified too much<br><br>Serial spring allows for force estimation while also protecting the motor |
| **Convey mechanical power to end effector to maintain configuration** | Spring-based Mechanism | Due to the parallel kinematics of the leg as well as the spring configuration |
| **Convey mechanical power to end effector for locomotion** | Parallel / Rope / Metals | Pantograph leg configuration is bioinspired (dogs)<br><br>Rope (Dyneema M20) along with a sufficiently stiff spring is used to hold the leg upright<br><br>Aluminium chosen due to its low weight and strength<br><br>One less motor as well as lesser moving parts reduces the mass, inertia and chances of failure<br><br>Leg lengths should be as short as possible such that it can still overcome obstacles (Application of linear forces reduces with leg length |
| **Apply linear forces to the ground** | Passive / Plantar Foot | Plantar feet is chosen to increase surface area of contact |
| **Apply forces to the mechanical interface** | Rigid Attachment | Low platform mass reduces the need for any specialized features |
| **Absorb external forces** | Damper | Simplest solution which leads to a reduction of overall leg mass and inertia (as compared to other solutions) |
| **Recuperate mechanical power** | Tendons | Converts moments on 3D printed part into linear forces (Ananthanarayanan 2012) |
| **Estimate power balance** | Force Sensor | Compliance in the leg reduces the closed-loop force control feedback; there is a need for a force sensor to estimate the forces involved |

**Concept 10 (Heavy Payload)**

| Front View | Side View |
|---|---|
| 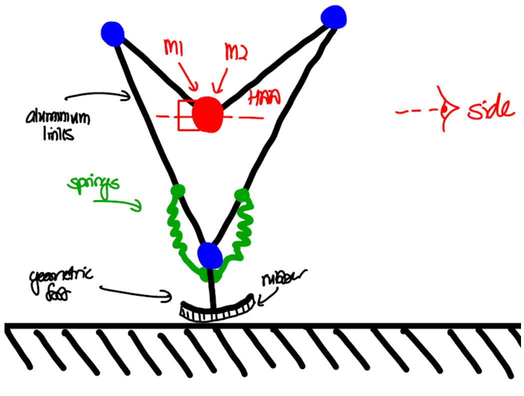 | 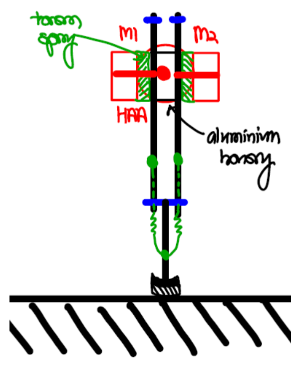 |

| Functions | Chosen Idea | Comments |
|---|---|---|
| **Convert electrical power into mechanical power** | Direct Drive Motor / Gearbox / Serial Spring | Choose a gear ratio such that:<br>● Motor provides sufficient torque<br>● Motor runs at high speeds (efficiency)<br>● Reflected inertia is not amplified too much<br><br>Serial spring allows for force estimation while also protecting the motor |
| **Convey mechanical power to end effector to maintain configuration** | Power from the Motors | Both motors share the load to provide the necessary torque |
| **Convey mechanical power to end effector for locomotion** | Parallel / Motors at Joints / Metals | Parallel leg configuration chosen due to simplicity<br><br>Aluminium chosen due to its low weight and strength<br><br>Leg lengths should be as short as possible such that it can still overcome obstacles (Application of linear forces reduces with leg length |
| **Apply linear forces to the ground** | Passive / Geometric Foot | Geometric feet is chosen to increase surface area of contact as a rolling point of contact |
| **Apply forces to the mechanical interface** | Spring-loaded Joint | Weight savings from this structured can be transferred into implementing better impact mitigation strategies |
| **Absorb external forces** | Damper | Simplest solution which leads to a reduction of overall leg mass and inertia (as compared to other solutions) |
| **Recuperate mechanical power** | Spring-based Mechanism | Foot is spring-loaded to store and release energy during locomotion |
| **Estimate power balance** | Force Sensor | Compliance in the leg reduces the closed-loop force control feedback; there is a need for a force sensor to estimate the forces involved |

## B.5 Evaluation Tree

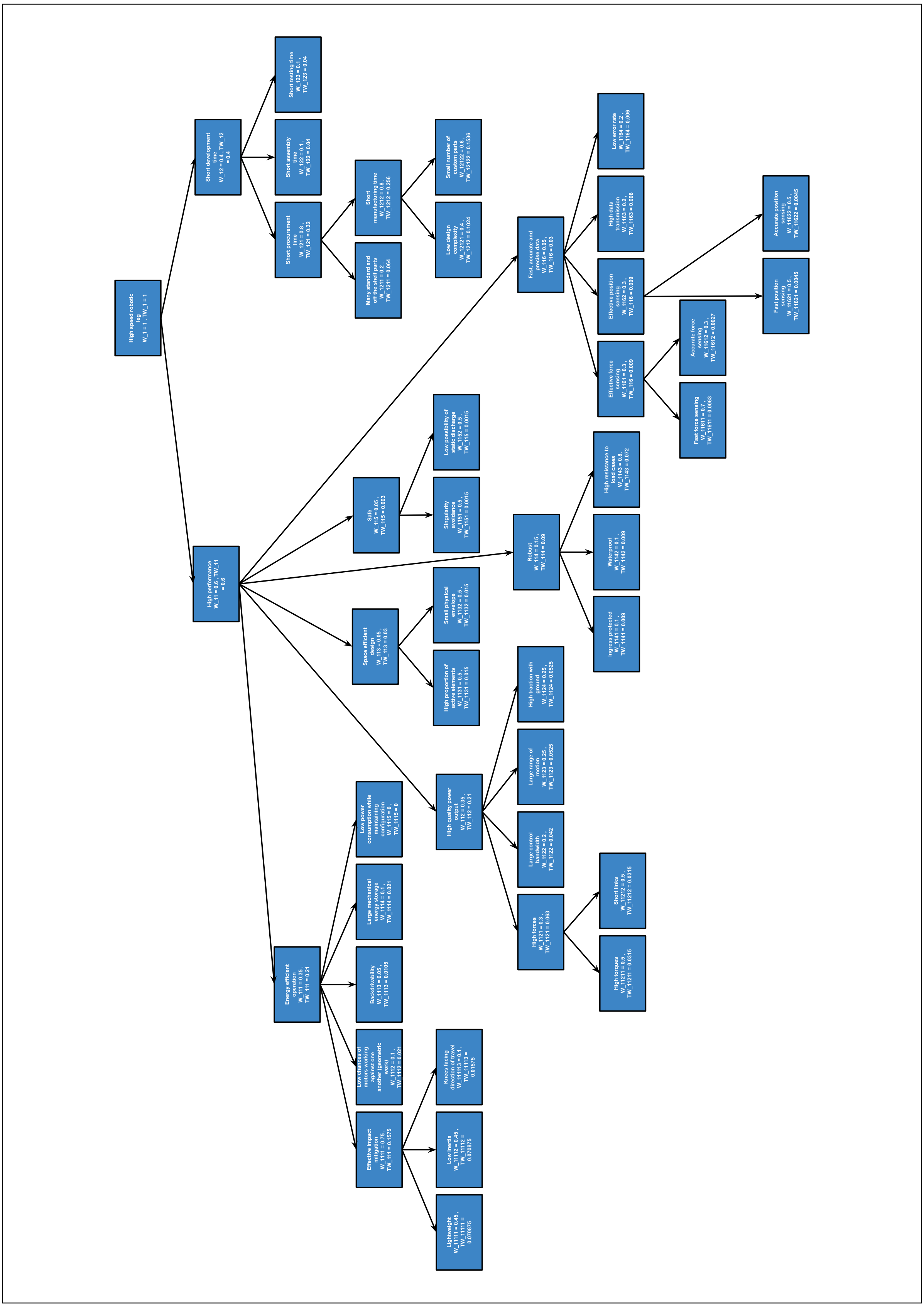

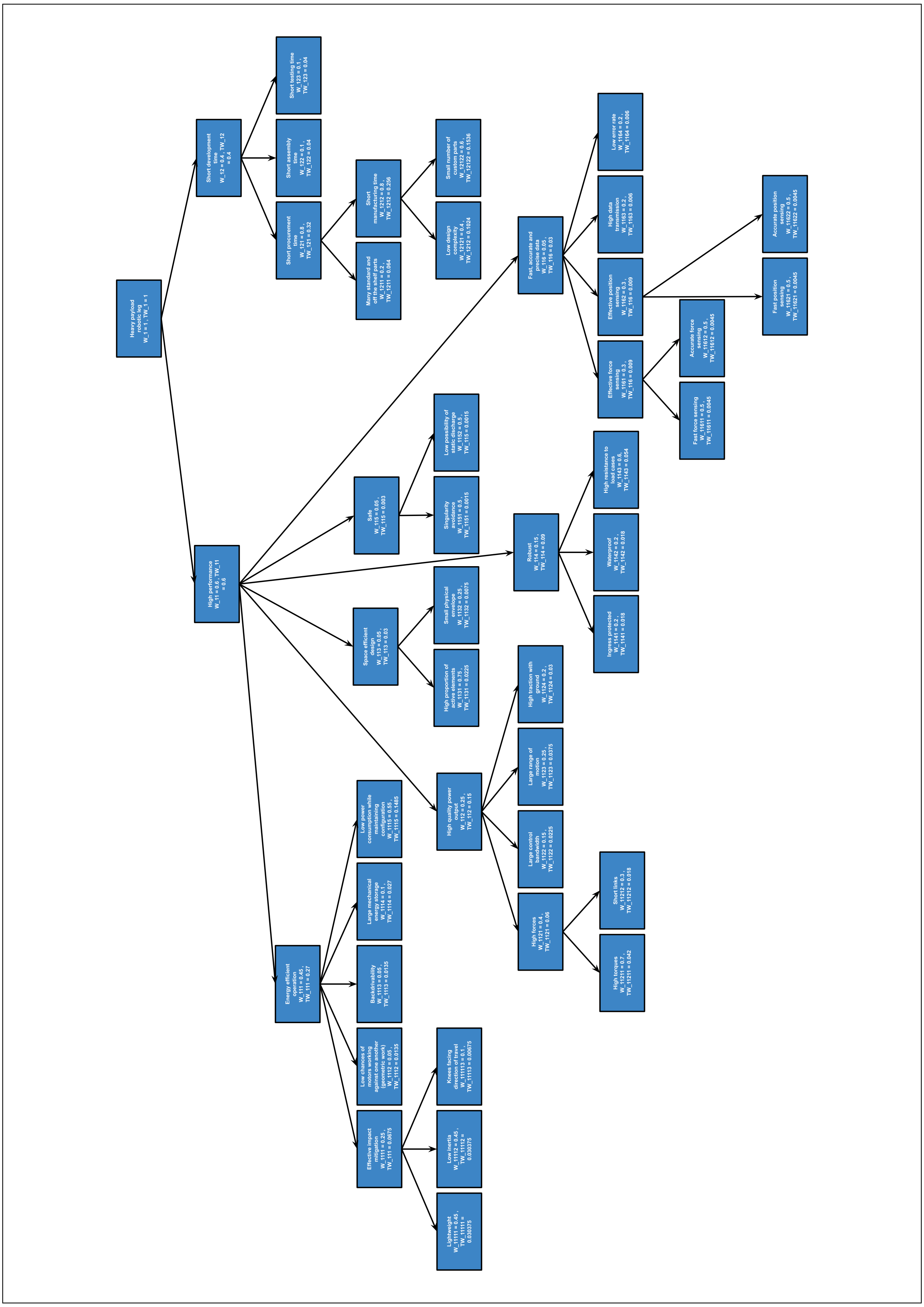

## B.6 Concept Evaluation

| ID | Pointer | HS Weightage | Concept 1 | | Concept 2 | | Concept 3 | | Concept 4 | | Concept 5 | |
|---|---|---|---|---|---|---|---|---|---|---|---|---|
| | | | Raw Score | Weighted Score | Raw Score | Weighted Score | Raw Score | Weighted Score | Raw Score | Weighted Score | Raw Score | Weighted Score |
| **11111** | **Lightweight** | 0.070875 | 6 | 0.42525 | 4 | 0.2835 | 8 | 0.567 | 6 | 0.42525 | 6 | 0.42525 |
| **11112** | **Low inertia** | 0.070875 | 8 | 0.567 | 4 | 0.2835 | 6 | 0.42525 | 6 | 0.42525 | 6 | 0.42525 |
| 11113 | Knees facing direction of travel | 0.01575 | 10 | 0.1575 | 10 | 0.1575 | 10 | 0.1575 | 0 | 0 | 0 | 0 |
| **1112** | **Low chances of motors working against one another (geometric work)** | 0.021 | 10 | 0.21 | 5 | 0.105 | 5 | 0.105 | 10 | 0.21 | 0 | 0 |
| 1113 | Backdrivability | 0.0105 | 6 | 0.063 | 8 | 0.084 | 6 | 0.063 | 4 | 0.042 | 6 | 0.063 |
| **1114** | **Large mechanical energy storage** | 0.021 | 0 | 0 | 6 | 0.126 | 6 | 0.126 | 8 | 0.168 | 6 | 0.126 |
| **1115** | **Low power consumption while maintaining configuration** | 0 | 0 | 0 | 0 | 0 | 0 | 0 | 6 | 0 | 0 | 0 |
| **11211** | **High torques** | 0.0315 | 5 | 0.1575 | 5 | 0.1575 | 5 | 0.1575 | 5 | 0.1575 | 5 | 0.1575 |
| 11212 | Short links | 0.0315 | 4 | 0.126 | 5 | 0.1575 | 5 | 0.1575 | 2 | 0.063 | 4 | 0.126 |
| **1122** | **Large control bandwidth** | 0.042 | 7 | 0.294 | 5 | 0.21 | 5 | 0.21 | 5 | 0.21 | 5 | 0.21 |
| **1123** | **Large range of motion** | 0.0525 | 4 | 0.21 | 2 | 0.105 | 4 | 0.21 | 1 | 0.0525 | 3 | 0.1575 |
| **1124** | **High traction with ground** | 0.0525 | 8 | 0.42 | 6 | 0.315 | 6 | 0.315 | 6 | 0.315 | 6 | 0.315 |
| **1131** | **High proportion of active elements** | 0.015 | 6 | 0.09 | 7 | 0.105 | 7 | 0.105 | 5 | 0.075 | 5 | 0.075 |
| **1132** | **Small physical envelope** | 0.015 | 3 | 0.045 | 4 | 0.06 | 4 | 0.06 | 2 | 0.03 | 4 | 0.06 |
| 1141 | Ingress protected | 0.009 | 4 | 0.036 | 5 | 0.045 | 6 | 0.054 | 4 | 0.036 | 4 | 0.036 |
| 1142 | Waterproof | 0.009 | 4 | 0.036 | 5 | 0.045 | 6 | 0.054 | 4 | 0.036 | 4 | 0.036 |
| **1143** | **High resistance to load cases** | 0.072 | 4 | 0.288 | 6 | 0.432 | 3 | 0.216 | 5 | 0.36 | 6 | 0.432 |
| **1151** | **Singularity avoidance** | 0.015 | 5 | 0.075 | 8 | 0.12 | 5 | 0.075 | 8 | 0.12 | 8 | 0.12 |
| 1152 | Low possibility of static discharge | 0.015 | 5 | 0.075 | 5 | 0.075 | 5 | 0.075 | 5 | 0.075 | 5 | 0.075 |
| 11611 | Fast force sensing | 0.0063 | 8 | 0.0504 | 8 | 0.0504 | 5 | 0.0315 | 5 | 0.0315 | 5 | 0.0315 |
| 11612 | Accurate force sensing | 0.0027 | 4 | 0.0108 | 4 | 0.0108 | 5 | 0.0135 | 5 | 0.0135 | 5 | 0.0135 |
| 11621 | Fast position sensing | 0.0045 | 5 | 0.0225 | 5 | 0.0225 | 5 | 0.0225 | 5 | 0.0225 | 5 | 0.0225 |
| 11622 | Accurate position sensing | 0.0045 | 5 | 0.0225 | 5 | 0.0225 | 5 | 0.0225 | 5 | 0.0225 | 5 | 0.0225 |
| 1163 | High data transmission | 0.006 | 5 | 0.03 | 5 | 0.03 | 5 | 0.03 | 5 | 0.03 | 5 | 0.03 |
| 1164 | Low error rate | 0.006 | 5 | 0.03 | 5 | 0.03 | 5 | 0.03 | 5 | 0.03 | 5 | 0.03 |
| 1211 | Many standard and off the shelf parts | 0.064 | 4 | 0.256 | 2 | 0.128 | 5 | 0.32 | 2 | 0.128 | 2 | 0.128 |
| 12121 | Low design complexity | 0.1024 | 6 | 0.6144 | 3 | 0.3072 | 7 | 0.7168 | 6 | 0.6144 | 5 | 0.512 |
| 12122 | Small number of custom parts | 0.1536 | 4 | 0.6144 | 2 | 0.3072 | 5 | 0.768 | 2 | 0.3072 | 2 | 0.3072 |
| 122 | Short assembly time | 0.04 | 6 | 0.24 | 6 | 0.24 | 8 | 0.32 | 6 | 0.24 | 6 | 0.24 |
| 123 | Short testing time | 0.04 | 5 | 0.2 | 5 | 0.2 | 5 | 0.2 | 5 | 0.2 | 5 | 0.2 |
| **Scores** | | | 156 | 5.36625 | 150 | 4.2151 | 162 | 5.60755 | 143 | 4.4401 | 133 | 4.3767 |
| **Maximum Weighted Score** | | | 5.60755 | | | | | | | | | |

Note:
1) Rating scale is from 1 to 10; 1 being the worst and 10 being the best (relative to ANYmal V2 which is a 5)

| ID | Pointer | HP Weightage | Concept 6 | | Concept 7 | | Concept 8 | | Concept 9 | | Concept 10 | |
|---|---|---|---|---|---|---|---|---|---|---|---|---|
| | | | Raw Score | Weighted Score | Raw Score | Weighted Score | Raw Score | Weighted Score | Raw Score | Weighted Score | Raw Score | Weighted Score |
| **11111** | **Lightweight** | 0.030375 | 4 | 0.1215 | 7 | 0.212625 | 3 | 0.091125 | 6 | 0.18225 | 6 | 0.18225 |
| **11112** | **Low inertia** | 0.030375 | 3 | 0.091125 | 7 | 0.212625 | 4 | 0.1215 | 6 | 0.18225 | 6 | 0.18225 |
| 11113 | Knees facing direction of travel | 0.00675 | 10 | 0.0675 | 10 | 0.0675 | 10 | 0.0675 | 0 | 0 | 0 | 0 |
| **1112** | **Low chances of motors working against one another (geometric work)** | 0.0135 | 10 | 0.135 | 5 | 0.0675 | 10 | 0.135 | 10 | 0.135 | 0 | 0 |
| 1113 | Backdrivability | 0.0135 | 8 | 0.108 | 6 | 0.081 | 6 | 0.081 | 4 | 0.054 | 6 | 0.081 |
| **1114** | **Large mechanical energy storage** | 0.027 | 0 | 0 | 6 | 0.162 | 9 | 0.243 | 8 | 0.216 | 6 | 0.162 |
| **1115** | **Low power consumption while maintaining configuration** | 0.1485 | 0 | 0 | 6 | 0.891 | 9 | 1.3365 | 6 | 0.891 | 0 | 0 |
| **11211** | **High torques** | 0.042 | 5 | 0.21 | 5 | 0.21 | 5 | 0.21 | 5 | 0.21 | 5 | 0.21 |
| 11212 | Short links | 0.018 | 4 | 0.072 | 5 | 0.09 | 4 | 0.072 | 2 | 0.036 | 4 | 0.072 |
| **1122** | **Large control bandwidth** | 0.0225 | 7 | 0.1575 | 5 | 0.1125 | 5 | 0.1125 | 5 | 0.1125 | 5 | 0.1125 |
| **1123** | **Large range of motion** | 0.0375 | 4 | 0.15 | 4 | 0.15 | 4 | 0.15 | 1 | 0.0375 | 3 | 0.1125 |
| **1124** | **High traction with ground** | 0.03 | 8 | 0.24 | 6 | 0.18 | 8 | 0.24 | 6 | 0.18 | 6 | 0.18 |
| **1131** | **High proportion of active elements** | 0.0225 | 4 | 0.09 | 6 | 0.135 | 4 | 0.09 | 5 | 0.1125 | 5 | 0.1125 |
| **1132** | **Small physical envelope** | 0.0075 | 3 | 0.0225 | 4 | 0.03 | 2 | 0.015 | 2 | 0.015 | 4 | 0.03 |
| 1141 | Ingress protected | 0.018 | 4 | 0.072 | 6 | 0.108 | 4 | 0.072 | 4 | 0.072 | 4 | 0.072 |
| 1142 | Waterproof | 0.018 | 4 | 0.072 | 6 | 0.108 | 4 | 0.072 | 4 | 0.072 | 4 | 0.072 |
| **1143** | **High resistance to load cases** | 0.054 | 7 | 0.378 | 4 | 0.216 | 7 | 0.378 | 5 | 0.27 | 6 | 0.324 |
| **1151** | **Singularity avoidance** | 0.015 | 8 | 0.12 | 5 | 0.075 | 6 | 0.09 | 8 | 0.12 | 8 | 0.12 |
| 1152 | Low possibility of static discharge | 0.015 | 5 | 0.075 | 5 | 0.075 | 5 | 0.075 | 5 | 0.075 | 5 | 0.075 |
| 11611 | Fast force sensing | 0.0045 | 8 | 0.036 | 5 | 0.0225 | 5 | 0.0225 | 5 | 0.0225 | 5 | 0.0225 |
| 11612 | Accurate force sensing | 0.0045 | 4 | 0.018 | 5 | 0.0225 | 5 | 0.0225 | 5 | 0.0225 | 5 | 0.0225 |
| 11621 | Fast position sensing | 0.0045 | 5 | 0.0225 | 5 | 0.0225 | 5 | 0.0225 | 5 | 0.0225 | 5 | 0.0225 |
| 11622 | Accurate position sensing | 0.0045 | 5 | 0.0225 | 5 | 0.0225 | 5 | 0.0225 | 5 | 0.0225 | 5 | 0.0225 |
| 1163 | High data transmission | 0.006 | 5 | 0.03 | 5 | 0.03 | 5 | 0.03 | 5 | 0.03 | 5 | 0.03 |
| 1164 | Low error rate | 0.006 | 5 | 0.03 | 5 | 0.03 | 5 | 0.03 | 5 | 0.03 | 5 | 0.03 |
| 1211 | Many standard and off the shelf parts | 0.064 | 3 | 0.192 | 4 | 0.256 | 2 | 0.128 | 2 | 0.128 | 2 | 0.128 |
| 12121 | Low design complexity | 0.1024 | 6 | 0.6144 | 6 | 0.6144 | 5 | 0.512 | 6 | 0.6144 | 5 | 0.512 |
| 12122 | Small number of custom parts | 0.1536 | 3 | 0.4608 | 4 | 0.6144 | 2 | 0.3072 | 2 | 0.3072 | 2 | 0.3072 |
| 122 | Short assembly time | 0.04 | 6 | 0.24 | 7 | 0.28 | 5 | 0.2 | 6 | 0.24 | 6 | 0.24 |
| 123 | Short testing time | 0.04 | 5 | 0.2 | 5 | 0.2 | 5 | 0.2 | 5 | 0.2 | 5 | 0.2 |
| **Scores** | | | 153 | 4.048325 | 164 | 5.29855 | 158 | 5.149325 | 143 | 4.6126 | 133 | 3.6372 |
| **Maximum Weighted Score** | | | 5.29855 | | | | | | | | | |

Note:
1) Rating scale is from 1 to 10; 1 being the worst and 10 being the best (relative to ANYmal V2 which is a 5)

## B.7 Detailed Leg Design Concepts

**Concept 1.1 (High Speed)**

**Front View**

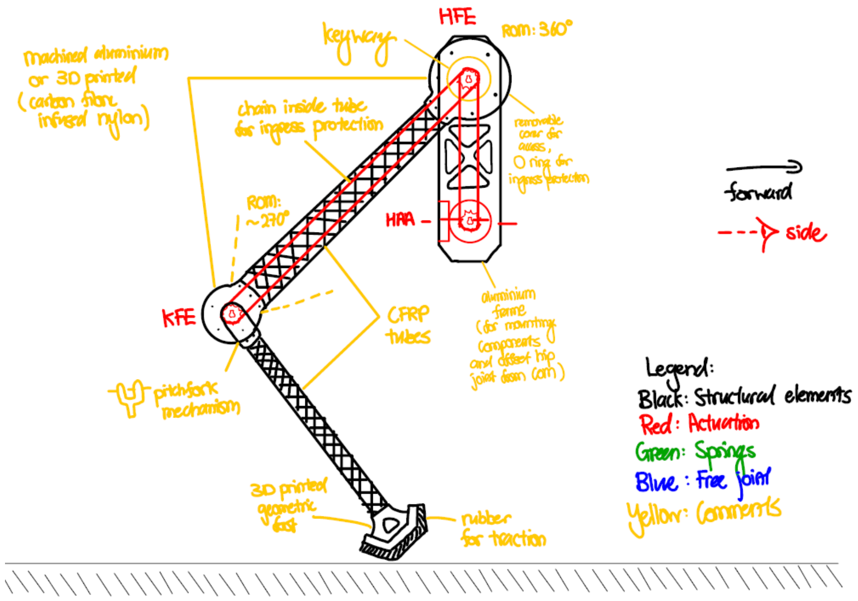


**Side View**

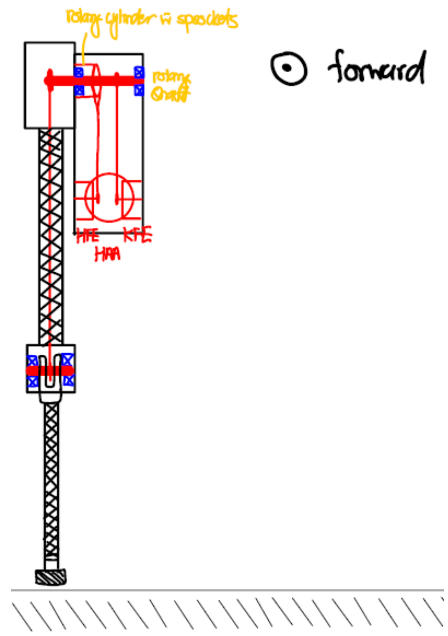

| | |
|---|---|
| **Description** | This high speed leg design strives for design simplicity (no compliant elements), effective impact mitigation (lightweight, low link inertia) and a better power balance between the various actuators (spider configuration) |

| Functions | Chosen Idea | Comments |
|---|---|---|
| **Convert electrical power into mechanical power** | Direct Drive Motor / Gearbox / No Spring | Choose a gear ratio such that:<br>● Motor provides sufficient torque<br>● Motor runs at high speeds (efficiency)<br>● Reflected inertia is not amplified too much |
| **Convey mechanical power to end effector to maintain configuration** | Power from Motors | Function is not particularly important for high speed<br><br>Neglecting the need of a specialized mechanism for this function leads to a reduction of overall leg mass and inertia |
| **Convey mechanical power to end effector for locomotion** | Serial / Chain / Composites | Spider configuration as it balances the actuator powers better (Abate 2016); knee facing forward so as to align the foot with the light axis (Abate 2015)<br><br>Chain is used so as to relocate the knee motor higher up the limb as well as to use standard parts; chain is used instead of belt due to higher tolerance for greater loads and simpler overall mechanism (e.g. do not need idlers)<br><br>Carbon fibre is used due to rigidity and availability; chain and other cables (e.g. cables for knee joint angle data) can placed within the tube for ingress protection<br><br>Leg lengths should be as short as possible such that it can still overcome obstacles (Application of linear forces reduces with leg length) |
| **Apply linear forces to the ground** | Passive / Geometric Foot | Geometric feet is chosen so as to increase surface area of contact<br><br>Minimal compliance in the leg aids in maximizing the closed-loop force control bandwidth (Wensing 2017) |
| **Apply forces to the mechanical interface** | Rigid Attachment | Low platform mass reduces the need for any specialized features |
| **Absorb external forces** | Damper | Simplest solution which leads to a reduction of overall leg mass and inertia (as compared to other solutions) |
| **Recuperate mechanical power** | Direct Transmission to Motors | Relying on backdrivability |
| **Estimate power balance** | Proprioceptive | Low gear ratio and low inertia leg permits this method of force estimation; inverse dynamics (Wensing 2017) |

**Concept 3.1 (High Speed)**

**Front View**

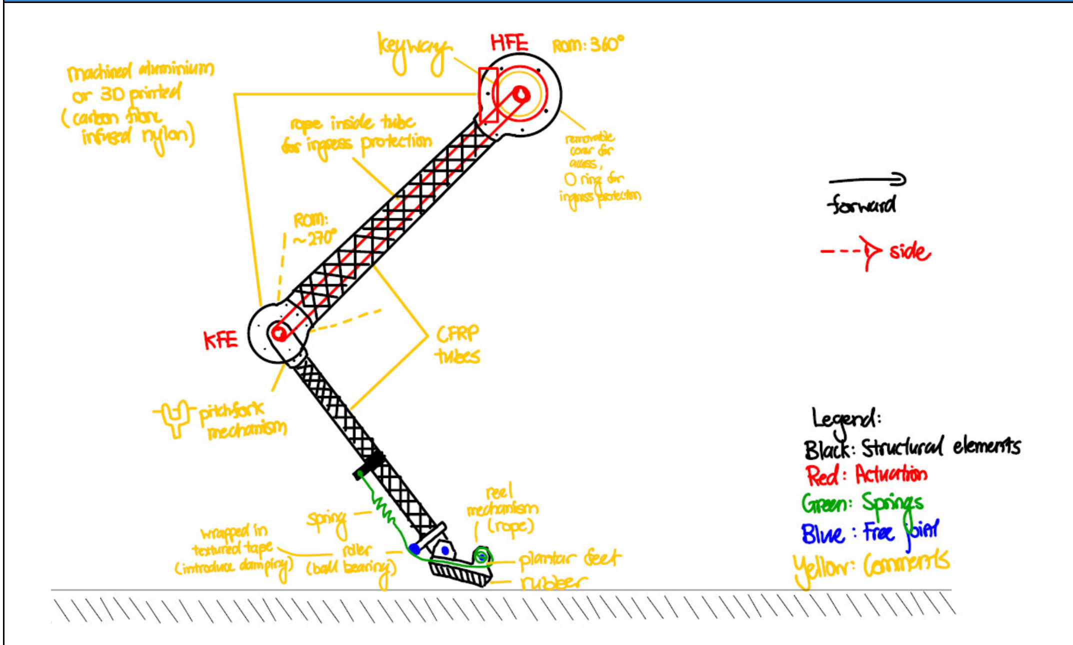


**Side View**

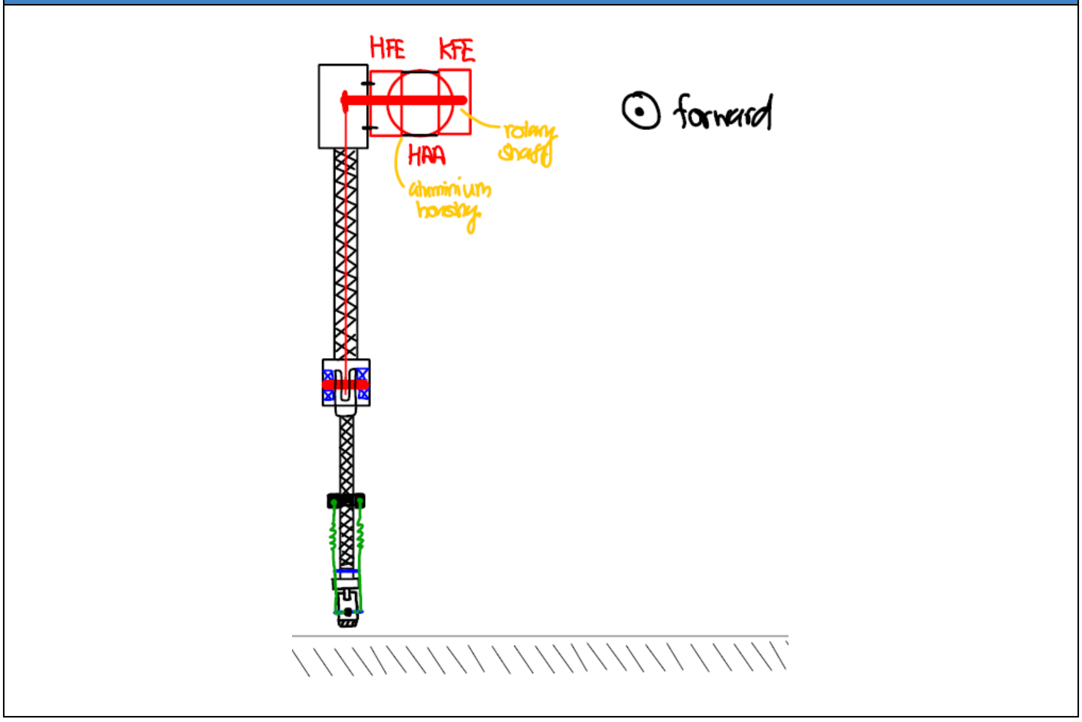

| Description | This high speed leg design strives for design simplicity (mammalian configuration) while incorporating an additional impact mitigation mechanism (spring-loaded feet) |
|---|---|

| Functions | Chosen Idea | Comments |
|---|---|---|
| **Convert electrical power into mechanical power** | Direct Drive Motor / Gearbox / No Spring | Choose a gear ratio such that:<br>● Motor provides sufficient torque<br>● Motor runs at high speeds (efficiency)<br>● Reflected inertia is not amplified too much |
| **Convey mechanical power to end effector to maintain configuration** | Power from Motors | Function is not particularly important for high speed<br><br>Neglecting the need of a specialized mechanism for this function leads to a reduction of overall leg mass and inertia |
| **Convey mechanical power to end effector for locomotion** | Serial-Parallel / Rope / Composites | Serial 2 link mammalian configuration is chosen due to its simplicity; knee facing forward so as to align the foot with the light axis (Abate 2015)<br><br>Rope so as to relocate the knee motor higher up the limb<br><br>Carbon fibre is used due to rigidity and availability; rope and other cables are placed within the limb for ingress protection<br><br>Leg lengths should be as short as possible such that it can still overcome obstacles (Application of linear forces reduces with leg length) |
| **Apply linear forces to the ground** | Passive / Plantar Foot | Spring-loaded plantar foot adds compliance so as to mitigate impacts while also storing mechanical energy<br><br>Plantar feet is chosen to increase surface area of contact |
| **Apply forces to the mechanical interface** | Rigid Attachment | Low platform mass reduces the need for any specialized features |
| **Absorb external forces** | Spring-based Mechanism | Passive spring-loaded foot stores and releases energy in an open loop manner<br><br>It is possible to wrap the rollers in the mechanism with a textured material so as to introduce damping into the spring-mass system; reduces unnecessary oscillations |
| **Recuperate mechanical power** | Spring-based Mechanism | Passive spring-loaded foot stores and releases energy in an open loop manner<br><br>It is possible to wrap the rollers in the mechanism with a textured material so as to introduce damping into the spring-mass system; reduces unnecessary oscillations |
| **Estimate power balance** | Force Sensor | Compliance in the leg reduces the closed-loop force control feedback; there is a need for a force sensor to estimate the forces involved |

**Concept 7.1 (Heavy Payload)**

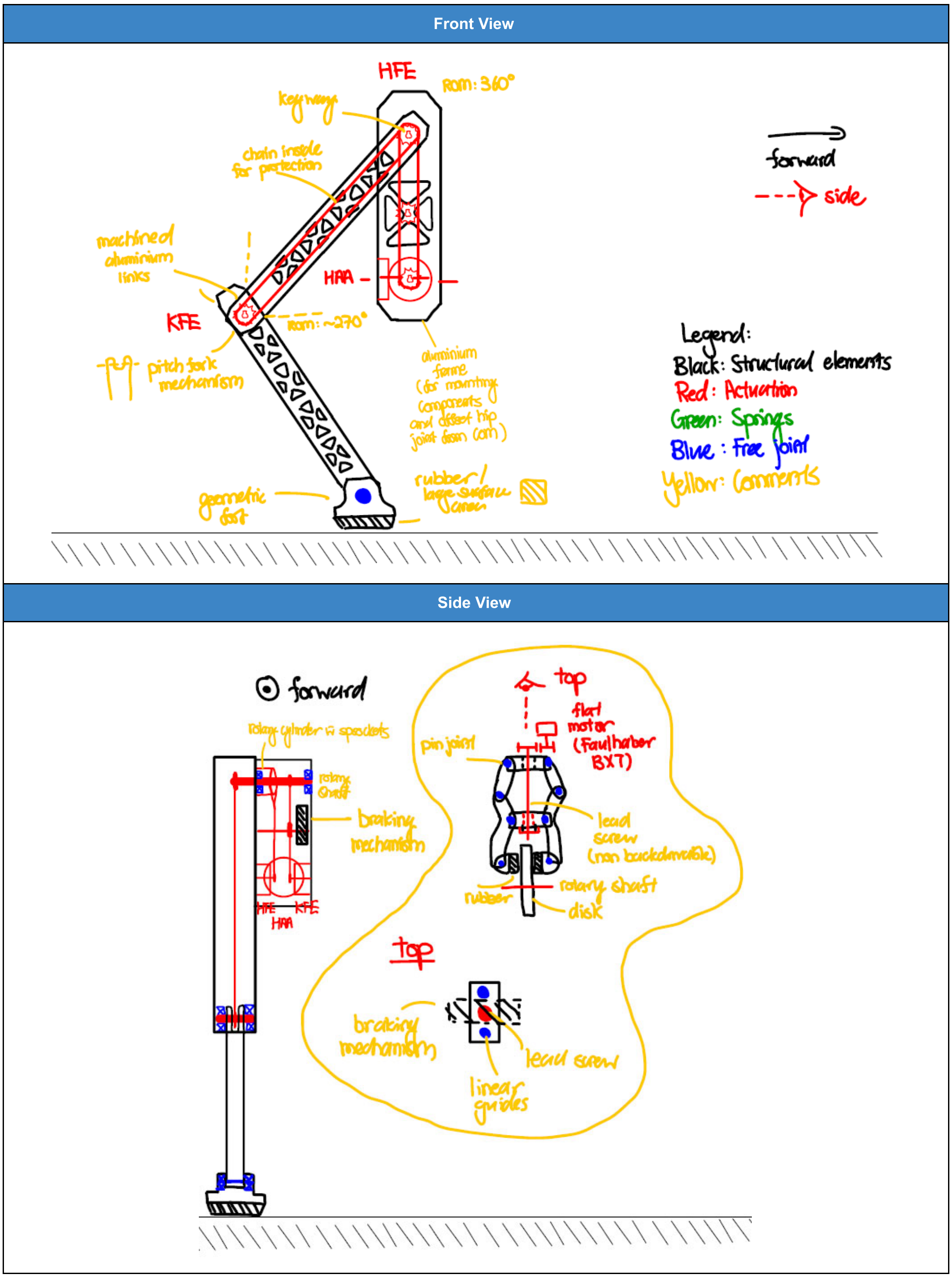

| | |
|---|---|
| **Description** | This heavy payload leg design strives for design simplicity (no compliant elements) while incorporating an active braking mechanism, hence enabling it to maintain any arbitrary configuration with a low power consumption |

| Functions | Chosen Idea | Comments |
|---|---|---|
| **Convert electrical power into mechanical power** | Direct Drive Motor / Gearbox / No Spring | Choose a gear ratio such that:<br>● Motor provides sufficient torque<br>● Motor runs at high speeds (efficiency)<br>● Reflected inertia is not amplified too much |
| **Convey mechanical power to end effector to maintain configuration** | Brakes | This leg relies on an active brake that jams the transmission system so as to maintain its configuration (Mechanism X channel on YouTube)<br><br>The braking mechanism is based on a clamping mechanism that is driven by a lead screw (non backdrivable); it is similar to a bicycle brake |
| **Convey mechanical power to end effector for locomotion** | Serial / Chain / Metals | Spider configuration as it balances the actuator powers better (Abate 2016); knee facing forward so as to align the foot with the light axis (Abate 2015)<br><br>Chain is used so as to relocate the knee motor higher up the limb as well as to use standard parts; chain is used instead of belt due to higher tolerance for greater loads and simpler overall mechanism (e.g. do not need idlers)<br><br>Aluminium chosen due to its low weight yet high strength<br><br>Leg lengths should be as short as possible such that it can still overcome obstacles (Application of linear forces reduces with leg length) |
| **Apply linear forces to the ground** | Passive / Geometric Foot | Geometric feet is chosen to increase contact surface area |
| **Apply forces to the mechanical interface** | Rigid Attachment | This keeps the design complexity of the leg low |
| **Absorb external forces** | Damper | Simplest solution which leads to a reduction of overall leg mass and inertia (as compared to other solutions) |
| **Recuperate mechanical power** | Direct Transmission to Motors | Relying on backdrivability |
| **Estimate power balance** | Force Sensor | Since there is no compliant element in the leg, it implies that a proprioceptive method of estimating the forces involved may be used<br><br>However, it is advisable to have a force sensor here so as not to damage the environment which the leg is in |

**Concept 8.1 (Heavy Payload)**

**Front View**

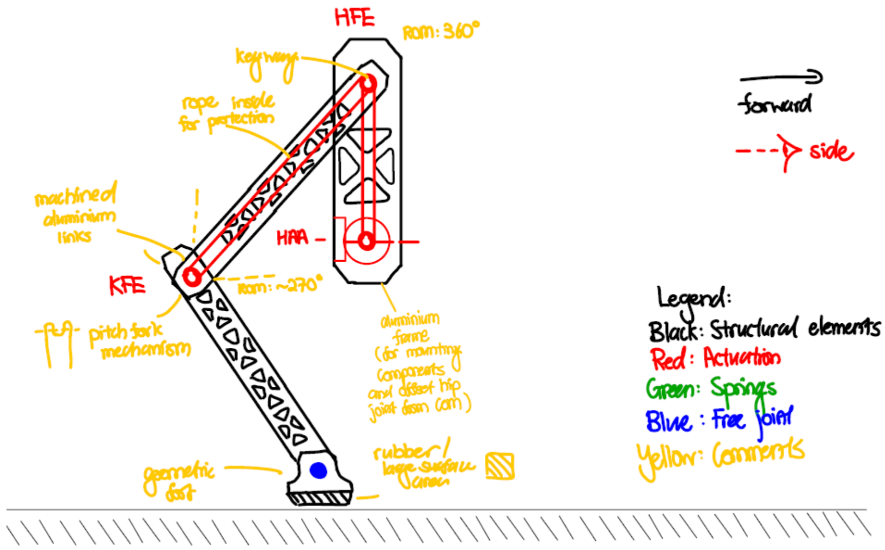


**Side View**

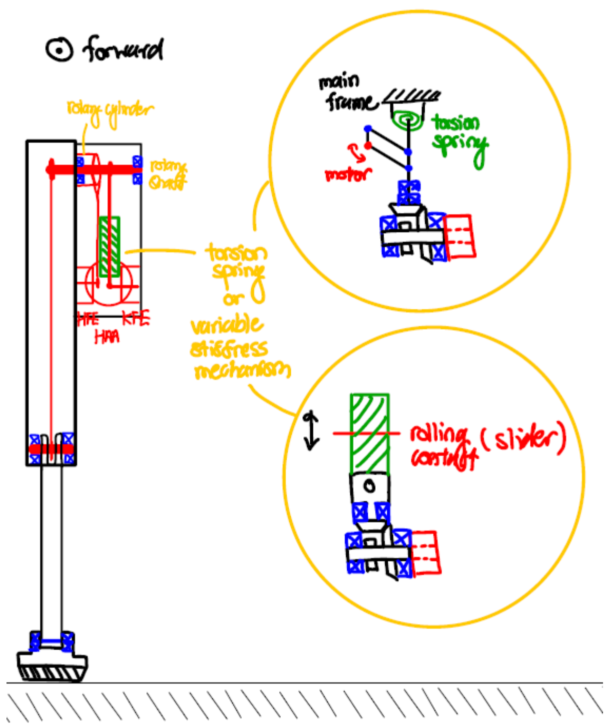

| Description | This heavy payload leg design seeks to take advantage of compliant elements to maintain an arbitrary configuration with a low power consumption |
|---|---|

| Functions | Chosen Idea | Comments |
|---|---|---|
| **Convert electrical power into mechanical power** | Direct Drive Motor / Gearbox / Parallel Spring | Choose a gear ratio such that:<br>• Motor provides sufficient torque<br>• Motor runs at high speeds (efficiency)<br>• Reflected inertia is not amplified too much<br><br>Parallel spring are either one of the two spring-based mechanisms explained below |
| **Convey mechanical power to end effector to maintain configuration** | Spring-based Mechanism | Two parallel springs mechanisms are proposed:<br><br>i) A simple torsion spring which can be engaged via a clutch at an arbitrary configuration<br><br>ii) A variable stiffness mechanism which is able to output a wide range of stiffnesses; changing the static configuration of the leg is synonymous with changing the stiffness of the mechanism (Chong 2017) |
| **Convey mechanical power to end effector for locomotion** | Serial / Rope / Metals | Spider configuration as it balances the actuator powers better (Abate 2016); knee facing forward so as to align the foot with the light axis (Abate 2015)<br><br>Rope is used so as to relocate the knee motor higher up the limb<br><br>Aluminium chosen due to its low weight yet high strength<br><br>Leg lengths should be as short as possible such that it can still overcome obstacles (Application of linear forces reduces with leg length) |
| **Apply linear forces to the ground** | Passive / Geometric Foot | Geometric feet is chosen to increase contact surface area |
| **Apply forces to the mechanical interface** | Rigid Attachment | This keeps the design complexity of the leg low |
| **Absorb external forces** | Spring-based Mechanism | Using the parallel spring (if engaged) |
| **Recuperate mechanical power** | Spring-based Mechanism | Using the parallel spring (if engaged) |
| **Estimate power balance** | Force Sensors | Compliance in the leg reduces the closed-loop force control feedback; there is a need for a force sensor to estimate the forces involved |

## B.8 Design Framework

**Overview**

This spreadsheet analyzes potential leg designs for the heavy payload robot as shown on the right

**Assumptions / Design Constraints**

1. The upper body of Halodi Eve is used as the torso
2. ANYmal C is used as the trunk
3. The initial leg design used will be based on Concept 7.3++
4. NEO actuators with limited additional gearing (mechanical advantage: [1,2] will be considered)
5. Sagittal plane (2D, X-Z coordinates) analysis; the robot is assumed to be symmetric about the X-Z plane
6. Hip height w.r.t. to the ground is a free design parameter; set to 0.6m

**Analysis Procedure**

1. Construct a low fidelity CAD model (intial design guess)
2. Static analysis (this spreadsheet)
3. Dynamic analysis (Towr, Vitruvio)
4. Obtain parameters required to do up a refined CAD model

**Sheets**

1. Overview: Provides an outline of the spreadsheet
2. Static Analysis (Initial Design Guess)
3. Dynamic Analysis (Initial Design Guess)
4. Static Analysis (Optimized, Engineered Legs)
5. Dynamic Analysis (Engineered Leg)

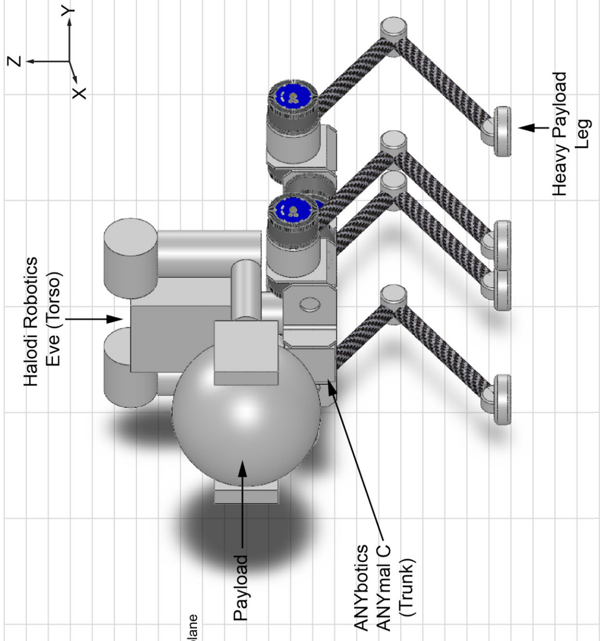

**Mass Distribution**

| Leg Components | Mass (kg) |
|---|---|
| HFE Actuator (NEO, geared) | 4.73 |
| KFE Actuator (NEO, geared) | 4.73 |
| AFE Actuator (NEO, ungeared) | 4.18 |
| Actuator Mounts | 1 |
| Knee Joint | 1 |
| Kendrion Brake (Size 09) | 1.2 |
| Ankle Joint | 1 |
| Distal Joint | 0.5 |
| Cylinders (CFRP, Aluminium) | 0.5 |
| Total Leg Mass | 18.84 |

| Subsystems | Mass (kg) |
|---|---|
| 4 Legs | 75.36 |
| ANYmal C Trunk | 11 |
| 2 Halodi Eve Arms | 19 |
| Halodi Eve Torso | 17 |
| Payload | 15 |
| m (Total robot mass) | 137.36 |

**Comments**
1. Blue boxes are inputs
2. Light blue ones are normal while dark blue ones are critical
3. Left foreleg is being shown

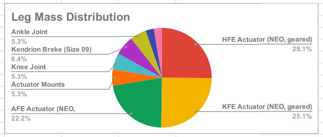


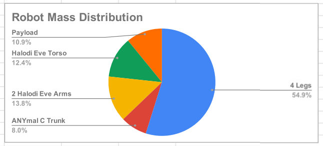


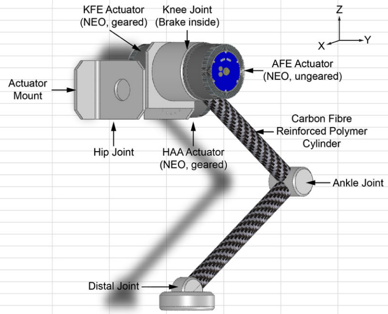


**Initial Leg Design Guess**

| Parameters | Value | Units |
|---|---|---|
| l_t (Thigh) | 0.05 | m |
| l_e (End effector) | 0.05 | m |

| Inputs | Value | Units |
|---|---|---|
| h_h (Hip height) | 0.6 | m |
| l_s (Shank) | 0.5 | m |
| l_f (Foot) | 0.5 | m |

| Output | Value | Units |
|---|---|---|
| θ_1 | 36.86989765 | ° |
| θ_2 | 36.86989765 | ° |

**Assumptions**
1. Based on Concept 7.3++ (Spider configuration with geometric end effector)
2. Hip height and link lengths are arbitrarily set
3. Stance phase with distal joint directly below knee joint

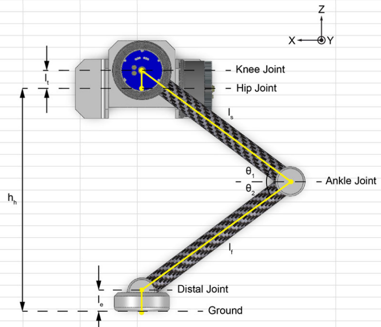


**Hip Heights**

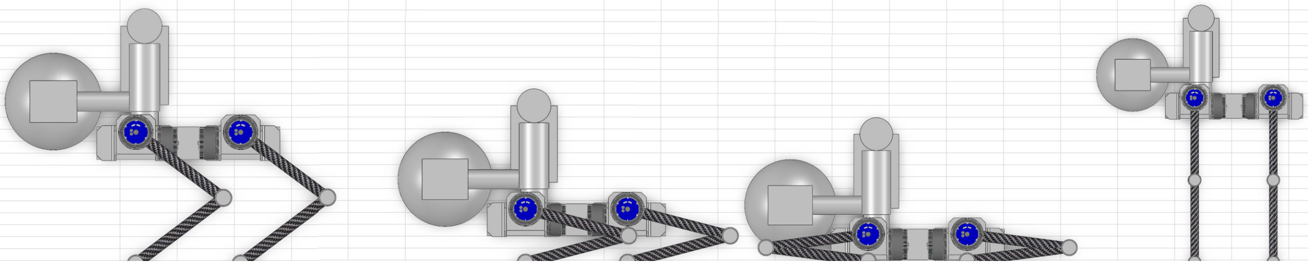

| Description | Hip Height (m) | |
|---|---|---|
| Left: Nominal stance; ankle joint directly below hip joint | 0.6 | |
| Middle Left: Minimum hip height in M configuration | 0.25 | Derived from CAD; minimum hip height that results in no collision |
| Middle Right: Minimum height in any configuration | 0.13 | Derived from CAD; minimum hip height that results in no collision |
| Right: Maximum hip height while maintaining configuration | 1 | |

**CoM Location and Reachability**

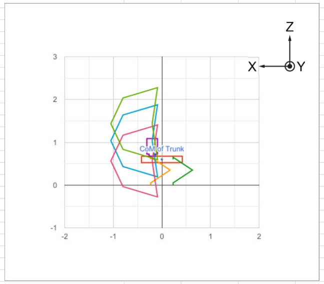


| Parameters | Value | Units | |
|---|---|---|---|
| ANYmal C Trunk Length (X) | 0.84 | m | |
| ANYmal C Trunk Height (Z) | 0.15 | m | |
| Hip attachment point displacement (X) | 0.23 | m | Derived from CAD, with respect to center of trunk |
| CoM of Trunk and Legs (X) | -0.02398179 | m | Derived from CAD, with respect to center of trunk |
| CoM of Trunk and Legs (Z) | -0.00578254 | m | Derived from CAD, with respect to center of trunk |
| Torso center of attachment displacement from Trunk CoM | 0.2 | m | |
| Halodi Eve Torso Length (X) | 0.22 | m | |
| Halodi Eve Torso Height (Z) | 0.36 | m | |
| Halodi Eve Torso Interface Diameter (X/Z) | 0.125 | m | |
| Halodi Eve Torso Interface Height (Z) | 0.1 | m | |
| Halodi Eve Arm Length (X) | 0.85 | m | To fingertips = 0.85m ; to palm = 0.7m |
| CoM of Torso and Payload (X, w.r.t center of attachment) | 0.14603917 | m | Derived from CAD, with arms at 90° |
| CoM of Torso and Payload (Z, w.r.t center of attachment) | 0.21892155 | m | Derived from CAD, with arms at 90° |
| CoM of Robot (X) | 0.1134022298 | m | With reference to center of trunk |
| CoM of Robot (Z) | 0.105493731 | m | With reference to center of trunk |

**Comments**

1. The shoulders of Halodi Eve have a joint range of ±97.5° (flexion,extension)
2. The hip of Halodi Eve have a joint range of ±30° (rotation); not considered in this 2D analysis

| Plotting Points | X Coordinates | Z Coordinates |
|---|---|---|
| CoM of Trunk | 0 | 0.6 |
| Top left of Trunk | -0.42 | 0.675 |
| Top right of Trunk | 0.42 | 0.675 |
| Bottom right of Trunk | 0.42 | 0.525 |
| Bottom left of Trunk | -0.42 | 0.525 |
| Top left of Trunk | -0.42 | 0.675 |
| Hip joint of Foreleg | -0.23 | 0.6 |
| Knee joint of Foreleg | -0.23 | 0.65 |
| Ankle joint of Foreleg | 0.17 | 0.35 |
| Distal joint of Foreleg | -0.23 | 0.05 |
| End effector of Foreleg | -0.23 | 0 |
| Hip joint of Hindleg | 0.23 | 0.6 |
| Knee joint of Hindleg | 0.23 | 0.65 |
| Ankle joint of Hindleg | 0.63 | 0.35 |
| Distal joint of Hindleg | 0.23 | 0.05 |
| End effector of Hindleg | 0.23 | 0 |
| Torso center of attachment | -0.2 | 0.675 |
| Bottom Left of Torso Interface | -0.2625 | 0.675 |
| Top Left of Torso Interface | -0.2625 | 0.725 |
| Bottom Left of Torso | -0.31 | 0.725 |
| Top Left of Torso | -0.31 | 1.085 |
| Top Right of Torso | -0.09 | 1.085 |
| Bottom Right of Torso | -0.09 | 0.725 |
| Top Right of Torso Interface | -0.1375 | 0.725 |
| Bottom Right of Torso Interface | -0.1375 | 0.675 |
| Torso center of attachment | -0.2 | 0.675 |
| Arm center of rotation (nominal) | -0.2 | 1.035 |
| Arm rotation lower limit (nominal) | -0.08905273661 | 0.1922718678 |
| Arm rotation bottom left limit (nominal) | -0.801040764 | 0.433959236 |
| Arm rotation left limit (nominal) | -1.05 | 1.035 |
| Arm rotation top left limit (nominal) | -0.801040764 | 1.636040764 |
| Arm rotation upper limit (nominal) | -0.08905273661 | 1.877728132 |
| Arm center of rotation (nominal) | -0.2 | 1.035 |
| Arm center of rotation (lowest stance) | -0.2 | 0.565 |
| Arm rotation lower limit (lowest stance) | -0.08905273661 | -0.2777281322 |
| Arm rotation bottom left limit (lowest stance) | -0.801040764 | -0.03604076401 |
| Arm rotation left limit (lowest stance) | -1.05 | 0.565 |
| Arm rotation top left limit (lowest stance) | -0.801040764 | 1.166040764 |
| Arm rotation upper limit (lowest stance) | -0.08905273661 | 1.407728132 |
| Arm center of rotation (lowest stance) | -0.2 | 0.565 |
| Arm center of rotation (highest stance) | -0.2 | 1.435 |
| Arm rotation lower limit (highest stance) | -0.08905273661 | 0.5922718678 |
| Arm rotation bottom left limit (highest stance) | -0.801040764 | 0.833959236 |
| Arm rotation left limit (highest stance) | -1.05 | 1.435 |
| Arm rotation top left limit (highest stance) | -0.801040764 | 2.036040764 |
| Arm rotation upper limit (highest stance) | -0.08905273661 | 2.277728132 |
| Arm center of rotation (highest stance) | -0.2 | 1.435 |

**Torques during stance**

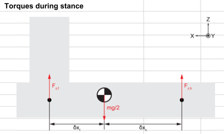


| Parameters | Value | Units | |
|---|---|---|---|
| g (Gravitational acceleration) | 9.81 | ms^-2 | |
| δx_f (Moment arm from CoM to foreleg) | 0.1165977702 | m | |
| δx_h (Moment arm from CoM to hindleg) | 0.3434022298 | m | |
| F_z,f = (δx_h/(δx_f+δx_h))(mg/2) | 502.9728849 | N | Obtained using the principle of moments |
| F_z,h = (δx_f/(δx_f+δx_h))(mg/2) | 170.7779151 | N | Obtained using the principle of moments |
| NEO Actuator (Ungeared) Peak Torque | 34.84848485 | Nm | |

| θ = θ_1 = θ_2 | τ_a,a (Nm) | τ_f,a (Nm) | τ_b,07 (Nm) | τ_b,08 (Nm) | τ_b,09 (Nm) | τ_b,10 (Nm) | h_h (m) | h_s (m) |
|---|---|---|---|---|---|---|---|---|
| 0 | 287.5 | 251.4864424 | 107.25 | 189.75 | 255.75 | 412.5 | 0 | 0.535 |
| 5 | 287.5 | 250.5294606 | 107.25 | 189.75 | 255.75 | 412.5 | 0.08715574275 | 0.6221557427 |
| 10 | 287.5 | 247.6657983 | 107.25 | 189.75 | 255.75 | 412.5 | 0.1736481777 | 0.7086481777 |
| 15 | 287.5 | 242.9172497 | 107.25 | 189.75 | 255.75 | 412.5 | 0.2588190451 | 0.7938190451 |
| 20 | 287.5 | 236.3199542 | 107.25 | 189.75 | 255.75 | 412.5 | 0.3420201433 | 0.8770201433 |
| 25 | 287.5 | 227.9241211 | 107.25 | 189.75 | 255.75 | 412.5 | 0.4226182617 | 0.9576182617 |
| 30 | 287.5 | 217.7936479 | 107.25 | 189.75 | 255.75 | 412.5 | 0.5 | 1.035 |
| 35 | 287.5 | 206.0056334 | 107.25 | 189.75 | 255.75 | 412.5 | 0.5735764364 | 1.108576436 |
| 40 | 287.5 | 192.6497918 | 107.25 | 189.75 | 255.75 | 412.5 | 0.6427876097 | 1.17778761 |
| 45 | 287.5 | 177.8277688 | 107.25 | 189.75 | 255.75 | 412.5 | 0.7071067812 | 1.242106781 |
| 50 | 287.5 | 161.6523692 | 107.25 | 189.75 | 255.75 | 412.5 | 0.7660444431 | 1.301044443 |
| 55 | 287.5 | 144.2466974 | 107.25 | 189.75 | 255.75 | 412.5 | 0.8191520443 | 1.354152044 |
| 60 | 287.5 | 125.7432212 | 107.25 | 189.75 | 255.75 | 412.5 | 0.8660254038 | 1.401025404 |
| 65 | 287.5 | 106.2827632 | 107.25 | 189.75 | 255.75 | 412.5 | 0.906307787 | 1.441307787 |
| 70 | 287.5 | 86.01342909 | 107.25 | 189.75 | 255.75 | 412.5 | 0.9396926208 | 1.474692621 |
| 75 | 287.5 | 65.08948089 | 107.25 | 189.75 | 255.75 | 412.5 | 0.9659258263 | 1.500925826 |
| 80 | 287.5 | 43.67016244 | 107.25 | 189.75 | 255.75 | 412.5 | 0.984807753 | 1.519807753 |
| 85 | 287.5 | 21.91848768 | 107.25 | 189.75 | 255.75 | 412.5 | 0.9961946981 | 1.531194698 |

| | | |
|---|---|---|
| Transmission mechanical advantage | 1.25 | |
| Planetary Gear mechanical advantage | 6.6 | |
| τ_a,a (Allowable ankle joint peak torque) | 287.5 | Nm |
| | | |
| **Sizing Permernant Magnet Brakes** | | |
| | | |
| **Kendrion Permernant Magnet Brake High Torque Line** | **Mass (kg)** | **Power (W)** |
| Size 07 | 0.6 | 14 |
| Size 08 | 1.15 | 18 |
| Size 09 | 1.2 | 19 |
| Size 10 | 1.86 | 22.5 |
| | | |
| **Stall Torques** | **Value** | **Units** |
| Size 07 | 13 | Nm |
| τ_b,07 (Size 07 Effective) | 107.25 | Nm |
| Size 08 | 23 | Nm |
| τ_b,08 (Size 08 Effective) | 189.75 | Nm |
| Size 09 | 31 | Nm |
| τ_b,09 (Size 09 Effective) | 255.75 | Nm |
| Size 10 | 50 | Nm |
| τ_b,10 (Size 10 Effective) | 412.5 | Nm |

| | | | | | | | | |
|---|---|---|---|---|---|---|---|---|
| 90 | 287.5 | 0 | 107.25 | 189.75 | 255.75 | 412.5 | 1 | 1.535 |
| | | | | | | | | |
| **θ = θ_1 = θ_2** | **τ_a,a (Nm)** | **τ_h,a (Nm)** | **τ_b,07 (Nm)** | **τ_b,08 (Nm)** | **τ_b,09 (Nm)** | **τ_b,10 (Nm)** | **h_h (m)** | **h_s (m)** |
| 0 | 287.5 | 85.38895755 | 107.25 | 189.75 | 255.75 | 412.5 | 0 | 0.535 |
| 5 | 287.5 | 85.06402679 | 107.25 | 189.75 | 255.75 | 412.5 | 0.08715574275 | 0.6221557427 |
| 10 | 287.5 | 84.09170742 | 107.25 | 189.75 | 255.75 | 412.5 | 0.1736481777 | 0.7086481777 |
| 15 | 287.5 | 82.47939938 | 107.25 | 189.75 | 255.75 | 412.5 | 0.2588190451 | 0.7938190451 |
| 20 | 287.5 | 80.23937331 | 107.25 | 189.75 | 255.75 | 412.5 | 0.3420201433 | 0.8770201433 |
| 25 | 287.5 | 77.38867716 | 107.25 | 189.75 | 255.75 | 412.5 | 0.4226182617 | 0.9576182617 |
| 30 | 287.5 | 73.94900644 | 107.25 | 189.75 | 255.75 | 412.5 | 0.5 | 1.035 |
| 35 | 287.5 | 69.94653914 | 107.25 | 189.75 | 255.75 | 412.5 | 0.5735764364 | 1.108576436 |
| 40 | 287.5 | 65.41173644 | 107.25 | 189.75 | 255.75 | 412.5 | 0.6427876097 | 1.17778761 |
| 45 | 287.5 | 60.37911092 | 107.25 | 189.75 | 255.75 | 412.5 | 0.7071067812 | 1.242106781 |
| 50 | 287.5 | 54.88696392 | 107.25 | 189.75 | 255.75 | 412.5 | 0.7660444431 | 1.301044443 |
| 55 | 287.5 | 48.97709398 | 107.25 | 189.75 | 255.75 | 412.5 | 0.8191520443 | 1.354152044 |
| 60 | 287.5 | 42.69447878 | 107.25 | 189.75 | 255.75 | 412.5 | 0.8660254038 | 1.401025404 |
| 65 | 287.5 | 36.08693281 | 107.25 | 189.75 | 255.75 | 412.5 | 0.906307787 | 1.441307787 |
| 70 | 287.5 | 29.2047435 | 107.25 | 189.75 | 255.75 | 412.5 | 0.9396926208 | 1.474692621 |
| 75 | 287.5 | 22.10028846 | 107.25 | 189.75 | 255.75 | 412.5 | 0.9659258263 | 1.500925826 |
| 80 | 287.5 | 14.82763687 | 107.25 | 189.75 | 255.75 | 412.5 | 0.984807753 | 1.519807753 |
| 85 | 287.5 | 7.442138018 | 107.25 | 189.75 | 255.75 | 412.5 | 0.9961946981 | 1.531194698 |
| 90 | 287.5 | 0 | 107.25 | 189.75 | 255.75 | 412.5 | 1 | 1.535 |

**Assumptions**

1. The legs are only able to output a force in the Z direction
2. The required Z force is solely provided by the ankle (w.r.t. spider configuration)
3. The end effector applies a force that is centered about it (no torques produced about distal joint)

**Insights**

1. The asymmetrical loadings arising from the asymmetrical design suggest that the two legs can be designed differently (different sized brakes for the two legs; we will assume that the same design will be used for both legs for now)
2. If weight reduction is a major priority, Size 07 brakes may be used for all of the legs, however the cost is that the shoulder height is limited to [1.44,1.53]m; anything lower will have to be supplied by the motors
3. If push-up is done quasistatically (minimal inertia torque), the torques required will be that of Column I

**Comments**

1. Green means that the torques are below the allowable peak ankle joint torque
2. Red means that the torques are above the allowable peak ankle joint torque
3. Brake torques are conditionally formatted to the torques for the foreleg ankle (maximum of the two); green means that the effective brake torques are above that of the ankle joint torque and vice versa for red
4. h_s denotes the height of the shoulder, heights are calculated through a model that equates the adjacent lengths of the two angles, heights are theoretical where collisions are not accounted for

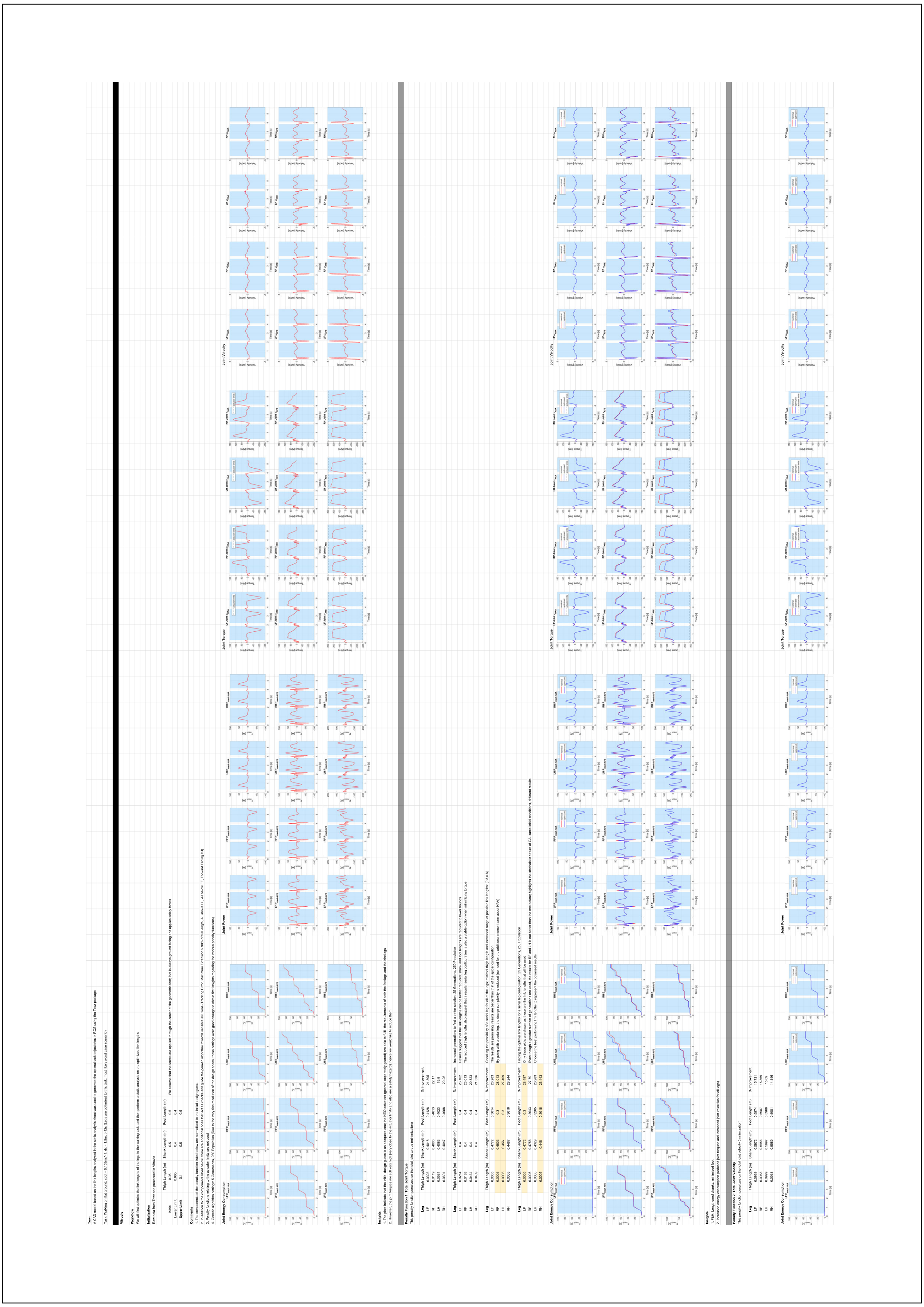

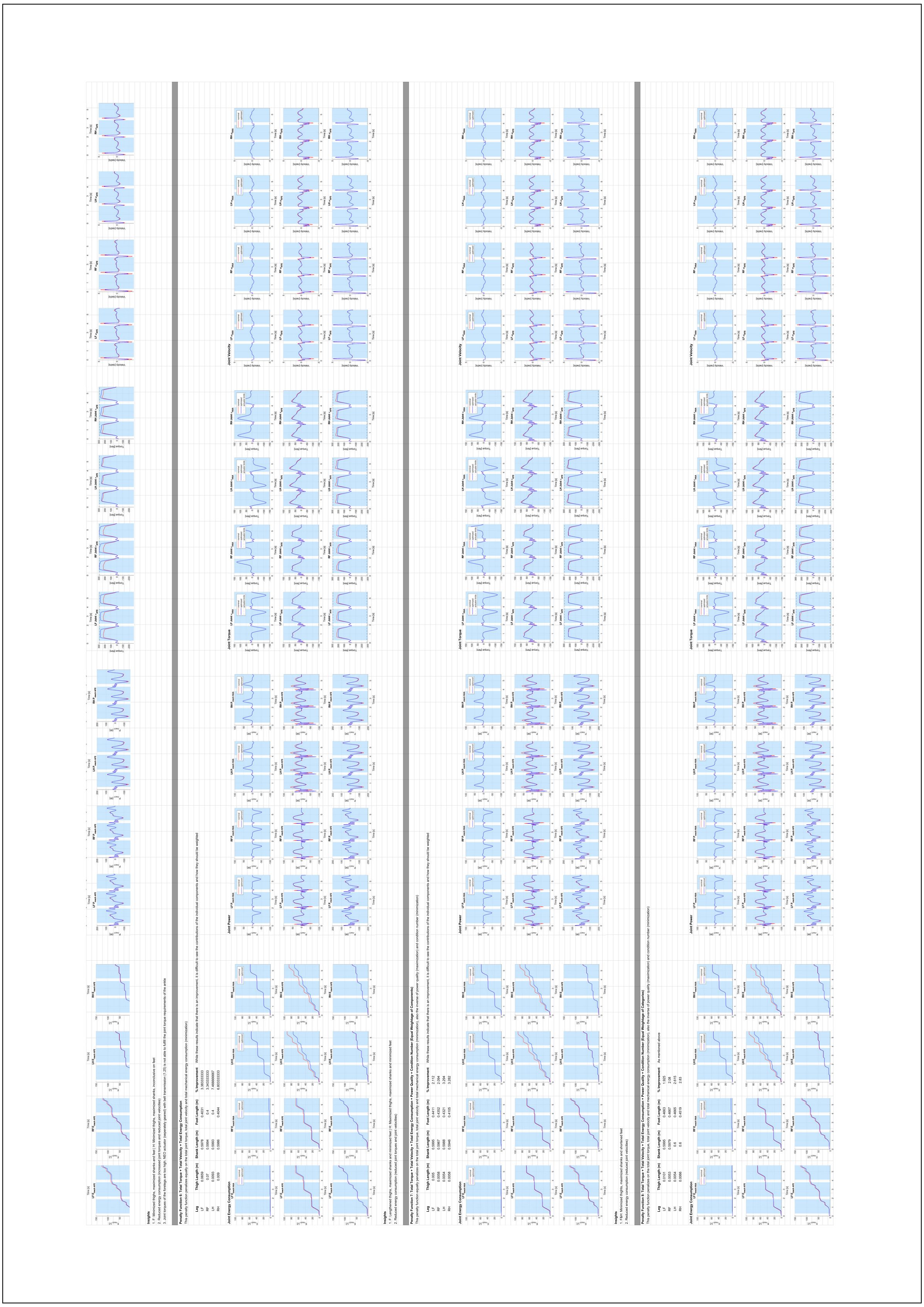

**Insights**

1. F: Inconclusive on thighs, maximized shanks and shortened feet | H: Minimized thights, maximized shanks, shortened feet
2. Reduced energy consumption (reduced joint torques)

**Conclusion**

1. In general, the dynamic analysis yields interesting results: i) Greatly differing optimal link lengths depending on which penalty function and trajectories are being used, ii) L/R symmetry is typically respected with regards to improvements
2. It is clear to see the effects of the optimization has on the leg design when it is optimized to a single objective
3. This is not the case for a multi-objective one as it is difficult to understand and control what the optimizer is doing (difficult in weighing the different objectives)
4. Given that the joint torques are the closest to the limits of the NEO actuators (limiting factor), we will proceed with the optimized link lengths when total torque was solely minimized; a demonstration of the optimal leg design procedure
5. Additionally, in a bid to reduce the design complexity, the concept is modified to a conventional serial leg configuration
6. The optimized link lengths are typically unequal and this may present a dilemma:

i) A short thigh and long shank requires a lesser braking torque (maybe able to use a smaller brake or gear ratio) and leg inertia (ankle joint is closer to the hip), but a greater knee torque is required (generally, depends on trajectory)

ii) A long thigh and short shank requires a small knee torque, but results in a greater breaking torque and leg inertia (vice versa to the case of the foreleg)

ii) The robotic is now more asymmetrical and does have a preferred direction of motion (robot level design matters vs. tasks, specialization vs. versatility)

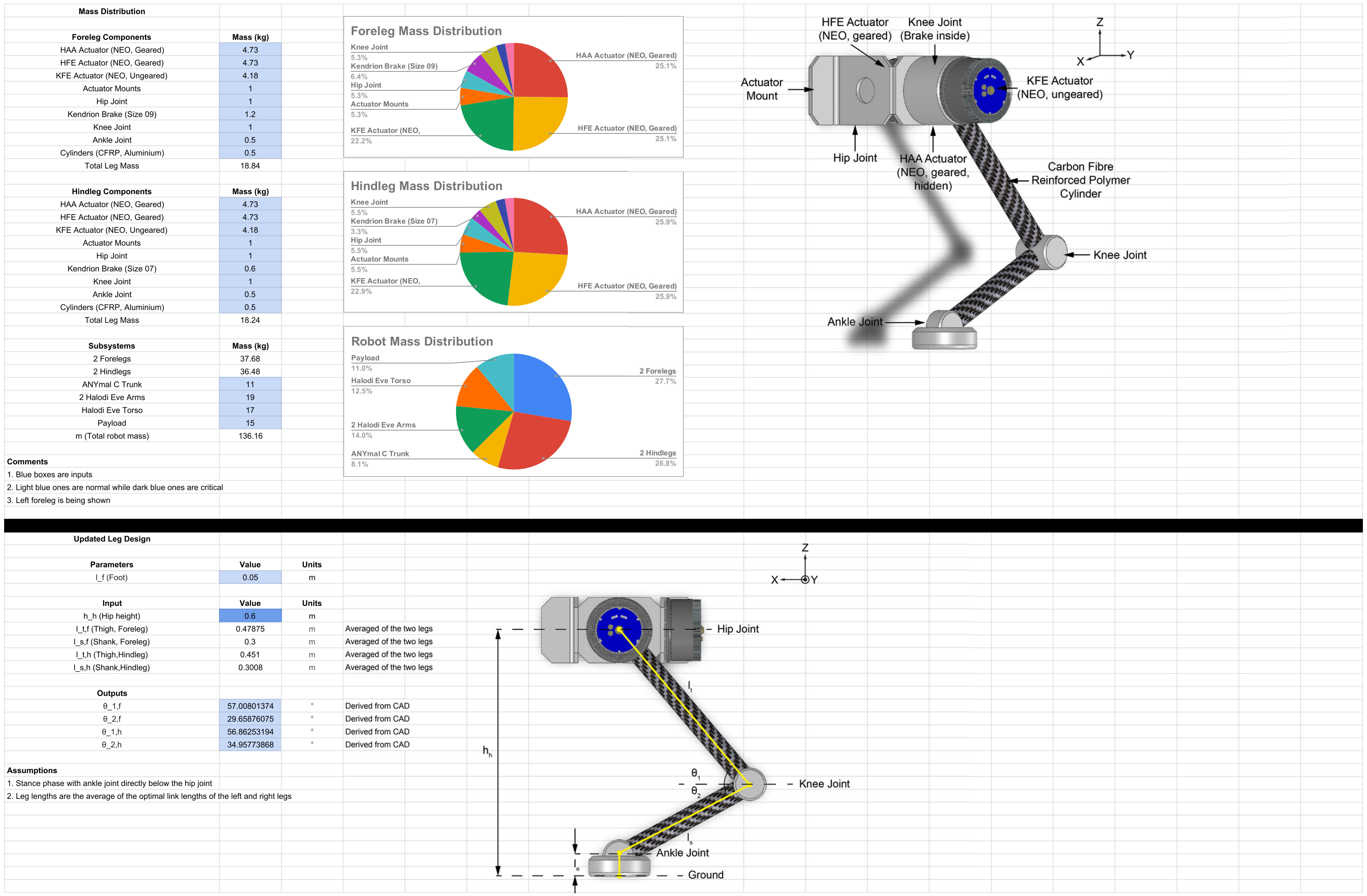

**Mass Distribution**

| Foreleg Components | Mass (kg) |
|---|---|
| HAA Actuator (NEO, Geared) | 4.73 |
| HFE Actuator (NEO, Geared) | 4.73 |
| KFE Actuator (NEO, Ungeared) | 4.18 |
| Actuator Mounts | 1 |
| Hip Joint | 1 |
| Kendrion Brake (Size 09) | 1.2 |
| Knee Joint | 1 |
| Ankle Joint | 0.5 |
| Cylinders (CFRP, Aluminium) | 0.5 |
| Total Leg Mass | 18.84 |

| Hindleg Components | Mass (kg) |
|---|---|
| HAA Actuator (NEO, Geared) | 4.73 |
| HFE Actuator (NEO, Geared) | 4.73 |
| KFE Actuator (NEO, Ungeared) | 4.18 |
| Actuator Mounts | 1 |
| Hip Joint | 1 |
| Kendrion Brake (Size 07) | 0.6 |
| Knee Joint | 1 |
| Ankle Joint | 0.5 |
| Cylinders (CFRP, Aluminium) | 0.5 |
| Total Leg Mass | 18.24 |

| Subsystems | Mass (kg) |
|---|---|
| 2 Forelegs | 37.68 |
| 2 Hindlegs | 36.48 |
| ANYmal C Trunk | 11 |
| 2 Halodi Eve Arms | 19 |
| Halodi Eve Torso | 17 |
| Payload | 15 |
| m (Total robot mass) | 136.16 |

**Comments**
1. Blue boxes are inputs
2. Light blue ones are normal while dark blue ones are critical
3. Left foreleg is being shown

**Updated Leg Design**

| Parameters | Value | Units |
|---|---|---|
| l_f (Foot) | 0.05 | m |

| Input | Value | Units | |
|---|---|---|---|
| h_h (Hip height) | 0.6 | m | |
| l_t,f (Thigh, Foreleg) | 0.47875 | m | Averaged of the two legs |
| l_s,f (Shank, Foreleg) | 0.3 | m | Averaged of the two legs |
| l_t,h (Thigh,Hindleg) | 0.451 | m | Averaged of the two legs |
| l_s,h (Shank,Hindleg) | 0.3008 | m | Averaged of the two legs |

| Outputs | | | |
|---|---|---|---|
| θ_1,f | 57.00801374 | ° | Derived from CAD |
| θ_2,f | 29.65876075 | ° | Derived from CAD |
| θ_1,h | 56.86253194 | ° | Derived from CAD |
| θ_2,h | 34.95773868 | ° | Derived from CAD |

**Assumptions**
1. Stance phase with ankle joint directly below the hip joint
2. Leg lengths are the average of the optimal link lengths of the left and right legs

**Updated Hip Heights**

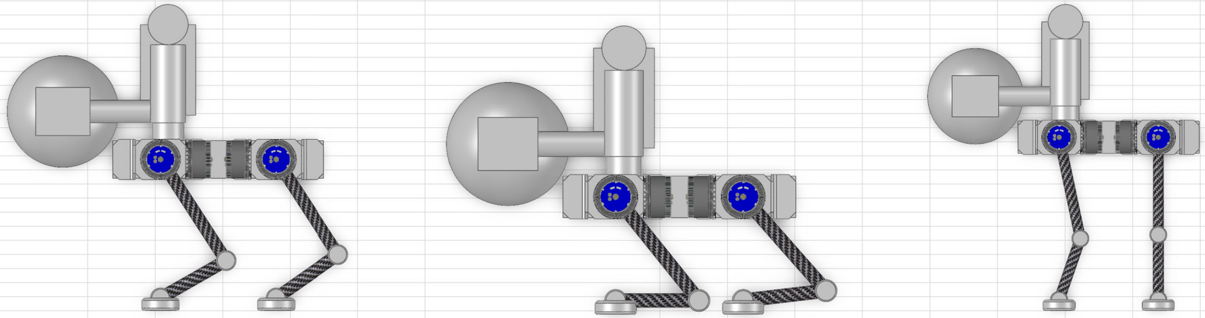

| Description | Hip Height (m) | |
|---|---|---|
| Left: Nominal stance; end effector directly below hip joint | 0.6 | |
| Middle: Minimum hip height | 0.423 | Derived from CAD; minimum hip height that results in no collision |
| Right: Maximum hip height while maintaining configuration | 0.802 | Determined by shortest leg |

**Comments**

1. Optimal link lengths are feasible due to the reasonable range of link lengths explored, however they have to be engineered: 1) Seeking a mm range, 2) Have yet to be sized for belt transmission, 3) At maximum hip height, there is unnecessary torque exerted on the foreleg

**Engineered Leg Design**

| Parameters | Value | Units | |
|---|---|---|---|
| Total length of foreleg | 0.77875 | m | |
| Total length of hindleg | 0.7518 | m | |
| Engineered Length of legs | 0.8 | m | Chose the rounded maximum as the length is needed to track the trajectory without overextension |

| Input | Value | Units | |
|---|---|---|---|
| h_h (Hip height) | 0.6 | m | |
| l_t,f (Thigh, Foreleg) | 0.484 | m | Calculated using the belt calculator below |
| l_s,f (Shank, Foreleg) | 0.316 | m | |
| l_t,h (Thigh,Hindleg) | 0.452 | m | Calculated using the belt calculator below |
| l_s,h (Shank,Hindleg) | 0.348 | m | |

| Outputs | | | |
|---|---|---|---|
| θ_1,f | 55.1468898 | ° | Derived from CAD |
| θ_2,f | 28.92128603 | ° | Derived from CAD |
| θ_1,h | 50.8732806 | ° | Derived from CAD |
| θ_2,h | 34.95085213 | ° | Derived from CAD |

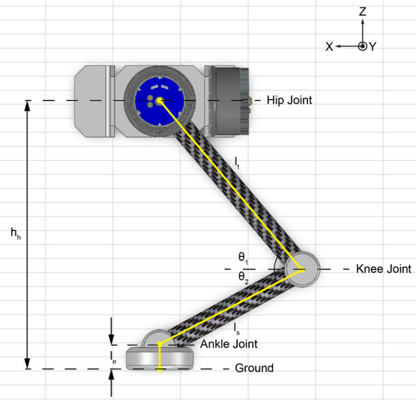


**Comment**

1. In order to be optimal for walking, the legs have a longer thigh than shank
2. The ratio of 0.5 can be viewed as the reference point for versatility while any deviation from that indicates a bias (specialization) to a certain task
3. Since the heavy payload robot already has asymmetry, it makes sense that the legs are asymmetry to reduce requirements of the task but not too much till it is unable to perform other tasks

**Engineered Hip Heights**

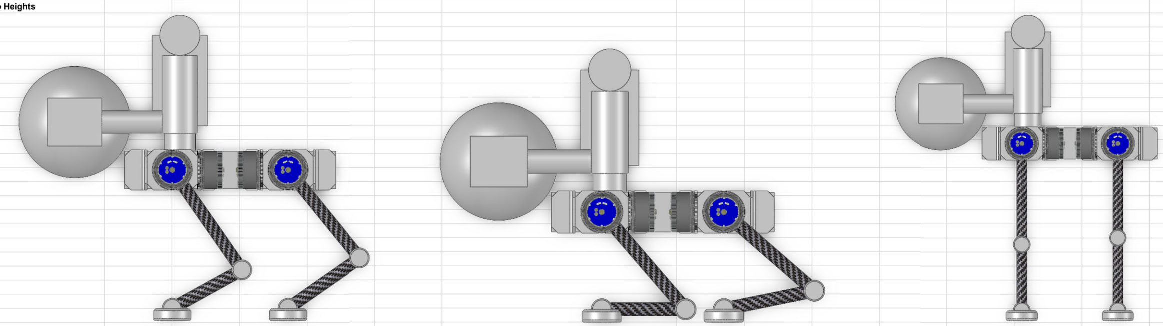

| Description | Hip Height (m) | |
|---|---|---|
| Left: Nominal stance; end effector directly below hip joint | 0.6 | |
| Middle: Minimum hip height | 0.416 | Derived from CAD;minimum hip height that results in no collision |
| Right: Maximum hip height while maintaining configuration | 0.85 | |

**CoM Location and Reachability**

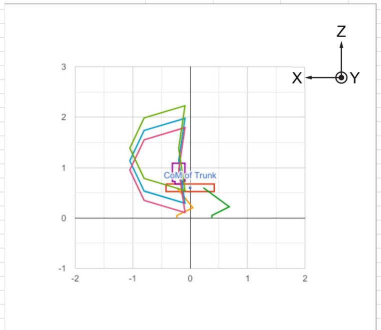


| Parameters | Value | Units | |
|---|---|---|---|
| ANYmal V3 Trunk Length (X) | 0.84 | m | |
| ANYmal V3 Trunk Height (Z) | 0.15 | m | |
| Hip attachment point displacement (X) | 0.23 | m | Derived from CAD, with respect to center of trunk |
| CoM of Trunk and Legs (X) | -0.0131287 | m | Derived from CAD, with respect to center of trunk |
| CoM of Trunk and Legs (Z) | -0.03781833 | m | Derived from CAD, with respect to center of trunk |
| Torso center of attachment displacement from Trunk CoM | 0.2 | m | |
| Halodi Eve Torso Length (X) | 0.22 | m | |
| Halodi Eve Torso Height (Z) | 0.36 | m | |
| Halodi Eve Torso Interface Diameter (X/Z) | 0.125 | m | |
| Halodi Eve Torso Interface Height (Z) | 0.1 | m | |
| Halodi Eve Arm Length (X) | 0.85 | m | To fingertips = 0.85m ; to palm = 0.7m |

| Plotting Points | X Coordinates | | | Z Coordinates | | | | |
|---|---|---|---|---|---|---|---|---|
| CoM of Trunk | 0 | 0.6 | | | | | | |
| Top left of Trunk | -0.42 | | 0.675 | | | | | |
| Top right of Trunk | 0.42 | | 0.675 | | | | | |
| Bottom right of trunk | 0.42 | | 0.525 | | | | | |
| Bottom left of trunk | -0.42 | | 0.525 | | | | | |
| Top left of trunk | -0.42 | | 0.675 | | | | | |
| Hip joint of Foreleg | -0.23 | | | 0.6 | | | | |
| Knee joint of Foreleg | 0.04659365069 | | | 0.20282 | | | | |
| Ankle joint of Foreleg | -0.2299963846 | | | 0.05 | | | | |
| Foot of Foreleg | -0.2299963846 | | | 0 | | | | |
| Hip joint of Hindleg | 0.23 | | | | 0.6 | | | |
| Knee joint of Hindleg | 0.6809859662 | | | | 0.22235 | | | |
| Ankle joint of Hindleg | 0.3801915145 | | | | 0.05 | | | |
| Foot of Hindleg | 0.3801915145 | | | | 0 | | | |
| Torso center of attachment | -0.2 | | | | | 0.675 | | |
| Bottom Left of Torso Interface | -0.2625 | | | | | 0.675 | | |
| Top Left of Torso Interface | -0.2625 | | | | | 0.725 | | |
| Bottom Left of Torso | -0.31 | | | | | 0.725 | | |
| Top Left of Torso | -0.31 | | | | | 1.085 | | |
| Top Right of Torso | -0.09 | | | | | 1.085 | | |
| Bottom Right of Torso | -0.09 | | | | | 0.725 | | |
| Top Right of Torso Interface | -0.1375 | | | | | 0.725 | | |
| Bottom Right of Torso Interface | -0.1375 | | | | | 0.675 | | |
| Torso center of attachment | -0.2 | | | | | 0.675 | | |
| Arm center of rotation (nominal) | -0.2 | | | | | | 1.135 | |
| Arm rotation lower limit (nominal) | -0.08905273661 | | | | | | 0.2922718678 | |
| Arm rotation bottom left limit (nominal) | -0.801040764 | | | | | | 0.533959236 | |
| Arm rotation left limit (nominal) | -1.05 | | | | | | 1.135 | |
| Arm rotation top left limit (nominal) | -0.801040764 | | | | | | 1.736040764 | |
| Arm rotation upper limit (nominal) | -0.08905273661 | | | | | | 1.977728132 | |
| Arm center of rotation (nominal) | -0.2 | | | | | | 1.135 | |
| Arm center of rotation (lowest stance) | -0.2 | | | | | | | 0.951 |
| Arm rotation lower limit (lowest stance) | -0.08905273661 | | | | | | | 0.1082718678 |
| Arm rotation bottom left limit (lowest stance) | -0.801040764 | | | | | | | 0.349959236 |
| Arm rotation left limit (lowest stance) | -1.05 | | | | | | | 0.951 |
| Arm rotation top left limit (lowest stance) | -0.801040764 | | | | | | | 1.552040764 |
| Arm rotation upper limit (lowest stance) | -0.08905273661 | | | | | | | 1.793728132 |

| | | | |
|---|---|---|---|
| CoM of Torso and Payload (X, w.r.t center of attachment) | 0.14603917 | m | Derived from CAD, with arms at 90° |
| CoM of Torso and Payload (Z, w.r.t center of attachment) | 0.21892155 | m | Derived from CAD, with arms at 90° |
| CoM of Robot (X) | 0.121400981 | m | With reference to center of trunk |
| CoM of Robot (Z) | 0.08643794115 | m | With reference to center of trunk |

| | | | |
|---|---|---|---|
| Arm center of rotation (lowest stance) | -0.2 | 0.951 | |
| Arm center of rotation (highest stance) | -0.2 | | 1.385 |
| Arm rotation lower limit (highest stance) | -0.08905273661 | | 0.5422718678 |
| Arm rotation bottom left limit (highest stance) | -0.801040764 | | 0.783959236 |
| Arm rotation left limit (highest stance) | -1.05 | | 1.385 |
| Arm rotation top left limit (highest stance) | -0.801040764 | | 1.986040764 |
| Arm rotation upper limit (highest stance) | -0.08905273661 | | 2.227728132 |
| Arm center of rotation (highest stance) | -0.2 | | 1.385 |

**Comments**
1. The shoulders of Halodi Eve have a joint range of ±97.5° (flexion,extension)
2. The hip of Halodi Eve have a joint range of ±30° (rotation); not considered in this 2D analysis

**Torques during stance**

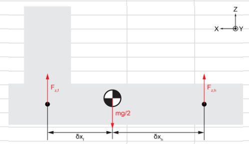


| Parameters | Value | Units | |
|---|---|---|---|
| g (Gravitational acceleration) | 9.81 | ms^-2 | |
| δx_f (Moment arm from CoM to foreleg) | 0.108599019 | m | |
| δx_h (Moment arm from CoM to hindleg) | 0.351400981 | m | |
| F_z,f = (δx_h/(δx_f+δx_h))(mg/2) | 510.1920563 | N | Obtained using the principle of moments |
| F_z,h = (δx_f/(δx_f+δx_h))(mg/2) | 157.6727437 | N | Obtained using the principle of moments |
| | | | |
| NEO Motor (Ungeared) Peak Torque | 34.84848485 | Nm | |
| Transmission mechanical advantage | 1.230769231 | | |
| Planetary Gear mechanical advantage | 6.6 | | |
| Safety factor | 1 | | Allow full range for this portion of the analysis |
| τ_k,a (Allowable knee joint peak torque) | 283.0769231 | Nm | |

| θ_f,1 | θ_f,2 | τ_k,a (Nm) | τ_f,k (Nm) | τ_b,07 (Nm) | τ_b,08 (Nm) | τ_b,09 (Nm) | h_h (m) | h_s (m) |
|---|---|---|---|---|---|---|---|---|
| 0 | #NUM! | 283.0769231 | 246.9329553 | 105.6 | 186.8307692 | 251.8153846 | #NUM! | #NUM! |
| 5 | #NUM! | 283.0769231 | 245.9933008 | 105.6 | 186.8307692 | 251.8153846 | #NUM! | #NUM! |
| 10 | #NUM! | 283.0769231 | 243.1814888 | 105.6 | 186.8307692 | 251.8153846 | #NUM! | #NUM! |
| 15 | #NUM! | 283.0769231 | 238.5189189 | 105.6 | 186.8307692 | 251.8153846 | #NUM! | #NUM! |
| 20 | #NUM! | 283.0769231 | 232.0410759 | 105.6 | 186.8307692 | 251.8153846 | #NUM! | #NUM! |
| 25 | #NUM! | 283.0769231 | 223.7972602 | 105.6 | 186.8307692 | 251.8153846 | #NUM! | #NUM! |
| 30 | #NUM! | 283.0769231 | 213.8502123 | 105.6 | 186.8307692 | 251.8153846 | #NUM! | #NUM! |
| 35 | #NUM! | 283.0769231 | 202.2756351 | 105.6 | 186.8307692 | 251.8153846 | #NUM! | #NUM! |
| 40 | #NUM! | 283.0769231 | 189.1616182 | 105.6 | 186.8307692 | 251.8153846 | #NUM! | #NUM! |
| 45 | #NUM! | 283.0769231 | 174.6079672 | 105.6 | 186.8307692 | 251.8153846 | #NUM! | #NUM! |
| 50 | 10.09358951 | 283.0769231 | 158.7254441 | 105.6 | 186.8307692 | 251.8153846 | 0.476146588 | 1.011146588 |
| 55 | 28.53615879 | 283.0769231 | 141.6349245 | 105.6 | 186.8307692 | 251.8153846 | 0.5974269852 | 1.132426985 |
| 60 | 40.01975377 | 283.0769231 | 123.4664776 | 105.6 | 186.8307692 | 251.8153846 | 0.6723606261 | 1.207360626 |
| 65 | 49.66155424 | 283.0769231 | 104.3583763 | 105.6 | 186.8307692 | 251.8153846 | 0.7295189631 | 1.264518963 |
| 70 | 58.40889731 | 283.0769231 | 84.45604475 | 105.6 | 186.8307692 | 251.8153846 | 0.7739826488 | 1.308982649 |
| 75 | 66.64549438 | 283.0769231 | 63.91095169 | 105.6 | 186.8307692 | 251.8153846 | 0.8076181196 | 1.34261812 |
| 80 | 74.57555253 | 283.0769231 | 42.87945769 | 105.6 | 186.8307692 | 251.8153846 | 0.8312652666 | 1.366265267 |
| 85 | 82.32858833 | 283.0769231 | 21.52162513 | 105.6 | 186.8307692 | 251.8153846 | 0.8453300118 | 1.380330012 |
| 90 | 90 | 283.0769231 | 0 | 105.6 | 186.8307692 | 251.8153846 | 0.85 | 1.385 |

| θ_h,1 | θ_h,2 | τ_k,a (Nm) | τ_h,k (Nm) | τ_b,07 (Nm) | τ_b,08 (Nm) | τ_b,09 (Nm) | h_h (m) | h_s (m) |
|---|---|---|---|---|---|---|---|---|
| 0 | #NUM! | 283.0769231 | 71.26808013 | 105.6 | 186.8307692 | 251.8153846 | #NUM! | #NUM! |
| 5 | #NUM! | 283.0769231 | 70.99688357 | 105.6 | 186.8307692 | 251.8153846 | #NUM! | #NUM! |
| 10 | #NUM! | 283.0769231 | 70.18535786 | 105.6 | 186.8307692 | 251.8153846 | #NUM! | #NUM! |
| 15 | #NUM! | 283.0769231 | 68.83967919 | 105.6 | 186.8307692 | 251.8153846 | #NUM! | #NUM! |
| 20 | #NUM! | 283.0769231 | 66.970089 | 105.6 | 186.8307692 | 251.8153846 | #NUM! | #NUM! |
| 25 | #NUM! | 283.0769231 | 64.59081599 | 105.6 | 186.8307692 | 251.8153846 | #NUM! | #NUM! |
| 30 | #NUM! | 283.0769231 | 61.71996787 | 105.6 | 186.8307692 | 251.8153846 | #NUM! | #NUM! |
| 35 | #NUM! | 283.0769231 | 58.37939353 | 105.6 | 186.8307692 | 251.8153846 | #NUM! | #NUM! |
| 40 | 5.744995604 | 283.0769231 | 54.59451676 | 105.6 | 186.8307692 | 251.8153846 | 0.3753752024 | 0.9103752024 |
| 45 | 23.302945 | 283.0769231 | 50.39414274 | 105.6 | 186.8307692 | 251.8153846 | 0.5072785282 | 1.042278528 |
| 50 | 33.39612864 | 283.0769231 | 45.81023887 | 105.6 | 186.8307692 | 251.8153846 | 0.5877997551 | 1.122799755 |
| 55 | 41.84175277 | 283.0769231 | 40.87769143 | 105.6 | 186.8307692 | 251.8153846 | 0.6523990116 | 1.187399012 |
| 60 | 49.50171499 | 283.0769231 | 35.63404007 | 105.6 | 186.8307692 | 251.8153846 | 0.7060715234 | 1.241071523 |
| 65 | 56.70718704 | 283.0769231 | 30.11919214 | 105.6 | 186.8307692 | 251.8153846 | 0.7505360453 | 1.285536045 |
| 70 | 63.62571941 | 283.0769231 | 24.37511898 | 105.6 | 186.8307692 | 251.8153846 | 0.7865181836 | 1.321518184 |
| 75 | 70.35646561 | 283.0769231 | 18.44553645 | 105.6 | 186.8307692 | 251.8153846 | 0.8143456734 | 1.349345673 |
| 80 | 76.96518736 | 283.0769231 | 12.37557224 | 105.6 | 186.8307692 | 251.8153846 | 0.83416626 | 1.36916626 |
| 85 | 83.50005347 | 283.0769231 | 6.211422458 | 105.6 | 186.8307692 | 251.8153846 | 0.8460430461 | 1.381043046 |
| 90 | 90 | 283.0769231 | 0 | 105.6 | 186.8307692 | 251.8153846 | 0.85 | 1.385 |

**Sizing Permernant Magnet Brakes**

| Kendrion Permernant Magnet Brake High Torque Line | Mass (kg) | Power (W) |
|---|---|---|
| Size 07 | 0.6 | 14 |
| Size 08 | 1.15 | 18 |
| Size 09 | 1.2 | 19 |

| Stall Torques | Value | Units |
|---|---|---|
| Size 07 | 13 | Nm |
| τ_b,07 (Size 07 Effective) | 105.6 | Nm |
| Size 08 | 23 | Nm |
| τ_b,08 (Size 08 Effective) | 186.8307692 | Nm |
| Size 09 | 31 | Nm |
| τ_b,09 (Size 09 Effective) | 251.8153846 | Nm |

**Assumptions**
1. Legs are only able to output a force in the Z direction
2. The required Z force is solely provided by the knee
3. The end effector applies a force that is centered about it

**Insights**
1. The asymmetrical loadings arising from the asymmetrical design suggest that the design of the two legs can be different; use Size 09 for forelegs, Size 07 for hindlegs (Updated as above)
2. If weight reduction is a major priority, Size 07 brakes may be used for all of the legs, however the cost is that the shoulder height is limited to [1.26,1.39]m; anything lower will have to be supplied by the motors
3. If push-up is done quasistatically (minimal inertia torque), the torques required will be that of Column I

**Comments**
1. Green means that the torques are below the allowable peak knee joint torque
2. Red means that the torques are above the allowable peak knee joint torque
3. Brake torques are conditionally formatted to the knee torques; green means that the effective brake torques are above that of the knee joint torque and vice versa for red
4. h_s denotes the height of the shoulder, heights are calculated through a model that equates the adjacent lengths of the two angles, a numerical error in the hip height signals that the hip height is unattainable, heights are theoretical where collisions are not accounted for

**Power Transmission**

| | | | |
|---|---|---|---|
| **HAA (NEO, Geared)** | Direct actuation | | |
| **Properties** | **Value** | **Units** | |
| Output peak torque | 230 | Nm | |
| Max output velocity | 18.8 | rads^-1 | |
| **HFE (NEO, Geared)** | Direct actuation | | |
| **Properties** | **Value** | **Units** | |
| Output peak torque | 230 | Nm | |
| Max output velocity | 18.8 | rads^-1 | |
| **KFE (NEO, Ungeared)** | Transmitted through belts | | |
| **Properties** | **Value** | **Units** | |
| Actuator peak torque | 34.84848485 | Nm | |
| Transmission mechanical advantage | 1.230769231 | | |
| Transmission peak torque | 42.89044289 | Nm | |
| Planetary Gear mechanical advantage | 6.6 | | |
| Output peak torque | 283.0769231 | Nm | |
| Max actuator velocity | 124.08 | rads^-1 | |
| Max output velocity | 15.275 | rads^-1 | |
| **Belt Sizing Calculator** | Based on Misumi transmission timing belts manual, transmission power derived from dynamic analysis | | |
| **Step 1** | From the dynamic analysis, the knee joint velocity during walking after optimization was kept within ±5rads^-1; worst case scenario (0.15ms^-1, with payload) | | |
| | This implies that the input motor speed is (5*(6.6*1.25)) = 41.25rads^-1 | | |
| As above | The worst case scenario is when the motor outputs maximum torque at this speed, Pt = 34.84848485*41.25 = 1.4375kW | | |
| | Limiting factor is not the tension in the belt but rather the transmission power of the belt | | |
| **Step 2** | | | |
| **Properties** | **Value** | **Units** | |
| Pt (Transmission power) | 1.4375 | kW | |
| Ko (Load Correction Factor) | 1.9 | Max output exceeding 300% of rated value, special motor (high torque), intermittent use (3-5h/day) | |
| | 1.3 | Starts / stops over 100 times/day or rapid acceleration / deceleration (MTS_M belts) | |
| | 2.47 | | |
| Kr (Speed Ratio Correction Coefficient) | 0 | | |
| Ki (Idlers Correction Coefficient) | 0 | Outside the tensioned side of the belt; since direction changes, we need two idlers on each side | |
| Ks=Ko+Kr+Ki (Overload Factor) | 2.47 | | |
| Pd=Pt*Ks (Design Power) | 3.550625 | kW | |
| Rotary speed of small pulley | 1184.87672 | rpm | |
| **Step 3** | | | |
| Fits inside MTS8M (Super High Torque Timing Belt) curve; nominal belt width: 60mm | | | |
| **Step 4** | | | |
| **Properties** | **Value** | **Units** | |
| Zd (No. of Teeth of Small Pulley) | 26 | | Allowable minimum number of teeth based on rpm is 24 |
| C' (Temporary Inter-shaft Distance) | 484 | mm | Ideal thigh length for foreleg: 478.75mm, feasible thigh length for foreleg: 484mm (belt length:1200mm) \| Ideal thigh length for hindleg: 451mm, feasible thigh length for hindleg: 452mm (belt length: 1136mm); closest belt length to optimized link lengths |
| Dp (Pitch Diameter of Large Pulley) | 81.49 | mm | 32 |
| dp (Pitch Diameter of Small Pulley) | 66.21 | mm | 26 |
| Lp' (Approximate Belt Circumference Length) | 1200.127216 | mm | Based on given formula |
| Lp (Belt Circumference Length) | 1136 | mm | Closest available belt length |
| b | 1807.986765 | mm | Based on given formula |
| C (Inter-shaft Distance) | 451.9321134 | mm | Based on given formula |
| Ps (Reference Transmission Capacity) | 22.67 | kW | Based on rpm of small pulley |
| θ (Contact Angle) | 178.0626648 | ° | Based on given formula, different from the above θ |
| Zm (No. of Teeth Engaged) | 12.86008135 | | Based on given formula |
| Km (Engagement Correction Coefficient) | 1 | | More than 6 |

**Step 5**

| Properties | Value | Units | |
|---|---|---|---|
| Wp (Reference Belt Width) | 60 | mm | |
| Bw' (Approximate Belt Width) | 9.397331275 | mm | |
| Bw (Belt Width) | 15 | mm | |
| | | | |
| Pd | 3.550625 | kW | |
| Kb (Width Correction Coefficient) | 0.21 | | |
| Ps*Km*Kb | 4.7607 | kW | Green means go, red means no go; change Zd or Bw if no go |
| Safety Factor | 1.340806196 | | |

**Step 6**

| Properties | Value | Units | |
|---|---|---|---|
| C | 451.9321134 | mm | |
| Ci (Minimum Adjustment Range, Inside) | 15 | mm | Loosening effect; need to account for in design |
| Cs (Minimum Adjustment Range, Outside) | 5 | mm | Tightening effect; can be done using idlers, need to account for in design |

**Belt Tautness**

| Properties | Value | Units | |
|---|---|---|---|
| Ti (Initial Tension) | 294 | N | Recommended value based on belt width |
| Y (Correction Coefficient) | 226 | | |
| t (Span Length) | 451.867531 | mm | |
| δ (Deflection) | 7.229880496 | mm | |
| Td (Load N Needed for Deflection d at Center of Span t) | 23.99351133 | N | |

**Parts Required: 26T pulley (HTPA26S8M150-A-C20), 32T pulley (HTPA32S8M150-A-C20), MTS8M (HTBN1200-MTS8M-150 (Foreleg), HTBN1136-MTS8M-150 (Hindleg))**

**Belt Properties**

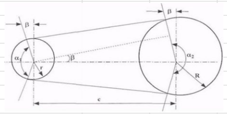

| Properties | Value | Units | |
|---|---|---|---|
| β | 0.9686424025 | ° | Based on given formula |
| α1 | 178.0627152 | ° | Based on given formula |
| α2 | 181.9372848 | ° | Based on given formula |
| | | | |
| Maximum allowable tension of MTS8M | 5472 | N | It was mentioned that it was approximately double of the standard S8M belt |
| Maximum Belt Tension (Small Pulley) | 1052.665303 | N | |
| Safety Factor | 5.198233461 | | |
| Maximum Belt Tension (Large Pulley) | 1052.655366 | N | |
| Safety Factor | 5.19828253 | | |

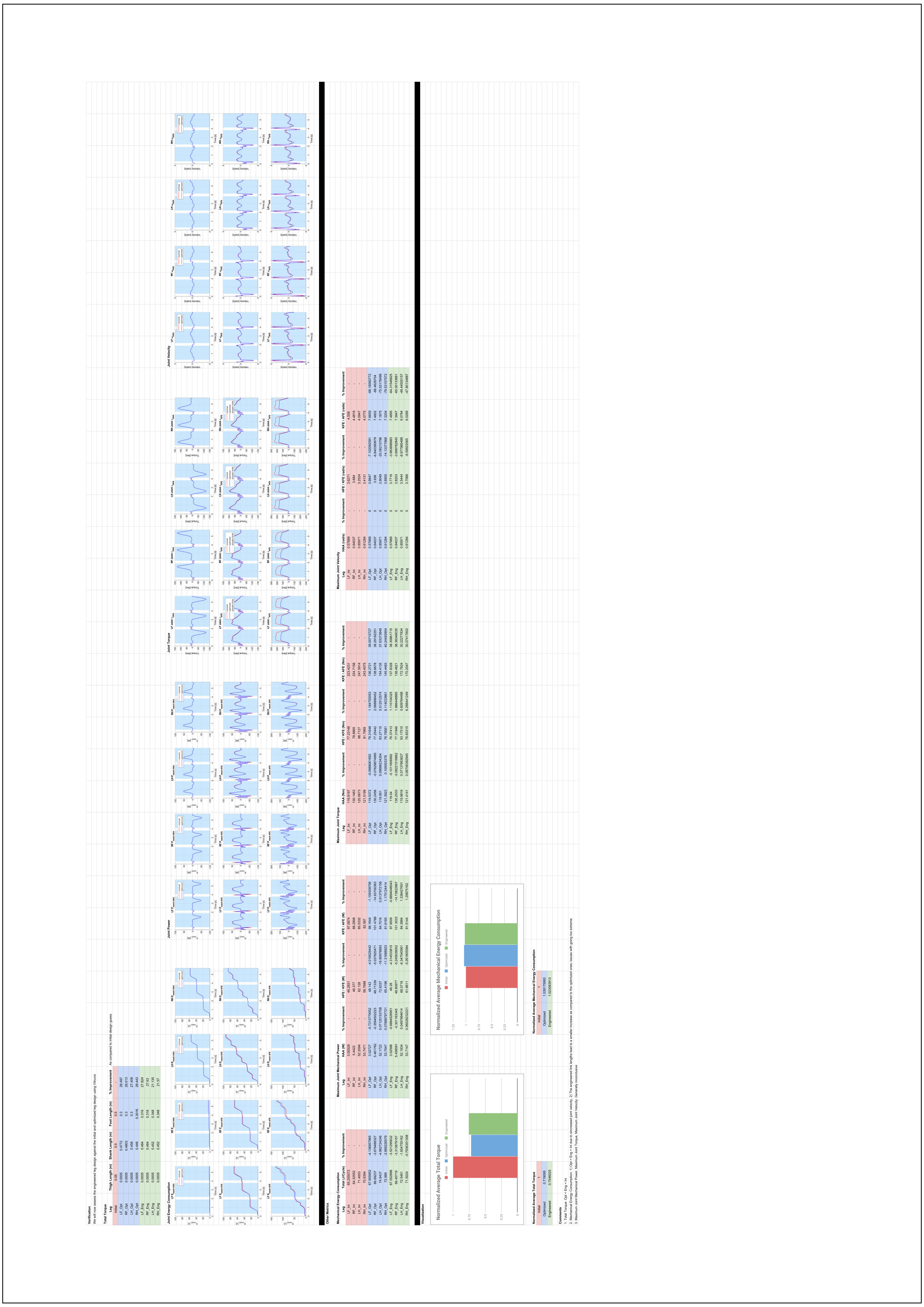

## B.9 Technical Requirements Evaluation

| ID | Requirement | Sign | Target | Type | Impt | Comments | Final CAD Predictions | Additional comments |
|---|---|---|---|---|---|---|---|---|
| **Vertex: Designing High-Performance Legs for Specialized Quadrupedal Robots** | | | | | | | | |
| **Technical Requirements List** | | | | | | | | |
| **Design** | | | | | | | | |
| D1 | The mass of the leg shall be | < | 20kg | D | 3 | Including actuators | 24.1kg | |
| D2 | The mass of active elements in the leg shall be | > | 12kg | D | 3 | Relates to transmission related components, 60% of mass | 18.3kg (76%) | |
| D3 | The link inertia of the leg shall be | < | 0.1kgm^2 | D | 3 | Measured at hip joint when the leg is fully extended | [1.86,1.41,0.950,0.00235,0.00233] kgm^2 (HAA, HFE, KFE, AAA, AFE) | On the sagittal plane |
| D4 | The dimensions of the leg when it is in its nominal stance shall be | < | 0.5m x 0.5m x 1.0 m | W | 3 | Length x Width x Height of envelope at nominal stance | 0.4m x 0.4m x 0.6.m | |
| D5 | The volume of the leg when it is fully compacted should be minimized | - | - | W | 3 | Length x Width x Height of envelope, ease of transporting around | Links can be easily removed | |
| D6 | The number of components of the leg shall be minimized | - | - | D | 5 | Strive for minimal design complexity, easy assembly and maintenance | Designed with this in mind | |
| D7 | Frictional losses in the power transmission of the leg shall be minimized | - | - | D | 4 | Energy efficiency, transparency | Designed with this in mind | |
| D8 | The possiblity of a static discharge of the leg shall be minimized | - | - | D | 4 | Safety; the robot is charging static electricity and rubber feet do not get rid of it | Since the whole leg is metallic, it is possible to ground the foot | |
| D9 | The components of the leg shall be ingress protected | - | IP65 | D | 5 | Possibility of wet missions, robustness | Permanent magnet brake is IP00 however is covered with a 3D-printed shell | |
| D10 | The components of the leg should be waterproof | - | IP68 | W | 3 | Possibility of wet missions, robustness | Permanent magnet brake is IP00 however is covered with a 3D-printed shell | |
| D11 | The leg should be kinematically redundant | - | - | W | 1 | To avoid singularities | Optimized such that it tracks the trajectories with <90% full extension | |
| **Functional** | | | | | | | | High-level matters |
| F1 | The kinematic velocity ellipsoid of the end effector shall be maximized | - | - | D | 3 | | Design sought to minimize total torque in the end | |
| F2 | The kinematic force ellipsoid of the end effector shall be maximized | - | - | D | 4 | | Design sought to minimize total torque in the end | |
| F3 | The dynamic force ellipsoid of the end effector shall be maximized | - | - | D | 4 | | Design sought to minimize total torque in the end | |
| F4 | The workspace volume of the end effector shall be maximized | - | - | D | 4 | With ANYmal V3 trunk; relates to range of motion | Design sought to minimize total torque in the end | |
| F5 | The normalized reachability of the end effector shall be maximized | - | - | D | 4 | Volume of reachable workspace / Volume of extended leg | Design sought to minimize total torque in the end | |
| **Performance** | | | | | | | | Characterization of the leg |
| P1 | The maximum load that the leg can bear while standing up from a fully crouched configuration shall be | > | 35kg | D | 5 | Mass(Platform + Payload) / 4 | 166kg | |
| P2 | The maximum shear force that can be applied at the end effector when the leg is in its nominal stance shall be maximized | - | - | D | 5 | Important for efficient power transmission the ground; see test on the right | Foot is designed with a layer of rubber for grip | |
| P3 | The bandwidth for force control of the leg shall be | > | 70Hz | D | 3 | The higher it is, the better it is to control; numbers from Hutter 2016 | BOTA Systems Rokubi Mini being used | |
| P4 | The maximum force that can be applied by the end effector shall be maximized | - | - | D | 4 | Thrust; stance phase | Not maximized as total torque is being reduced | |
| P5 | The maximum velocity of the end effector shall be maximized | - | - | D | 3 | Preparing for next step; swing phase | Not maximized as total torque is being reduced | |
| P6 | The positioning accuracy of the end effector shall be | < | 10mm | D | 3 | Accuracy; within a few mm but through the transmission it adds up (especially long links and transmissions) | Not tested | |
| P7 | The positioning repeatability of the end effector shall be | < | 10mm | D | 3 | Precision; within a few mm | Not tested | |
| P8 | The end effector shall be able to track specific trajectories | - | 60% stance, 40% swing (Walk) | D | 5 | Related to gaits | Optimized for walking (Towr trajectory) | |
| P9 | The minimum obstacle height that the leg can overcome shall be | > | 375mm | D | 4 | Average height of a 20L bucket | Possible | |

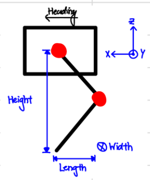


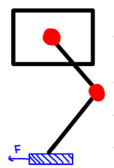


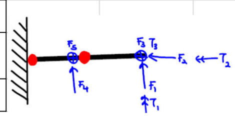

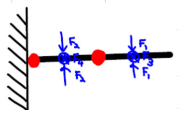

| | | | | | | | | |
|---|---|---|---|---|---|---|---|---|
| P10 | The structure of the leg shall withstand impact loads | - | Load cases | D | 5 | Load cases to be determined (not only for walking but also falling); shank broke multiple times as load case was not accounted for | Shanks are made of titanium and should be able to withstand such impacts | Load cases to simulate walking and falling |
| **Interface** | | | | | | | | |
| I1 | There should be a common electrical interface between the leg and the ANYmal V3 trunk | - | - | W | 2 | LEMO connectors | Everything except the permanent magnet brake does not use a LEMO connector | |
| I2 | There should be a common mechanical interface between the leg and the ANYmal V3 trunk | - | - | W | 2 | Compatible with HAA actuator | Was designed to the Capler-leg rail | |
| I3 | The time required to replace the leg should be | < | 15 mins | W | 3 | To facilitate troubleshooting | Not tested | |
| I4 | The leg shall be able to be mounted onto the Capler-leg rail | - | - | D | 5 | To facilitate testing; using the Capler-leg rail interface | Designed with this in mind | |
| I5 | The leg shall have a mechanism that allows additional weight to be easily added | - | - | D | 5 | To facilitate testing; using the Capler-leg rail interface | Pushed to the Capler-leg rail instead | |
| I6 | The length of the power and data cables in the leg shall be minimized | - | - | D | 2 | To ensure the robustness of operation | Designed with this in mind | |
| I7 | The twisting of the power and data cables in the leg shall be minimized | - | - | D | 4 | To ensure the robustness of operation | Designed with this in mind | |
| I8 | The movement of the power and data cables in the leg shall be minimized | - | - | D | 4 | To ensure the robustness of operation | Designed with this in mind | |
| I9 | The power and data cables of the leg should be integrated into its structure | - | - | W | 2 | To ensure the robustness of operation | Designed with this in mind | |
| I10 | The power and data cables of the leg shall be detachable | - | - | D | 3 | To ensure the robustness of operation; especially for the actuators | Designed with this in mind | |
| I11 | Safe data communication should be ensured | > | 100 Mbps | W | 3 | To ensure the robustness of operation | Not tested | |